



QEX

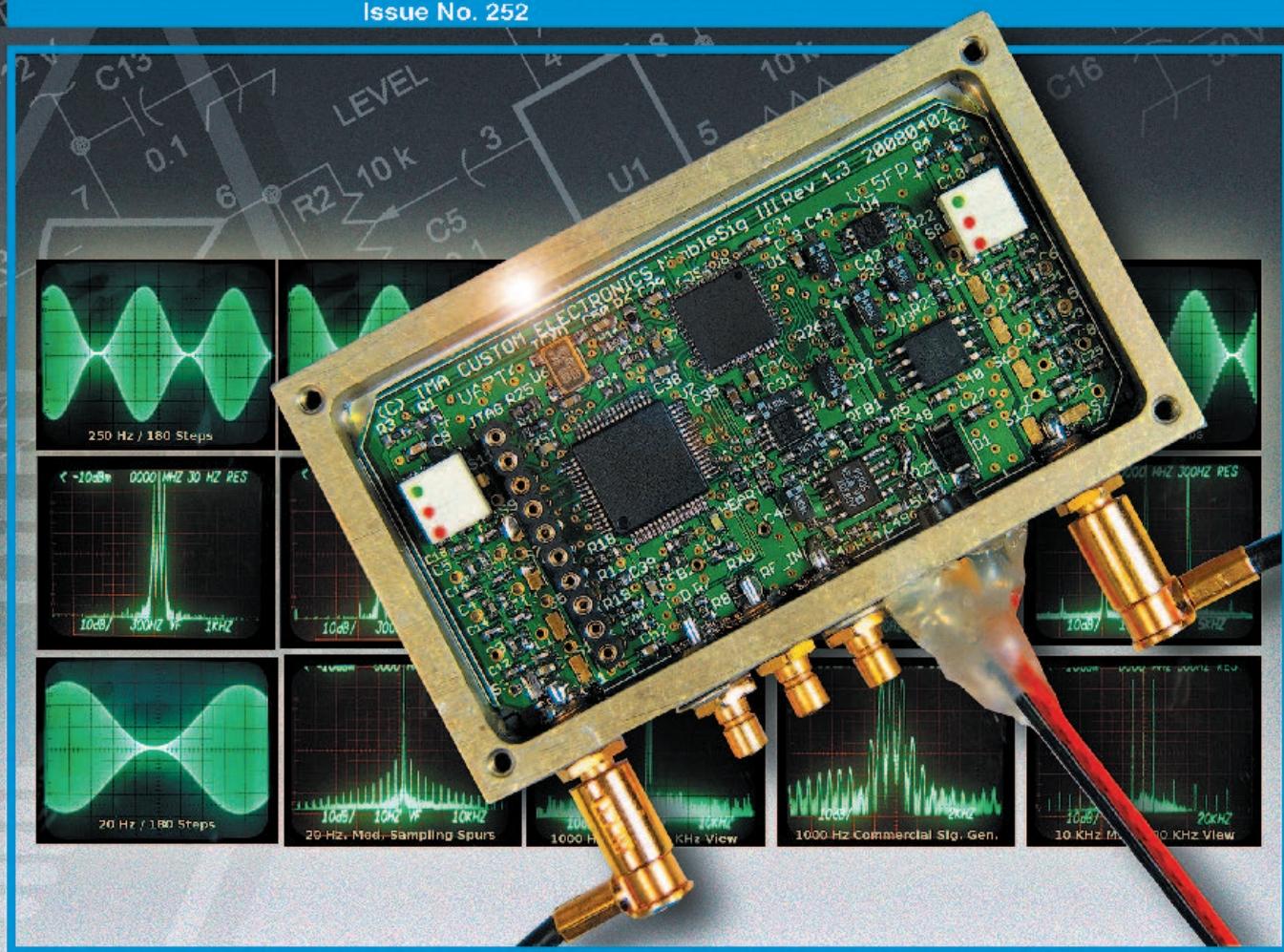
\$5

January/February 2009

www.arrl.org

A Forum for Communications Experimenters

Issue No. 252



VA7TA introduces NimbleSig III, a versatile, dual-output, DDS RF generator that provides signals over a range from 100 kHz to 200 MHz, with 1 Hz resolution.

ARRL The national association for
AMATEUR RADIO

225 Main Street
Newington, CT USA 06111-1494

TOKYO HY-POWER

Two of the **LIGHTEST** and **MOST COMPACT** Amplifiers in the Industry!



NEW!

600W OUT, Weighing only 22.5lbs.

HL-1.1KFX
Lightweight HF Linear

Outstanding for Field Works and DX-peditions!



This world-class compact HF amplifier has built-in switching mode power supply to save the weight. It is compatible with wide AC line of 100 to 250V, and is best suited for DX-peditioners.

Features

- The amplifier allows operation in full break-in CW mode due to the use of the amplifier's high speed antenna relays.
- The amp utilizes a sophisticated circuit to run the various high speed protection circuits such as overdrive, high antenna SWR, DC overvoltage, band mis-set etc.
- An analog multimeter allows the operator to monitor Pf (Forward output power), Pr (Reflected power), Vd (Drain voltage of power FET), Id (Drain current) etc.

Specifications

Frequency:
1.8 ~ 28MHz all amateur bands including WARC bands

Mode:
SSB, CW, RTTY

RF Drive:
75 ~ 90W

Output Power:
SSB 600W PEP max.
CW 600W.
RTTY 500W (5 minutes)

Final Transistor:
SD 2933 x 4
(MOS FET by ST micro)

Circuit:
Class AB parallel push-pull

Cooling Method:
Forced Air Cooling

Multi-Meter:
Output Pf 1kW, Reflected Power 100W, Drain Voltage Vd 60V, Drain Current Id 50A

Input/Output Connectors:
Type M-J (UHF SO-239)

AC Power:
1.4kVA max. when TX
AC 100 ~ 250V (Auto Select)

Dimensions:
9.1 x 5.6 x 14.3 inches (WxHxD)

Weight:
Approx. 22.5 lbs.



NEW!

Compact 45W Power Amp.

HL-45B
HF/50MHz 45W
Linear Power Amplifier

To go with the popular Yaesu FT-817 series.



Features

- HL-45B is a solid-state HF/50MHz band linear power amplifier with the maximum output power of 45W. Designed RF drive power is 5W.
- This amplifier is particularly designed for the use with popular portable radio of YAESU FT-817. When combined with FT-817, you can enjoy a unique and very comfortable feature of automatic band selection as well as send-receive switching, by connecting the amp and radio with the supplied special control cable.
- LED power level meter will always indicate the relative output power level for the convenience of the operator.

Specifications

Frequency:
HF Band (1.8 ~ 28MHz and 50MHz Amateur Bands)

Mode: SSB(A3E), CW(A1A), FM(F3E)

RF Output Power:
SSB (PEP)/CW 45W

RF Drive Power: 5W max.

DC Power: DC 13.8V, 8.5A max.

In/Out Impedance: 50Ω

In/Out Connectors: SO-239

Major Circuits and Functions:

1. Class AB wide band linear power amp
2. Automatic/manual switching output low pass filters
3. WARNG (Protection circuit) for over-voltage and over-drive
4. LED meter for indicating transmitting power level

5. Send-receive switching remote terminal
6. ALC

Final RF Power Transistor:
RD30HVF
(by Mitsubishi Electric) x 2

Accessory Parts:
DC Power cord (Red/Black) x 1
Coax jumper cable with PL-259 connectors x 1
Remote control cable for FT-817 x 1
Spare fuse 10A x 2

Dimensions:
150(W) x 47(H) x 211(D) mm
(5.9 x 1.9 x 8.3 inches)

Weight:
Approx. 1.6kgs. (3.4lbs.)

More Fine Products from TOKYO HY-POWER



HC-1.5KAT
HF 1.5KW
Auto Tuner



HL-350VDX
VHF/2m 330W
Amplifier



HL-1.5KFX
HF/6m 1kW Linear
Auto Band Set with modern ICOM, Yaesu, Kenwood Radios

TOKYO HY-POWER

TOKYO HY-POWER LABS., INC. - USA
Technical Support
28301 Tomball Parkway, Suite #500-210
Tomball, TX 77375
Phone 713-818-4544
e-mail: thpsupport@airmail.net

TOKYO HY-POWER LABS., INC. - JAPAN
1-1 Hatanaka 3chome, Niiza Saitama 352-0012
Phone: +81 (48) 481-1211 FAX: +81 (48) 479-6949
e-mail: info@thp.co.jp
Web: <http://www.thp.co.jp>



Exclusively from Ham Radio Outlet!

www.hamradio.com

Western US/Canada 1-800-854-6046	Southeast 1-800-444-7927	Northeast 1-800-644-4476
Mountain/Central 1-800-444-9476	Mid-Atlantic 1-800-444-4799	New England/Eastern Canada 1-800-444-0047



QEX (ISSN: 0886-8093) is published bimonthly in January, March, May, July, September, and November by the American Radio Relay League, 225 Main Street, Newington, CT 06111-1494. Periodicals postage paid at Hartford, CT and at additional mailing offices.

POSTMASTER: Send address changes to: QEX, 225 Main St, Newington, CT 06111-1494 Issue No 251

Harold Kramer, WJ1B
Publisher

Larry Wolfgang, WR1B
Editor

Lori Weinberg, KB1EIB
Assistant Editor

Zack Lau, W1VT
Ray Mack, W5IFS
Contributing Editors

Production Department

Steve Ford, WB8IMY
Publications Manager

Michelle Bloom, WB1ENT
Production Supervisor

Sue Fagan, KB1OKW
Graphic Design Supervisor

David Pingree, N1NAS
Senior Technical Illustrator

Advertising Information Contact:

Janet L. Rocco, W1JLR
Business Services
860-594-0203 – Direct
800-243-7768 – ARRL
860-594-4285 – Fax

Circulation Department

Cathy Stepina, QEX Circulation

Offices

225 Main St, Newington, CT 06111-1494 USA
Telephone: 860-594-0200
Fax: 860-594-0259 (24 hour direct line)
e-mail: qex@arrl.org

Subscription rate for 6 issues:

In the US: ARRL Member \$24,
nonmember \$36;

US by First Class Mail:
ARRL member \$37, nonmember \$49;

International and Canada by Airmail: ARRL member
\$31, nonmember \$43;

Members are asked to include their membership
control number or a label from their QST when
applying.

In order to ensure prompt delivery, we ask that you periodically check the address information on your mailing label. If you find any inaccuracies, please contact the Circulation Department immediately. Thank you for your assistance.



Copyright © 2008 by the American Radio Relay League Inc. For permission to quote or reprint material from QEX or any ARRL publication, send a written request including the issue date (or book title), article, page numbers and a description of where you intend to use the reprinted material. Send the request to the office of the Publications Manager (permission@arrl.org).

About the Cover

Thomas M. Alldread, VA7TA introduces us to his NimbleSig III. This dual-output, DDS RF generator provides signals over a range from 100 kHz to 200 MHz, with 1 Hz resolution. The frequencies can be set independently with a simple computer interface, and the built-in low lever RF power meter makes this a versatile building block for many applications.



In This Issue

Features

3 NimbleSig III—Part 1
By Thomas M. Alldread, VA7TA

21 Experimental Determination of Ground System Performance for HF Verticals—Part 1
By Rudy Severns, N6LF

26 Unusual Terrain Influence on VHF/UHF Propagation
By Bisharat, Chenoweth, Edwards, Kolar, Nielsen, Noel, Romriell, Wilken, Hawley

32 A Small, Simple, USB-Powered Vector Network Analyzer
By Prof. Dr. Thomas C. Baier, DG8SAQ

37 Octave for SWR
By Maynard Wright, W6PAP

41 A Protocol for Multicast Weather Data Distribution
By Nick Luther, K9NL

48 Experimental Determination of Ground System Performance for HF Verticals—Part 2
By Rudy Severns, N6LF

57 TAPR Announces HPSDR Mercury Direct-Sampling Receiver

Columns

53 SDR: Simplified
By Ray Mack, W5IFS

62 Reader's Page
By Larry Wolfgang, WR1B

58 Letters to the Editor

63 2008 QEX Index

62 Upcoming Conferences

64 In the Next Issue of QEX

Index of Advertisers

American Radio Relay League:..... Cover III
Atomic Time:..... 64
Down East Microwave Inc:..... 64
JWM Engineering: 31
Kenwood Communications:..... Cover IV

National RF, Inc: 47
Nemal Electronics International, Inc:..... 56
RF Parts 59, 61
Teri Software:..... 36
Tokyo Hy-Power Labs, Inc: Cover II
Tucson Amateur Packet Radio: 40

The American Radio Relay League



The American Radio Relay League, Inc. is a noncommercial association of radio amateurs, organized for the promotion of interest in Amateur Radio communication and experimentation, for the establishment of networks to provide communications in the event of disasters or other emergencies, for the advancement of the radio art and of the public welfare, for the representation of the radio amateur in legislative matters, and for the maintenance of fraternalism and a high standard of conduct.

ARRL is an incorporated association without capital stock chartered under the laws of the state of Connecticut, and is an exempt organization under Section 501(c)(3) of the Internal Revenue Code of 1986. Its affairs are governed by a Board of Directors, whose voting members are elected every three years by the general membership. The officers are elected or appointed by the Directors. The League is noncommercial, and no one who could gain financially from the shaping of its affairs is eligible for membership on its Board.

"Of, by, and for the radio amateur," ARRL numbers within its ranks the vast majority of active amateurs in the nation and has a proud history of achievement as the standard-bearer in amateur affairs.

A *bona fide* interest in Amateur Radio is the only essential qualification of membership; an Amateur Radio license is not a prerequisite, although full voting membership is granted only to licensed amateurs in the US.

Membership inquiries and general correspondence should be addressed to the administrative headquarters:

ARRL
225 Main Street
Newington, CT 06111 USA
Telephone: 860-594-0200
FAX: 860-594-0259 (24-hour direct line)

Officers

President: JOEL HARRISON, W5ZN
528 Miller Rd, Judsonia, AR 72081

Chief Executive Officer: DAVID SUMNER, K1ZZ

The purpose of QEX is to:

- 1) provide a medium for the exchange of ideas and information among Amateur Radio experimenters,
- 2) document advanced technical work in the Amateur Radio field, and
- 3) support efforts to advance the state of the Amateur Radio art.

All correspondence concerning QEX should be addressed to the American Radio Relay League, 225 Main Street, Newington, CT 06111 USA. Envelopes containing manuscripts and letters for publication in QEX should be marked Editor, QEX.

Both theoretical and practical technical articles are welcomed. Manuscripts should be submitted in word processor format, if possible. We can redraw any figures as long as their content is clear. Photos should be glossy, color or black-and-white prints of at least the size they are to appear in QEX or high-resolution digital images (300 dots per inch or higher at the printed size). Further information for authors can be found on the Web at www.arrl.org/qex/ or by e-mail to qex@arrl.org.

Any opinions expressed in QEX are those of the authors, not necessarily those of the Editor or the League. While we strive to ensure all material is technically correct, authors are expected to defend their own assertions. Products mentioned are included for your information only; no endorsement is implied. Readers are cautioned to verify the availability of products before sending money to vendors.

Larry Wolfgang, WR1B

lwolfgang@arrl.org

Empirical Outlook

Happy New Year! Isn't this an exciting time? Every January we have the opportunity to wipe the slate clean, and start over with a fresh outlook. As I write this in early December, I am thinking about my personal and professional goals for 2009, and what "resolutions" I might make this year. Of course only a few weeks into the new year many of us will have made our New Year's Resolutions, and already hopelessly broken them. I know that my perennial goals to get more exercise and lose some weight will be some of the most difficult challenges I will face. Every year, though, I seem to think that a fresh start will give me the opportunity to make this year different.

I also have some professional goals that I hope will be reflected in the pages of QEX in the coming months. I recently registered to take the ARRL Continuing Education on-line Antenna Modeling Course, so that I will better understand some of the issues surrounding antenna modeling. Making that public is a bit difficult, because now you know I am taking the course, so you will expect me to complete it. It is a significant time investment, but one I know will be worthwhile.

Throughout 2008, we have watched the QEX circulation numbers climb after several years of holding steady. Can we continue to grow our circulation? I am sure it will be challenging, but we will try. The first challenge will be to produce a magazine that more hams want to read.

The ARRL Headquarters staff works very hard to bring you the technical content that you want, and have come to expect from QEX. We will continue to strive to meet your expectations, but we will need your help to achieve that goal. We need to hear from you to know what kinds of articles you want to read, and of course, we also need you to write those articles! We can't succeed without you.

For the last few months, we have all struggled with the downturn in the world economy. Will people have the money to continue to enjoy their hobbies? From past experience, it seems that during difficult economic times, Amateur Radio can still thrive. I suspect that part of the reason is that people tend to turn to simpler pleasures. Amateur Radio is a pastime that we can enjoy just about anywhere. It can help us learn about new technologies (that may just turn into a new employment opportunity) and can be enjoyed with little expense. Many of us may even turn to building more of our own equipment, both for the simple pleasure of building a gadget with our own hands and then enjoying the thrill of using it on the air. QEX will continue to bring you many new project ideas.

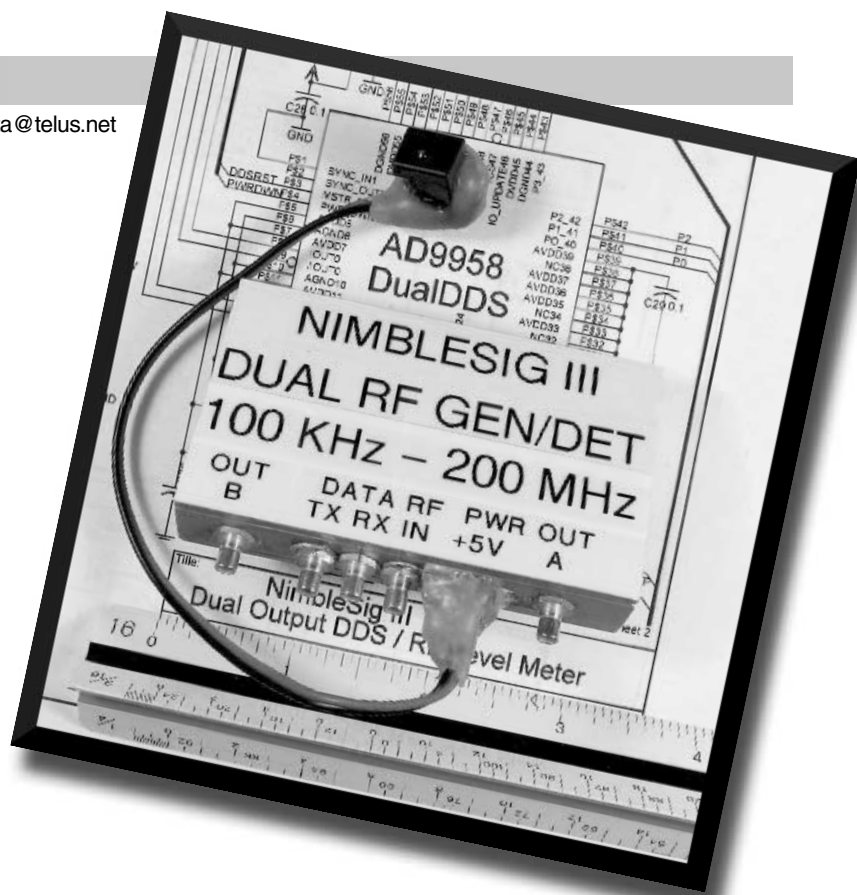
I am very excited about this issue of QEX. We are introducing a series of articles by past QEX Editor Rudy Severns, N6LF, about some antenna experiments he conducted. Rudy plans to describe his experiments in each issue throughout 2009. His experimental setup and test instrumentation are described here, as well as an experiment that verifies an interesting prediction from NEC modeling of vertical antennas with shortened ground radials. This issue also begins a three-part series by Thomas Alldread, VA7TA, about his NimbleSig III DDS RF signal generator, featured on our cover. This versatile project may well find its way into a number of other projects and test equipment. Let us know how you use it.

QEX Proofreader and "Out of the Box" contributing editor Ray Mack, W5IFS, introduces a column about software defined radio. SDR is certainly a hot topic, not only in Amateur Radio but in all kinds of communications fields. Ray will lead us through some hardware and software experiments to help us learn about digital signal processing and other SDR topics. I look forward to reading Ray's future columns, and hope you will, too!

A couple of months ago, reader Gary Johnson, WB9JPS, wrote with an idea for a new section within the pages of QEX. Gary suggested that we include photos of various Amateur Radio and electronic projects that our readers have built or are working on. Gary mentioned that he has seen such photo pages in *Fine Woodworking* magazine, and I immediately thought about the project photos I've seen in a couple of the woodworking magazines to which I subscribe. It's always fun to see what other folks have made, even if there is no way I could ever duplicate their efforts. So, I am offering some QEX page space for you to show off your handiwork. E-mail your photos to qex@arrl.org, or mail a photo CD to QEX at ARRL Headquarters. We can't promise to print every photo we receive, but we will select some of the best offerings for our "Readers' Page." You don't have to send professional quality photos, but they should be sharply focused and carefully lighted. Be conscious of your surroundings, and try to keep background clutter and other distractions to a minimum. Keep in mind that we will be printing your photos in black and white. Photos should show something you have built, and can be an original project design or your interpretation of something presented in QEX, QST or even a kit, if there is something interesting or unique about your construction. Include a sentence or two, up to a short paragraph to describe your project. Show us what you've got!

NimbleSig III —Part 1

*Build this dual output DDS
RF generator and low-level RF
power meter.*



This article describes the design and construction details for a stable, frequency agile, dual output, direct digital synthesizer (DDS) based RF signal generator module with a built in RF level meter. This module is intended to be used as a building block to provide the signal source and RF level measurement functions for many possible applications such as signal generators, swept frequency spectrum displays, receivers, transmitters and RF modems. It could provide both local oscillator signals for a dual conversion receiver or a pair of frequency locked signals for applications that require a quadrature phase offset local oscillator signal pair. The signal outputs can be described as frequency agile as they can be altered very quickly by command without any settling time requirement. The output frequencies can be independently set with 1 Hz resolution anywhere within the 100 kHz to 200 MHz range. The firmware provides an ASCII command line type interface, which enables control directly from a PC equipped with suitable serial port interface. Any conventional terminal program that supports 115,200 Baud (such as *HyperTerminal*) is all that is needed for the PC software to establish keyboard control of the dual DDS and signal level meter. When used as a building block for more complex applications control could be provided by any dedicated host microcontroller that has a UART peripheral capable of 115 Kbaud and that is programmed to send the necessary commands to the NimbleSig module.

During the past decade and a half I have been following the development of DDS technology and have designed and built about a dozen DDS generators. My first DDS generator had a relatively low clock rate of 50 MHz, which limited the maximum output frequency to about 20 MHz. I built it, along with an analog to digital converter (ADC), on a wire-wrapped ISA card that

filled a whole slot in my then state of the art 486 based PC. I controlled the DDS/ADC chips directly from the ISA computer bus with an application I dubbed "PanaBand," which was written in the PASCAL language. Figure 1 is an example of the PanaBand full screen, VGA, color graphics display (considered high resolution in the early 1990s) that shows the IF output frequency spectrum from my HF transceiver. In addition to the frequency spectrum display PanaBand also provided GUI style mouse and point and click control of my transceiver via the serial port interface. The ability to view the frequency and strength of all the signals on the selected HF band with digital display accuracy and to also be able to tune to any one of them with just a "click of the mouse" seemed pretty wonderful in the early 1990s. Although my old PanaBand project will not be described here it is an example of what can be done with DDS technology when placed under computer control. The seemingly open-ended realm of possible applications associated with computer controlled DDS signal sources hooked me on further experimentation with this technology.

My first version of this series of DDS signal source designs only provided a single output up to 160 MHz. It also provided AM/FM modes and had a built in RF level meter. It used a 32 bit, 50 MHz ARM microcontroller with 64 KB of program memory space. To my very pleasant surprise, that

project won second place in the Luminary Micro Inc sponsored "Design Stellaris 2006" international design competition, which was hosted by Circuit Cellar Magazine.¹

NimbleSig III (NS3), described here, is my most recent DDS module design. It is relatively enhanced in that it provides two independent RF signal outputs with 1 Hz frequency step resolution up to 200 MHz. Either generator output can be AM/FM modulated at specified modulation indexes at rates from 1 Hz to 20 kHz. Alternately each RF generator can be simultaneously set to the same frequency to provide a pair of signals with accurate relative phase offsets. These offsets can be changed in very fine steps across the full 360° range. The built in RF power meter can measure levels with typical 1 dB accuracy from -50 to +10 dBm from just above the audio spectrum to about 500 MHz.

NS3 uses a relatively recent DDS chip from Analog Devices Incorporated (ADI), which is clocked at 500 MHz. The 50 MHz, ARM7 NXP (formally Philips) controller used here has 512 KB of program memory space. This large instruction code space provides room for many enhancements to the firmware as only about 20% of the program memory space is currently used. Also new in this version is a 64 KB EEPROM, which is provided for non-volatile (NV) storage of internal initialization and calibration data. A

¹Notes appear on page 20.

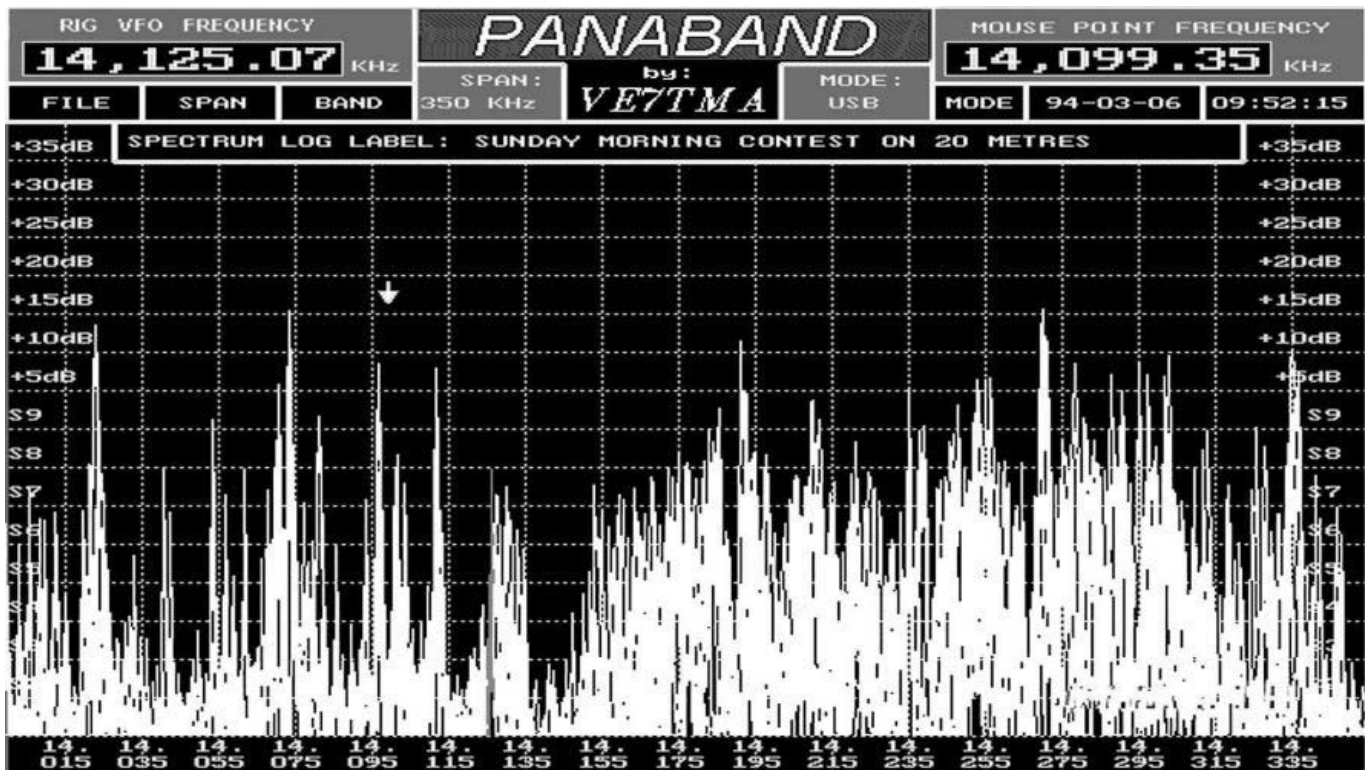


Figure 1 — A Kenwood TS-850S transceiver IF spectrum display, based on early 1990s DDS technology.

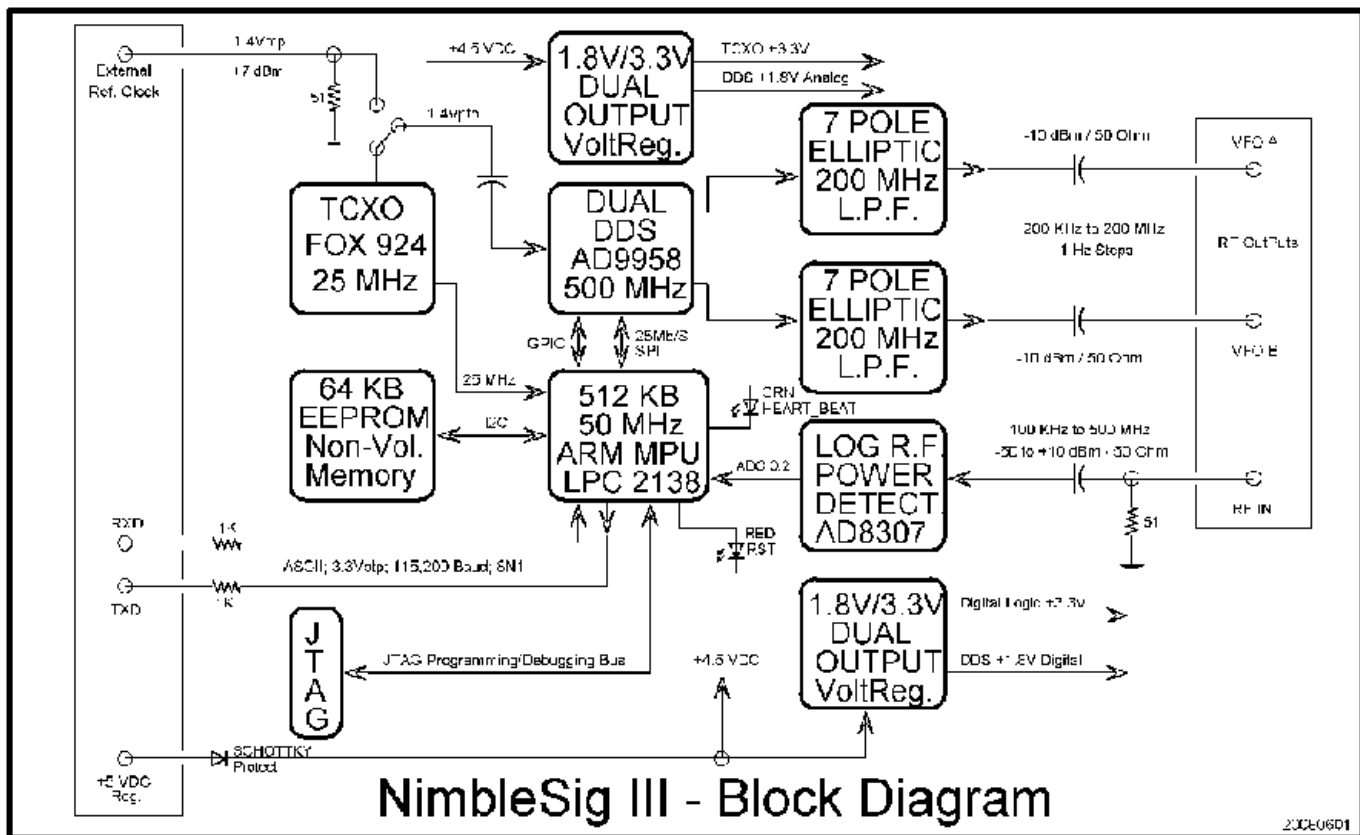


Figure 2 — The NimbleSig III block diagram illustrates the main sections of the circuit.

16 KB block of this NV memory space is allocated for storing external host controller application data such as initialization values and frequency channel information.

As shown in the lead photo, modern surface mount technology makes it possible to fit all the functionality and power of NimbleSig III into a very small ($2 \times 3 \times 0.5$ inch) package.

Hardware

Block and Level Diagram

As shown in the Figure 2 block diagram, the reference clock for the MPU is provided by the internal 25 MHz, FOX 924, temperature-controlled crystal oscillator (TCXO) IC, which by optional default also provides the reference clock for the DDS. Both the DDS and MPU have internal phase lock loops that are programmed to multiply the clock reference input to the actual internal clock frequency, which, as mentioned in the introduction, is 50 MHz for the MPU and 500 MHz for the DDS.

At room temperature the TCXO provides good enough frequency stability for many DDS applications. Using my relatively stable oven-controlled crystal oscillator (OCXO) referenced frequency counter, I have observed a day-to-day variation of less than 10 Hz when operating continuously at 100 MHz within a room-temperature controlled environment.

Although the TCXO provides quite a respectable degree of stability it may not be sufficiently stable for applications that are critically frequency dependent or where the DDS cannot be left powered up for a long enough lead time to stabilize. Also, the DDS internal PLL, which in the case of the TCXO operation is set to multiply the reference clock frequency by 20, has the disadvantage of significantly increasing the phase noise. The DDS data sheet indicates a phase noise improvement of about 20 dB can be obtained by driving the clock input directly with a 500 MHz, low phase noise reference signal. Although I believe the TCXO/PLL combination is more than adequate for most applications much better phase noise performance should be possible if an external, low sideband noise, high overtone crystal oscillator (such as the Butler type) is used to drive a suitable multiplier to obtain a relatively quiet 500 MHz, 1 mW clock source.

As shown in the upper left of Figure 2, an external clock signal may be optionally injected for the DDS frequency reference. The maximum drive amplitude is 1.4 V p-p into a 50 Ω load, which, considering a sine wave source, works out to about 5 mW or +7 dBm. The DDS specification states the injection level should be in the range of -5

to +3 dBm (2 mW). The external input is directly terminated in 50 Ω and the clock is subsequently capacitive coupled to the DDS input, which floats on an internally generated dc bias.

The ADI AD9958 IC has a pair of internal DDS engines, which use the clock signal as a reference to generate sine wave output signals on frequencies specified by data stored in the associated internal registers. The AD9958 is described in detail within the manufacturer's data sheet.² A great deal of information on the theory of DDS signal generation, including an Amateur Radio related project (AN-557) can be found within Analog Devices' library of DDS application notes.³

The DDS receives data and control signals from the MPU. The register data for setting the operating mode, frequency, phase and amplitude is sent serially via a high speed, 25 Mb/S, serial peripheral interface (SPI) bus. There are 3 control registers containing, in total, 6 bytes of data common to both DDS engines. In addition data is stored for each individual engine by 21 dedicated registers containing 82 bytes of channel specific information that includes frequency, amplitude and relative phase offset values. The SPI bus consists of four lines, namely "master input/slave output" (MISO) data, "master output/slave input" (MOSI) data, "serial clock" (SCLK) and "slave select" (SS). The MPU acts as the master and the DDS the slave. Details of the general operation of the SPI bus can be found on the Internet (see Note 4) and more specific information on the SPI format used for this application can be found within the DDS data sheet (see Note 2) and the MPU users manual.^{4,5}

There are nine additional control lines connecting the DDS and MPU that have various functions including chip select, DDS reset, DDS power control, register data update strobe and modulation step selection.

The two RF outputs from the DDS, which contain both the desired output signals and the undesired images, are fed into seven pole, elliptic design type, low pass filters that strip off the images and any other out of band signals. These image regions, which extend from 300 MHz to 750 MHz and beyond, are attenuated by a minimum of 50 dB by the filters.

The RF output levels are set to -10 dBm with frequency dependent amplitude calibration data that is stored within the EEPROM by the calibration subroutines. This data is sent to the DDS by the MPU each time a new frequency command is implemented. The output levels may be reduced by command in 0.1 dB steps to -20 dBm. It is also possible to bypass the calibration and operate at unlevelled, full output, which is about -4 dBm mid spectrum.

The RF level detector is designed around the popular, broadband AD8307 logarithmic response power detector IC from ADI. It has a bandwidth specification of dc to 500 MHz. The variable dc output from the detector is connected to one of the 10 bit analog-to-digital converter inputs of the MPU.

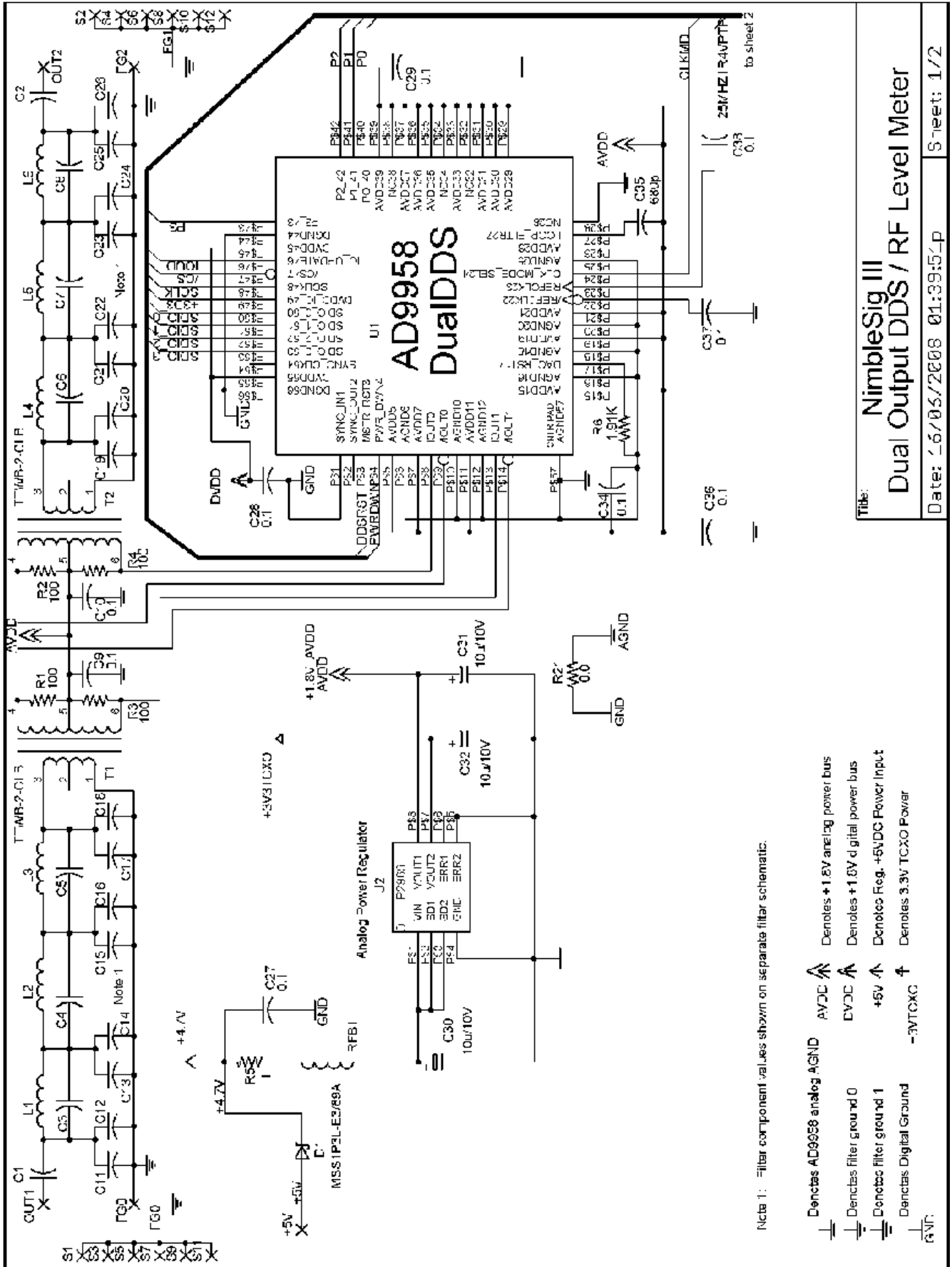
The RF detector IC has a significant response roll off between HF and UHF. Calibration data to compensate for this frequency roll off along with correction data for the device dependent logarithmic response variations is stored within the EEPROM during calibration. If the approximate frequency (specified in units of MHz) is supplied with the power measurement command, the level reading is adjusted for the frequency specified. Also during calibration, data from a curve fitting algorithm that matches the dynamic range response of the specific logarithmic detector IC is also saved in EEPROM.

As shown in the block diagram the EEPROM data is conveyed to and from the MPU via an Inter-Integrated Circuit (I²C – for "I squared C") bus. Details on the general operation of the I²C bus can also be found on the Internet.⁶ More specific information on the protocol for this application can be found in Microchip's 24LC512 EEPROM data sheet.⁷

A UART peripheral within the MPU provides the 115,200 Baud, ASCII serial data communications link to the outside world. The data on the receive data (RXD) and transmit data (TXD) lines is in the positive 3.3 V, unipolar format typically found on 3.3 V microcontroller I/O pins. This simple logic level interface was selected as it offers both direct compatibility to a host controller microprocessor as well as indirect compatibility to either USB or legacy RS-232 serial port PC interfaces. Although this interface requires either an RS-232C level conversion or USB protocol conversion device to interface to a standard personal computer it was chosen as it provides the most universal fit for all perceived applications. The RXD and TXD MPU pins are protected from induced transients or other abnormal line conditions with 1K resistors.

Two LEDs are provided to indicate status of the MPU. A red LED, designated RST, illuminates when the MPU reset line is pulled low to force the MPU to the reset state. A green LED, designated HEART, flashes at 72 PPM to indicate the firmware is executing. These indicators are not important to the normal operation of the module but can save a lot of time during programming, troubleshooting and debugging by indicating rather vague operational status "at a glance".

Six additional I/O lines make up the "Joint Test Action Group" (JTAG) bus,



Title: **NimbleSig III
Dual Output DDS / RF Level Meter**

Date: 1/6/05/2008 01:39:51p

Sheet: 1/2

Note 1: Filter component values shown on separate filter schematic.

- Denotes AD9958 analog AGND
- Denotes +1.8V analog power bus
- Denotes +1.8V digital power bus
- Denotes Filter ground 0
- Denotes Filter ground 1
- Denotes Reg. +5VDC Power Input
- Denotes Digital Ground
- Denotes 3.3V TCXC Power

Figure 3 — Section 1 of the NimbleSig III schematic diagram.

which is used for programming and debugging the software. These lines terminate on a SIP connector that provides connection to the software development system for programming and debugging.

The LPC2138 MPU used here is a variant of ARM Incorporated's ARM7 family manufactured by NXP (previously Philips) Semiconductors. The ARM 7 family of 32 bit MPUs are relatively powerful processors in comparison to the 8 bit microcontrollers more commonly seen in amateur radio projects. The ARM 7 is clocked roughly 10 times faster, processes 4 bytes at a time and in this case has more than 10 times the program memory space normally found in 8 bit MPU chips. One of the primary reasons for the use of an ARM processor is that it is well supported by software development tools that provide 64-bit arithmetic to calculate the DDS 32-bit frequency tuning words on the fly, which for this application, eliminates rounding error.

The extra MPU power and memory space also provides the foundation for a plain text, command line style, man/machine interface. There is an abundance of storage room for help pages, register dump tables and calibration routines. The firmware has commands that provide the user full access to read or write to any of the DDS registers. The user is also given the power to change the DDS initialization values without the need to reprogram the MPU (The user may revert back to the original default parameters for recovery if needed).

A very important consideration for the use of the LPC2138 MPU is that there are good quality and affordable integrated development environment (IDE) software tools available to write and maintain the software for this family of ARM processors. Rowley Associates' *Crossworks for ARM*, which uses the well proven GNU GCC C compiler, was used to develop the NS3 firmware. Rowley Associates offer a non-commercial, hobbyist/student level license for this fully functional (not crippled or limited), professional quality, well supported IDE package at a much reduced price that is within reach of most serious radio amateur equipment builders.⁸

Considering all the advantages of the ARM processor the additional cost of just a few dollars over a more common 8 bit processor chip seems, in the author's opinion, well justified.

The two, dual output voltage power regulators shown in Figure 2 play a very important role in this design. Experience has proven that noise on the power rails is a major problem for DDS generators. If digital noise gets superimposed on the analog voltage bus to the DDS, noise sidebands of sig-

nificant level can appear across the spectrum. Also any noise on the TCXO power causes FM sidebands to appear. The most effective means for obtaining clean power for a DDS generator is by isolating the analog/digital buses from each other with dedicated voltage regulators. Fortunately, semiconductor manufacturers have introduced low cost, dual output voltage regulators in small packages that serve this need nicely. Separate voltage supply rails with dedicated regulators are provided here for the 3.3 V digital devices, 3.3 V TCXO supply, 1.8 V DDS digital supply and 1.8 V DDS analog supply. Power for the regulators is supplied from an external, regulated +5 V dc supply. The +5 V source passes through a low forward voltage drop, reverse polarity protection diode prior to distribution to the regulator inputs.

Circuit Description

The first schematic sheet shown in Figure 3 shows the details of the AD9958 DDS and analog power regulator circuitry.

The various ground and power bus designators are shown at the lower left of the page. As shown there are four separate ground planes, namely, analog ground, digital ground, filter 0 ground and filter 1 ground. These ground planes are isolated from each other by PC board design. This design approach helps prevent the coupling of digital noise into the analog circuitry and crosstalk between the generator outputs that could otherwise be caused by noise voltage gradients on a relatively simplistic, single ground plane.

The +5 V dc power input (center – left) is first routed through a Schottky diode that provides reverse polarity protection with only about a 0.4 V forward voltage drop. The diode output of 4.7 V supplies the RF Detector and the regulator inputs. The LP2966 dual output voltage regulators are of the ultra low voltage drop-out type. With the provided 1.3 V headroom, these devices have sufficient control margin to provide well regulated 3.3 V outputs.

The 4.7 V power bus is bypassed with a 0.1 μ F bypass capacitor (C27) to guard against possible RF noise superimposed on the 5 V power source. The power passes through a 1 Ω resistor (R5) that provides a small amount of low frequency isolation between the analog and digital grounds. This resistor also provides a convenient point to check the analog regulator input current. The load side of R5 feeds an RF bead that provides an impedance to RF current flow between the analog and digital grounds. C30, a tantalum input filter capacitor, provides a low impedance bypass of the analog regulator IC input to analog ground. As shown, the 1.8 V and 3.3 V regulator outputs are

bypassed by two additional tantalum electrolytic capacitors (C31, C32). As the 3.3 V output only powers the TCXO, it operates with a light load of approximately 5 mA. In contrast the 1.8 V output feeds the DDS analog bus, which is a relatively heavy load of around 100 mA.

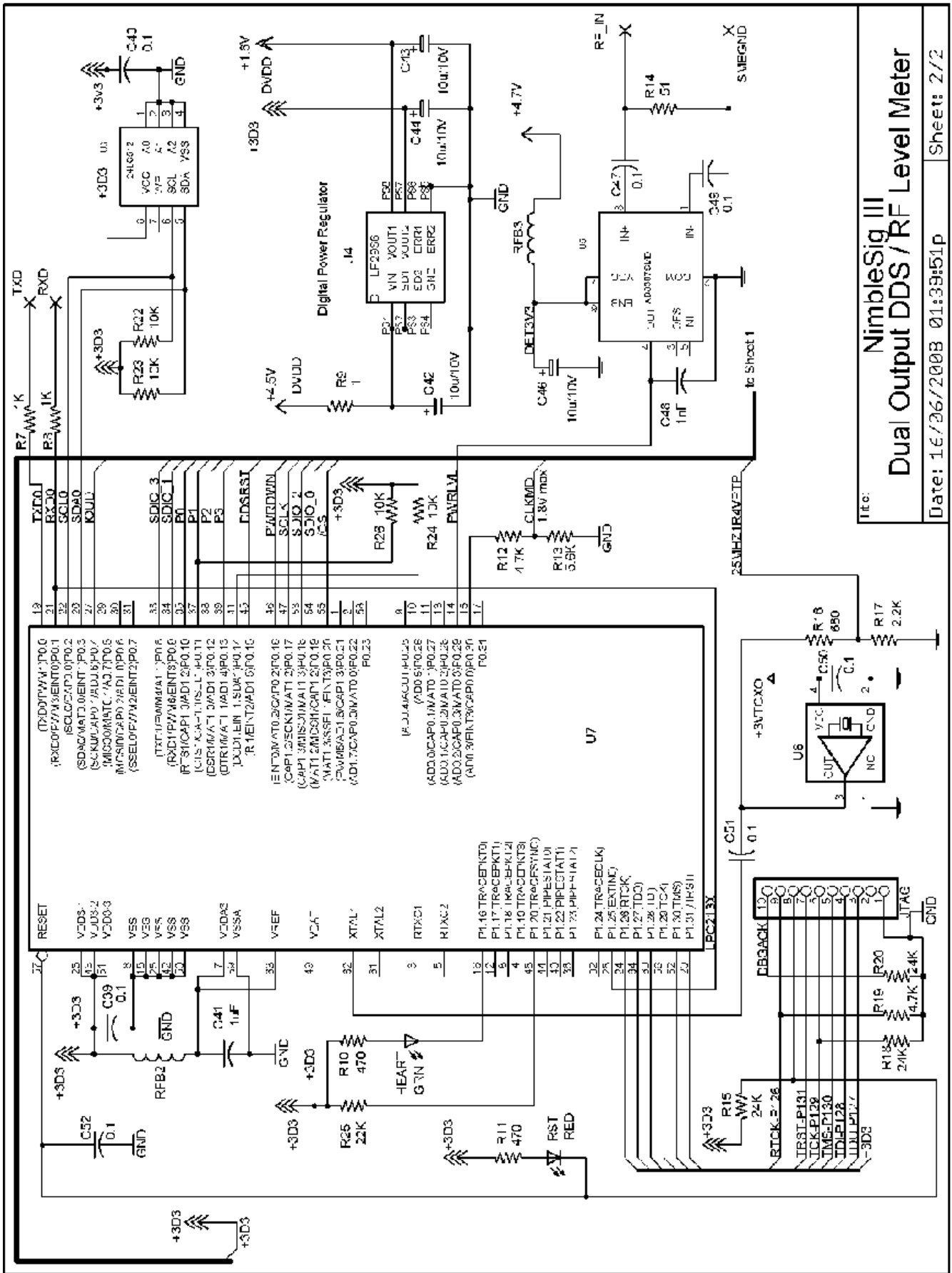
The functions of the common components connected to the AD9958 DDS are described in Table 3, "Pin configuration and Function Descriptions" within the device datasheet given at the reference of Note 2. The 16 connections between the DDS and the MPU are shown entering a bus that reappears on sheet 2. Balanced lines on the PC board connect the push-pull RF outputs from the DDS to the associated transformer-coupled low pass filters. These balanced lines help prevent crosstalk between generator outputs. The transformer coupling isolates the filter grounds and provides efficient push-pull coupling of RF from the DDS outputs to the filter inputs. Power for the DDS DAC outputs is injected into the primary center taps of the transformers. Resistors R1, R2, R3 and R4 moderate the out of band impedance extremes presented to the DDS outputs, which if not moderated would cause excessive intermodulation distortion from image products. Capacitors C9 and C10 are RF bypasses for the center tap power injection points. A detailed description of the low pass filter design is given below.

Figure 4 is the schematic for the MPU, TCXO, EEPROM, digital power regulator and RF detector circuitry. The 3.3 V and 1.8 V digital power is supplied from the dual digital power regulator U4. R9 provides a small amount of power decoupling from the 4.7 V bus and also provides a convenient test point for measurement of the input current to the regulator. Tantalum electrolytic capacitors C42, C43 and C44 ensure regulator stability. The 1.8 V output load is 60 to 80 mA. The 3.3 V output load that supplies the MPU, EEPROM and RF level detector is estimated to be less than 50 mA.

As shown in the upper left of the diagram 3.3 V digital power is injected into pins 23, 43, 49 and 51 of the MPU. RFB2 and C41 provide decoupled injection of this power to the analog ADC reference voltage pin 7.

R10 and R11 are current limiting resistors for the indicator LEDs. R15, 18, 19, 22, 23, 24, 26, 25 and R18, 19, 20 are logic pull-up and pull-down resistors respectively.

C51 couples the 3.3 V p-p, 25 MHz square wave reference clock from the TCXO output to the XTAL1 clock injection pin of the MPU. R16 and 17 form a voltage divider to drop the amplitude to 1.4 V p-p for injection into the DDS. Note that if the external reference clock option is desired, R16 is omitted and R17 is changed to 51 Ω for



Title: **NimbleSig III
Dual Output DDS/RF Level Meter**

Date: 1E/26/2008 01:39:51p

Sheet: 2/2

Figure 4 — Section 2 of the NimbleSig III schematic diagram.

terminating the external clock signal source. The external signal connection point is the high end of R17.

R12 and R13 form a voltage divider to drop the 3.3 V logic level output from the MPU GPIO P30.0 pin to match the 1.8 V logic level of the DDS clock mode select input.

The TXD and RXD pads provide connection points for the ASCII data communications connection to the host computer. R7 and R8 protect the MPU RXD, TXD internal interface circuitry from direct exposure to outside connection, extraneous voltages and/or shorts to ground.

The power to the 64KByte EEPROM, U3 is bypassed by C40. The power to the RF level detector U5 is decoupled by ferrite bead RFB3 and bypassed with tantalum capacitor C46. C48 bypasses the RF from the detector output, yet provides a fast enough response time to measure audio modulation envelope peaks. C47 and C49 couple the input RF to the detector from the 51 Ω input termination R14.

The JTAG programming/debugging interface connector consists of a 10 pin, 0.010 inch pitch, machined quality, gold-plated SIP socket connector strip. This was selected as a commonly available, space efficient, low profile alternative to the usual 20 pin header used for ARM JTAG interfacing for which there was insufficient mounting space. A simple adapter board has been designed to convert to the 20 pin standard. The operation of the JTAG interface is complex and black magic to the author. There is much JTAG information available on the web but as I have found the JTAG operation to be transparent I decided there would be little practical benefit for me to learn the details of the operation of this complex interface. I can say it works wonderfully well!

Elliptic Low Pass Filters

Figures 5 and 6 show the schematic and simulated response of the 200 MHz LPF. The parallel resonant circuit traps comprised of L1/C3 [L6/C8], L2/C4 [L5/C7] and L3/C5 [L4/C6] provide rejection nulls in the stop band at 300, 250 and 500 MHz respectively. The 250 MHz notch was chosen to establish the corner of the stop band at the half clock frequency. The 300 MHz null provides the needed attenuation for the “500 MHz clock minus output frequency” lower sideband image that is present when the DDS is used to generate frequencies close to 200 MHz. Image signals would otherwise appear as spurious outputs. As described within ADI’s application note AN-939, the level of the image sidebands will taper off towards the 500 MHz clock frequency.⁹ The combination of the Nyquist level tapering effect and rejection

of the filters for all intents and purposes eliminate the image signals.

The Elliptic LPF design, which is based on ADI’s application note AN-837, was designed using two freeware software packages.¹⁰ Tonne Software’s *SVC Filter Designer* was used to do the preliminary design and Linear Technology’s *LTCSpice* program was used to analyze the design.^{11, 12} This design uses parallel pairs of capacitors for the shunt capacitance elements to help ensure a low RF impedance connection to the associated LPF ground plane at UHF. All the frequency determining components are SMD package-size category 0402. With measurements of only 0.4 mm × 0.2 mm, these components are indeed quite small!

The roll off of the filter frequency response in conjunction with the roll off of output level from the DAC at the upper end of the first Nyquist zone limits the leveled -10 dBm output amplitude maximum frequency to approximately 195 MHz. (See Note 9.) At

200 MHz the maximum output level drops to about -12 dBm. Possibly the 200 MHz filter loss could be reduced slightly with higher Q inductors and/or shifting the LPF cutoff frequency slightly higher. At the time of this writing, I plan to re-design the LPF corner frequency to around 230 MHz with the first notch at 300 MHz instead of 250 MHz. The need for establishing deep attenuation at 250 MHz is questionable considering the lowest-frequency, full-level image product would be at 300 MHz. This re-design may slightly reduce the attenuation in the 195-200 MHz region. If I find the modification provides a worthwhile performance improvement I will post the design details on my Web page.¹³

Assembly Description

Figure 7 is a close up view of the component side of the fully populated PCB mounted into the chassis. The largest chip,

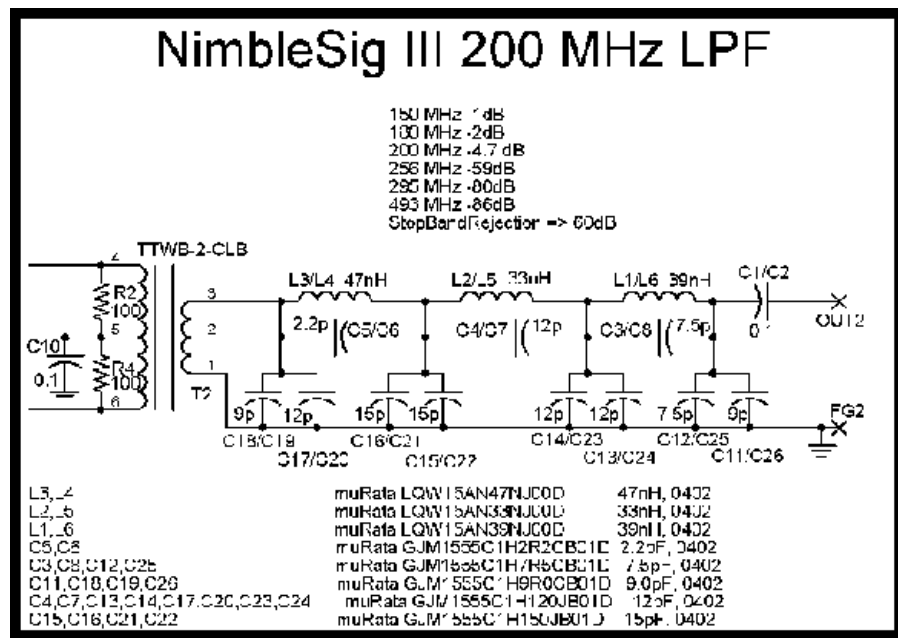


Figure 5 — Elliptic low pass filter schematic with parts list.

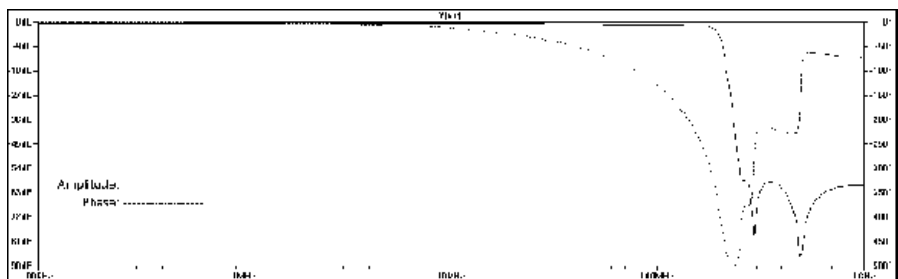


Figure 6 — Simulated LPF frequency response.

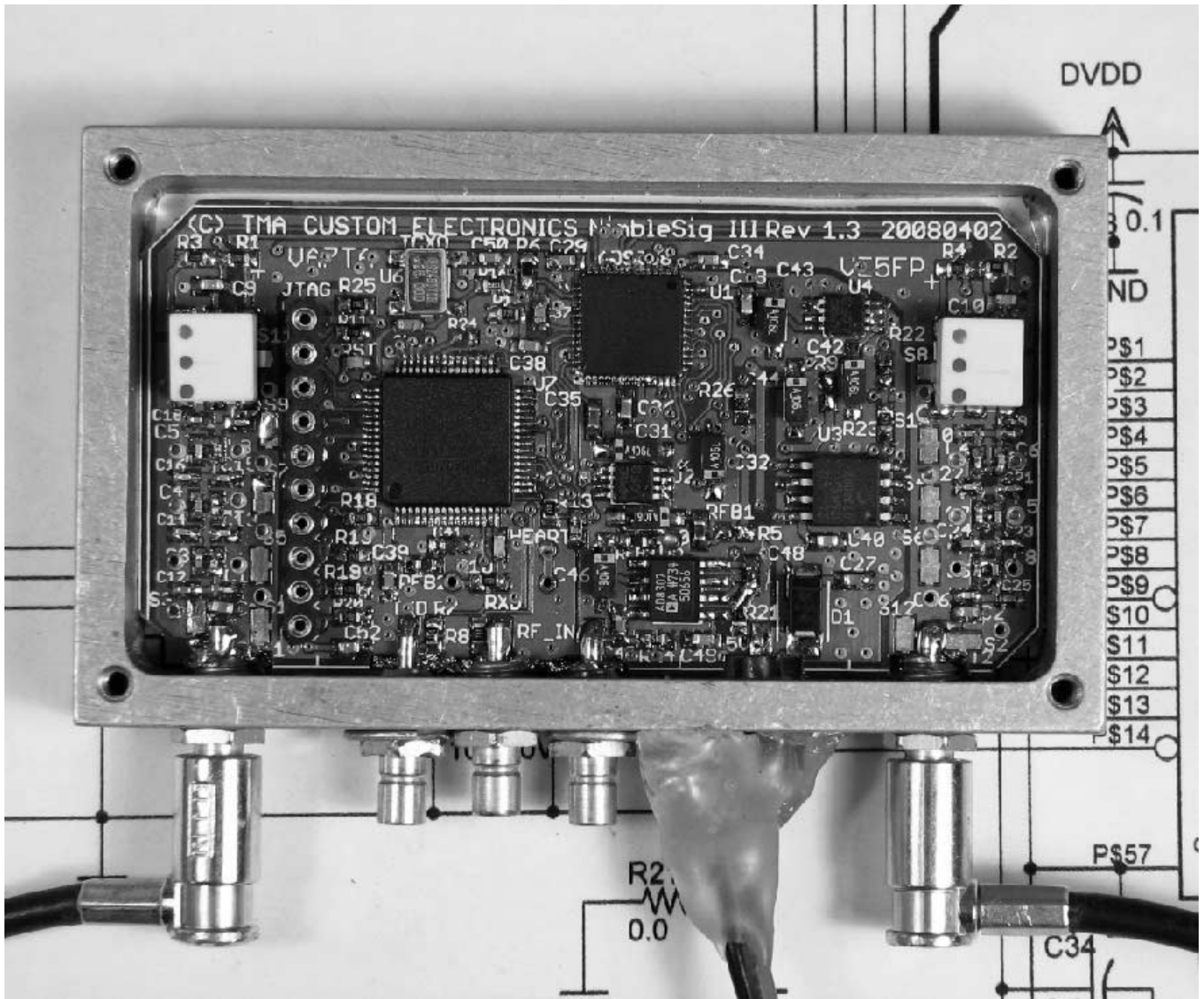


Figure 7 — This photo shows the component side of the populated NimbleSig III circuit board.

mounted left of center, is the LPC2138 MPU. The next largest chip in the upper center is the AD9958 DDS. The small chip in the metal case located above the MPU is the TCXO. The AD8307 RF power detector is mounted right of center at the bottom close to the RF input connector. To the right of the detector is the input protection diode, D1. The 24LV512 EEPROM is the chip above D1. The two remaining small ICs are the LP2966 dual output voltage regulators. The red LED reset indicator is above the top left corner of the MPU and the green LED heart beat indicator is below the opposite corner.

The JTAG connector is to the left of the MPU. Although the silkscreen labeling seems to indicate otherwise please note that pin 1 is actually at the top of the connector just below the “JTAG” silkscreen label. The PCB silkscreen labeling on this first manu-

facturing run of PC boards is disrupted by the vias, which are not covered by silkscreen. The vias were intentionally left uncovered to provide connection points for testing the prototype. The labeling should be easier to read in the future, if I have another batch of boards made with the vias covered with the silkscreen.

The frequency determining components for the two low pass filters are located along the opposite ends of the PCB between the RF transformers (white blocks) and the output connectors (shown with RF cables attached). The three, tightly spaced, central SMB connectors, left-to-right, provide the TXD, RXD and RF IN (level meter input) external connections. The power input is bypassed and anchored to a ground lug under the RF input connector. The power passes through the chassis via an RF bead that serves as a

feed through insulator and provides some RF isolation. A boot formed from hot glue provides insulation for the power connections and strain relief for the cable. Although the glue is rather messy, it has proven effective for protecting these connections and the power cable.

With the exception of the JTAG connector all components are of the surface mount type. As mentioned above 0402 size components are used for the filters. With a few exceptions the rest of the ceramic capacitors and resistors are the larger 0603 size.

The components shown were hand soldered under an 8X power binocular microscope using a fine tip, 290°C, temperature-controlled pencil soldering iron with 0.015 inch (28 AWG) Kester 63/37 RA core solder. Any excess solder was sopped up with the 0.025 inch desoldering braid. For the first

step before installing any components I used a flux pen manufactured by Kester to coat all the PCB connections with flux. I also used the flux pen to coat the contacts on the pinless DDS chip, which made soldering this package much easier.

I wish to mention that until I was introduced to surface mount construction techniques about 5 years ago I avoided projects based on surface mount devices. Now having experience with surface mount design and construction I avoid the use of leaded, through hole components where possible. The ability to construct with surface mount devices has opened up many project horizons for me. I would also like to mention, how-

ever, that this project would be a poor choice for one's first attempt at surface mount construction. Some of the components used here are very small and others have fine pin spacing. This project is intended for those with a reasonably good collection of surface mount construction tools and the acquired skill set to use them proficiently.

My preferred sequence for manually soldering components to a board is to build and test the regulated power supplies first. I then install the the passive components whilst routinely checking with my trusty, continuity buzzer equipped Ohmmeter for power bus shorts as I go along. Finally I mount the signal ICs leaving the relatively precious DDS

chip for the last. I check for any grounded power supply buses after installing each IC. Using this method one can usually find the cause of an accidental power bus short fairly quickly. Since typical power buses have wide distribution trouble shooting a shorted bus after all the components are installed can be very difficult due to the maze of shorted connection point possibilities. I also usually take the time to check for adjacent pin shorts with my Ohmmeter before applying power. The use of a low test voltage Ohmmeter with a continuity buzzer that provides the ability to test for adjacent pin shorts without taking your eyes away from the finely spaced leads is a big asset for this job. To avoid false posi-

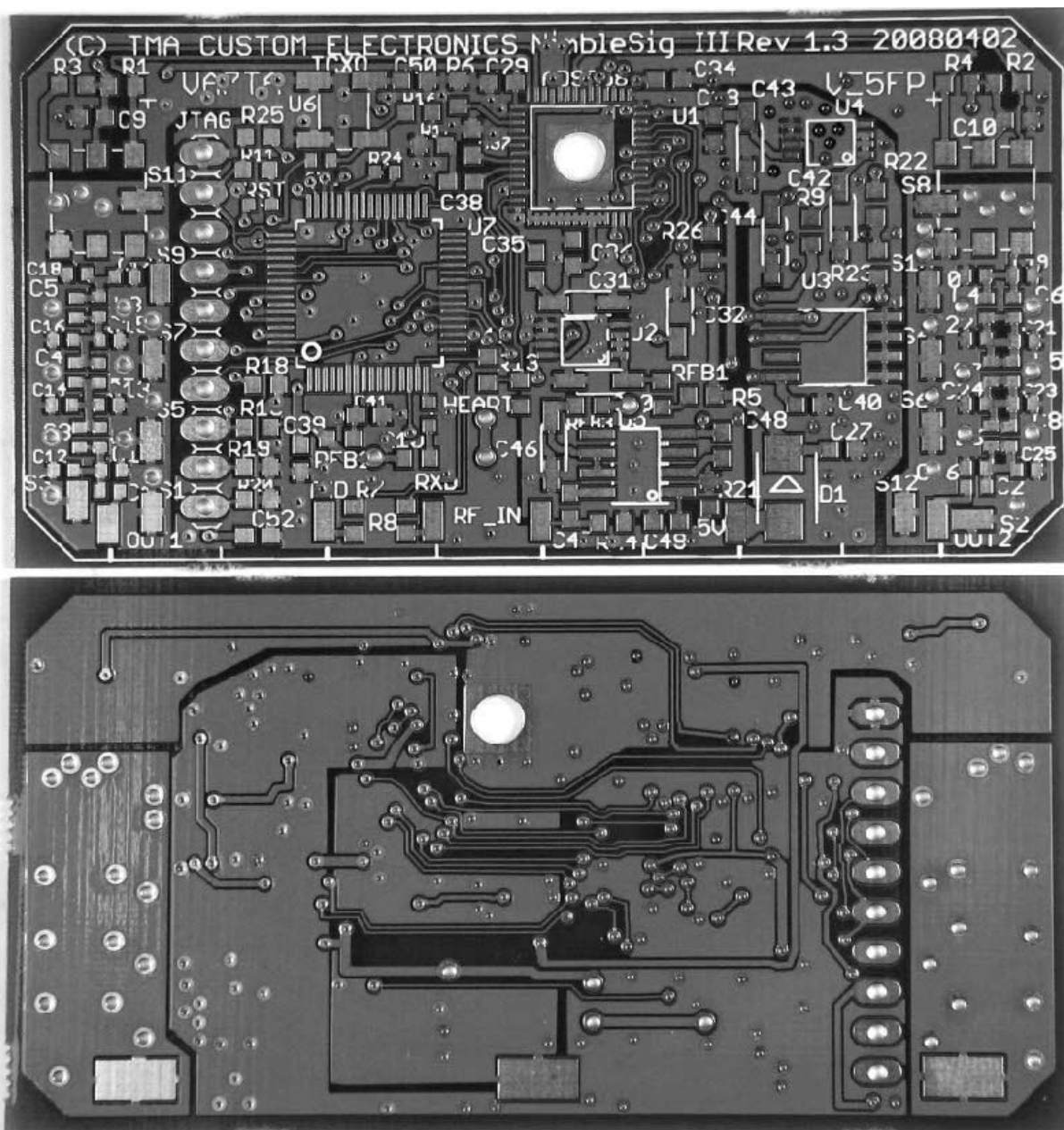


Figure 8 — The component side of the circuit board is shown in Part A. Part B shows the bottom of the circuit board.

tives from device internal protection diodes, it is important that the test voltage, imposed by the continuity meter probes, is well below 0.5 V. Fortunately the continuity buzzer feature provided in most modern day digital multimeters meet this requirement.

The PCB is a relatively simple double-sided board compared to the relatively expensive four-layer board type usually specified for DDS applications. The four-layer boards more readily provide low RF impedance ground planes. The two-layer board used here provides the requisite low impedance analog ground via a large ground post, which connects the analog ground pad of the DDS chip direct to the chassis. Additionally, there are four isolated ground planes provided by the artwork design, which are bonded at the chassis connector apron. This design significantly reduces the coupling of noise and crosstalk between circuit sections.

Figure 8A shows the component side of the PCB artwork. The large, 0.125 inch diameter plated through hole in the center of the DDS footprint provides access from

underneath for soldering the analog ground center pad of the DDS chip. This facilitates the installation of the DDS chip using a conventional soldering iron. The author has had a 100% success rate using an inexpensive soldering iron with a blunt, 0.100 inch diameter tip that has been filed flat. The soldering iron is adjusted to 280°C with a Variac transformer. A small coil of solder is inserted in the hole and the soldering iron tip inserted into the hole, branding iron style, for 5 seconds or less. This does a good job of soldering the DDS pad to analog ground and also provides a good contact area for the analog ground post.

The balanced lines that couple the push pull outputs from the DDS to the respective low pass filter input transformers can be seen along the top edge of the PCB. As mentioned above, the maximum separation of the filters along with the balanced lines helps provide good isolation between the generator outputs. The exposure to the coupling of stray RF noise into the RF level meter input from the rest of the circuitry is minimized by the

placement of the “RF_IN” pad right beside the detector chip input pin.

Figure 8B shows the bottom side of the PCB artwork, which shows the four distinct ground planes. The analog ground post connection to the ground pad of the DDS is the large plated through hole under the DDS chip. Analog ground wings extend under the balanced lines to the underside of the LPF transformer primary connections. The analog ground also extends below the DDS under the analog power regulator to the large analog ground pad near the center bottom of the photo. The two filter grounds extend from underneath the connections to the transformer secondaries to the corresponding filter ground pads near the bottom corners of the board. The digital ground extends from the left side of the DDS down to the very bottom and across to the RF detector, EEPROM, digital voltage regulator and JTAG connector areas. The digital and analog grounds are connected together with a zero Ohm resistor located near the RF detector. The ground pads are ultimately bonded by soldering to

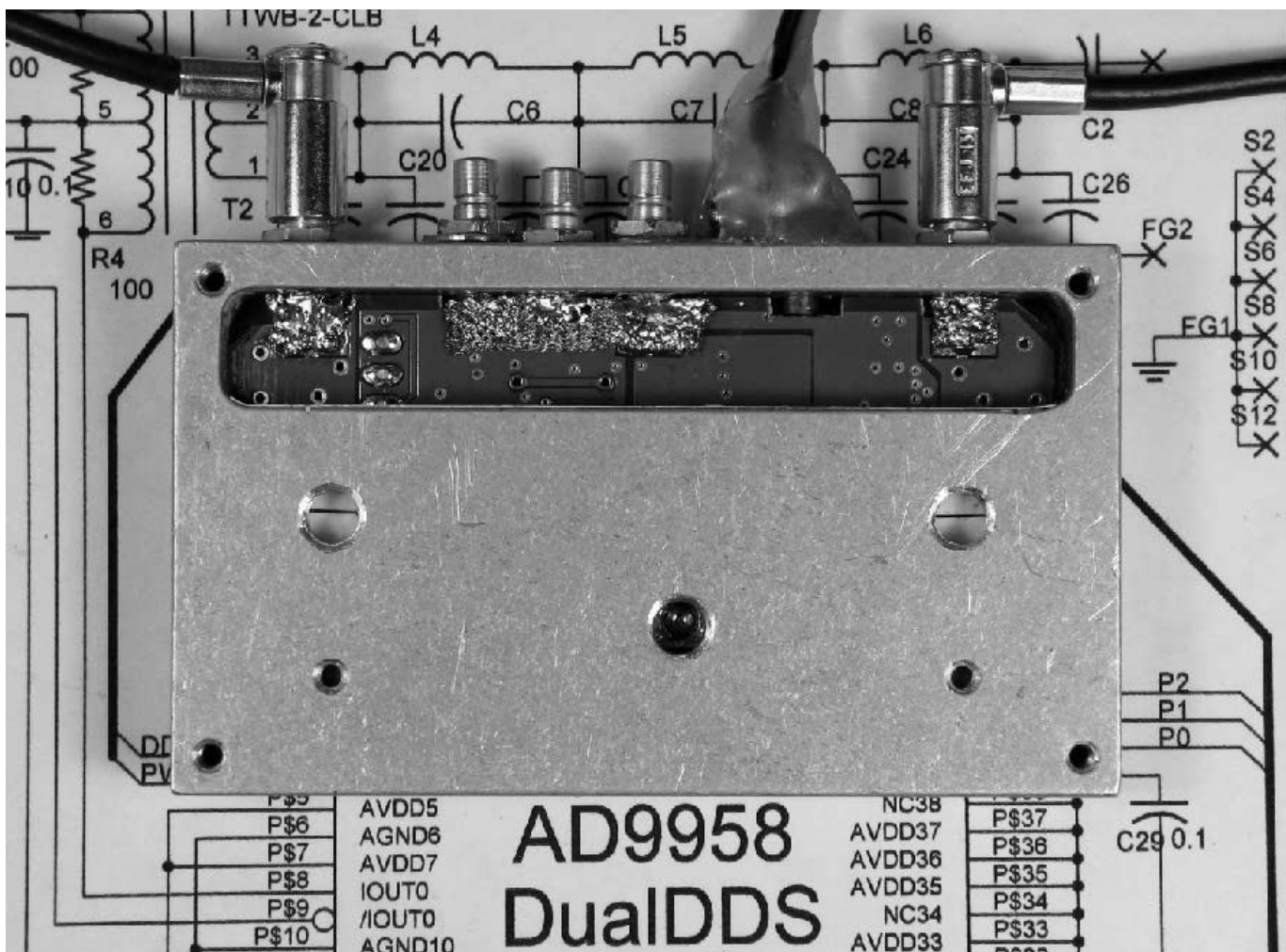


Figure 9 — Grounding braid bonds the circuit board grounds to the coaxial SMB connectors.

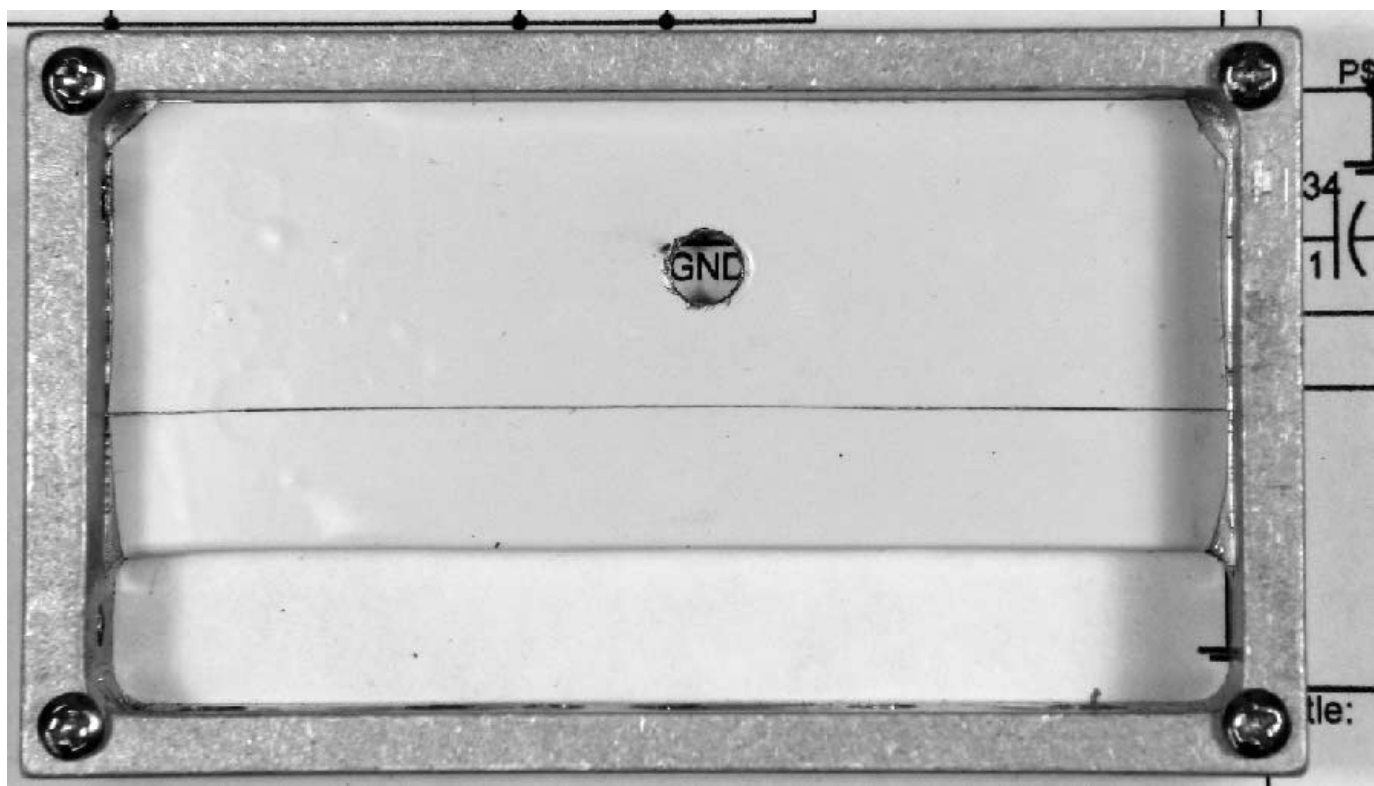
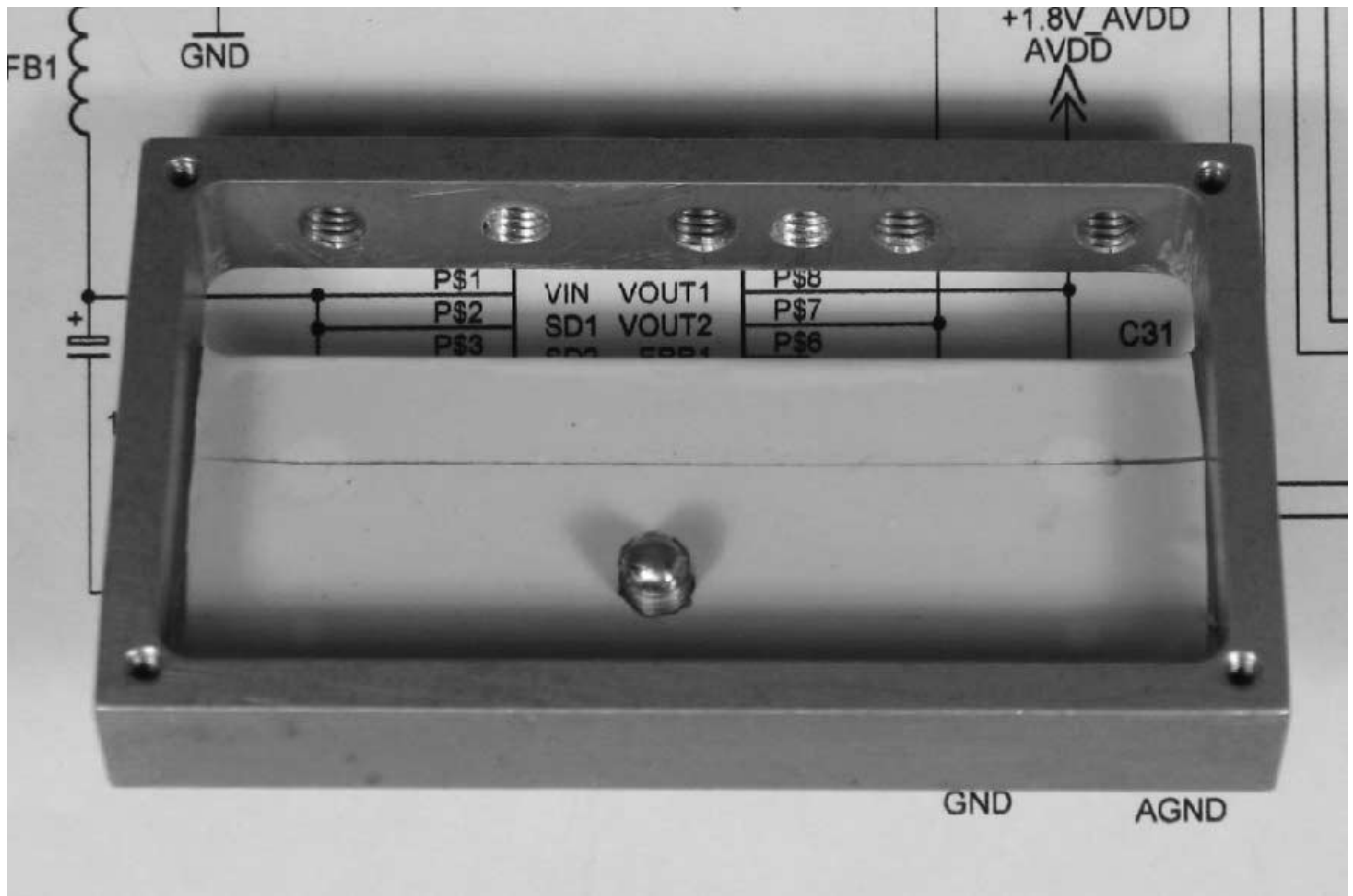


Figure 10 — Part A shows the analog ground post. Part B shows the tapped hole for the analog ground post.

the outer conductor threads of the coaxial connectors.

The board is mounted to the chassis by soldering the component side pads to the respective connector center pins and by bonding the ground pads on the bottom side of the board with braid to the connector threads as shown in Figure 9. A large soldering iron with lots of thermal mass is needed for soldering to the threads. Do not use a soldering gun for this job as the magnetic field from the tip may induce destructive currents into the semiconductor circuitry. The back of the board rests on the analog ground post shown in Figure 10. The tip of the brass screw is covered with a blob of solder to provide a soft contact surface with good galvanic compatibility. The chassis cover shown in Figure 11 has a bumper made up from commonly available, self-adhesive rubber feet. This somewhat resilient bumper presses against the top of the DDS chip holding it firmly against the ground post.

The reason for providing the ground post is to lower the RF impedance of the analog ground by providing a low Z path via the relatively large chassis surface area to the bonding point for the multiple grounds at the RF connectors. The PCB analog ground plane copper area would by itself provide sufficient heat sinking for the DDS chip without the presence of the ground post. As the AD9958 runs with a relatively low, 1.8 V core voltage, this chip does not dissipate nearly as much power as some of the earlier DDS devices that required better cooling. Thus depending on the mechanical design of the enclosure a chassis ground connection alternative to the ground post such as a short length of flexible grounding braid or other low RF impedance path to the chassis could be used. Use caution if soldering to the ground post pad, because it would be quite easy to overheat and possibly

destroy the DDS chip, which is thermally coupled to the pad.

The square corners of the PCB, which are intended to be trimmed off to fit the surplus die cast aluminum chassis used here, can be used with standoffs to provide an alternative mounting method. As shown in Figure 12, photos A and B, there is just enough room to drill 3/32 inch holes for 2-56 machine screw hardware. Note that the holes need to be drilled with a degree of precision and although not shown here the use of nylon screws and insulating washers is necessary to ensure the board ground planes remain electrically isolated from the chassis.

The PCB artwork shown here is the first revision, in which the majority of the first run problems were corrected. For this revision of the board, however, there remains the need for two, easy-to-install jumpers and if desired, a test point to simplify entry into the internal system programming mode. The errata details are available on my Web site. (See Note 13.) If there is sufficient interest these items will be corrected for the next manufacturing run of boards.

Performance Test Results

Frequency Spectrum Purity

Obtaining a clean spectrum from a DDS generator is somewhat of a design challenge and thus is also rewarding to achieve. Spectrum purity tests are consequently high on the priorities list for proof of performance. Since both the DDS and MPU chips are digital devices, if all is not well with the circuit design and layout, the spectrum can become polluted with unwanted spurs at significant levels. As illustrated by the array of spectrum analyzer photos in Figure 13, the signal from NimbleSig III is very clean. In order to display the full 200 MHz spectrum with the

noise floor sufficiently low to reveal the spurs my legacy spectrum analyzer was pushed to its limits. It was necessary to increase the sweep duration to 100 seconds for most of the tests. The adjustment of the baseline clipper was quite critical and a good compromise between the high intensity needed to clearly paint the narrow spurs, prevention of variable persistence storage blooming, viewing of the noise floor while retaining readability of the text fonts proved to be tedious. Please note that the center frequency readout text field data of 0000 MHz, which appears in all of the Figure 13 photos, is caused by a malfunction in the logic circuitry within my spectrum analyzer. This is just a problem with the readout circuitry, which fortunately does not affect the fundamental performance of the analyzer. I hope to someday obtain the triple connector card extender I need to troubleshoot this logic circuit.

The photos across row 1 show the full 200 MHz spectrum with output frequencies, from left to right, of 10, 20, 40 and 50 MHz. As shown, most spurs are greater than 60 dB down from the carrier. Note that the 50 MHz example has the highest spur of the group at 100 MHz. As this spur drops down with just a slight shift of carrier frequency, I wonder if this spur is made worse when the output carrier is a direct sub multiple of the reference clock frequency.

The row 2 photos are also full 200 MHz spectrum sweeps. Photos A2 and B2 both show the carrier frequency set to 103.333 MHz, but the reference clock source differs. In photo A2 the DDS was running with the PLL set to 20:1 multiplication using the internal 25 MHz TCXO as the reference. In photo B2 the PLL was disabled with the DDS locked to an external, 500 MHz injected reference. Clearly, as one would expect, the spectrum is cleaner with the DDS

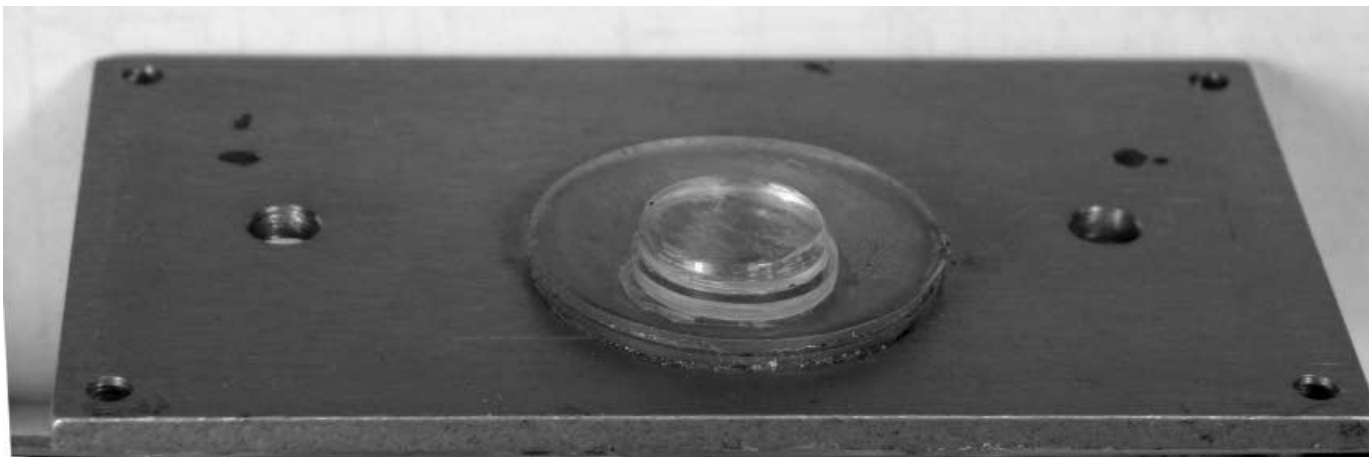


Figure 11 — This is the DDS chip compression bumper, as described in the text.

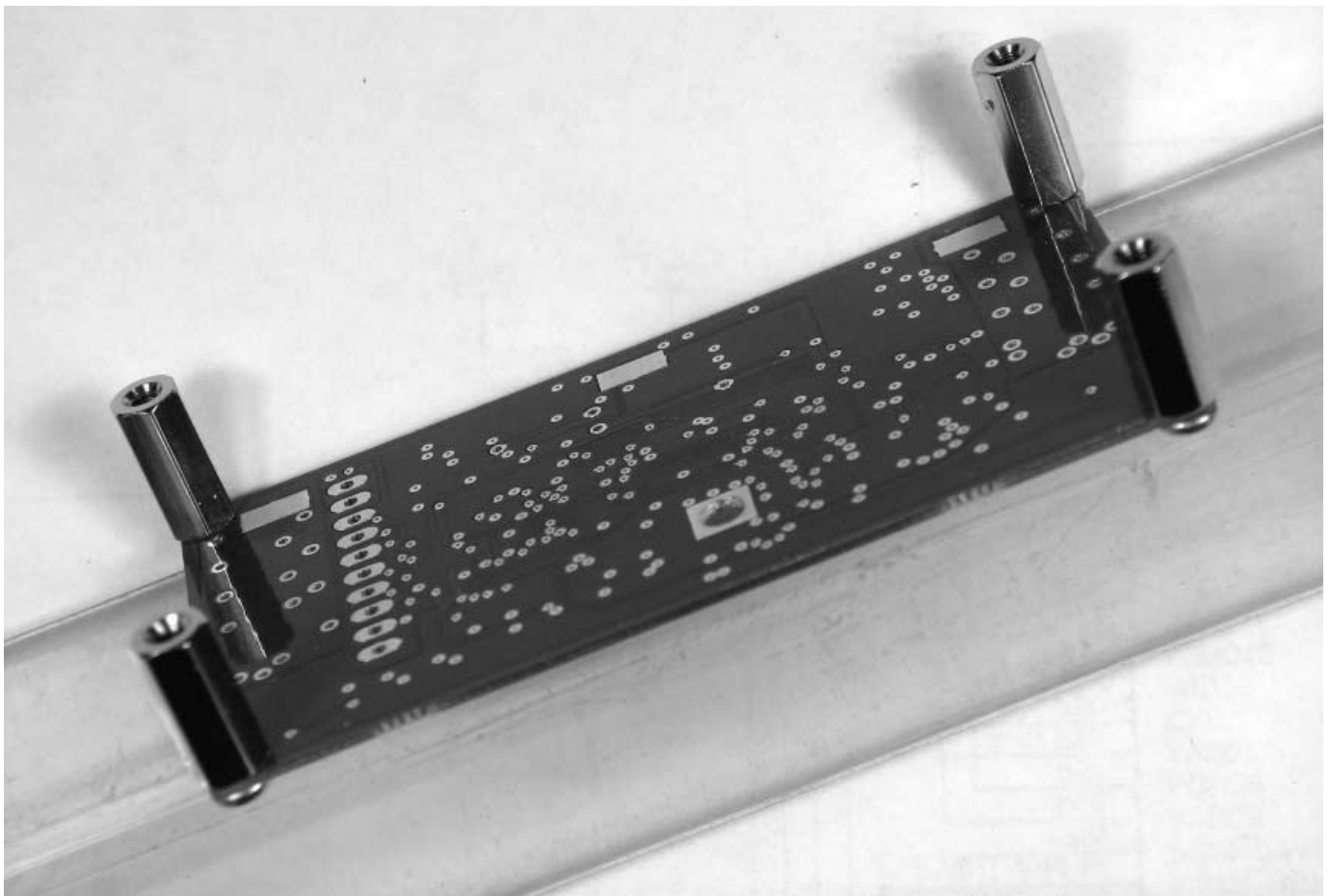
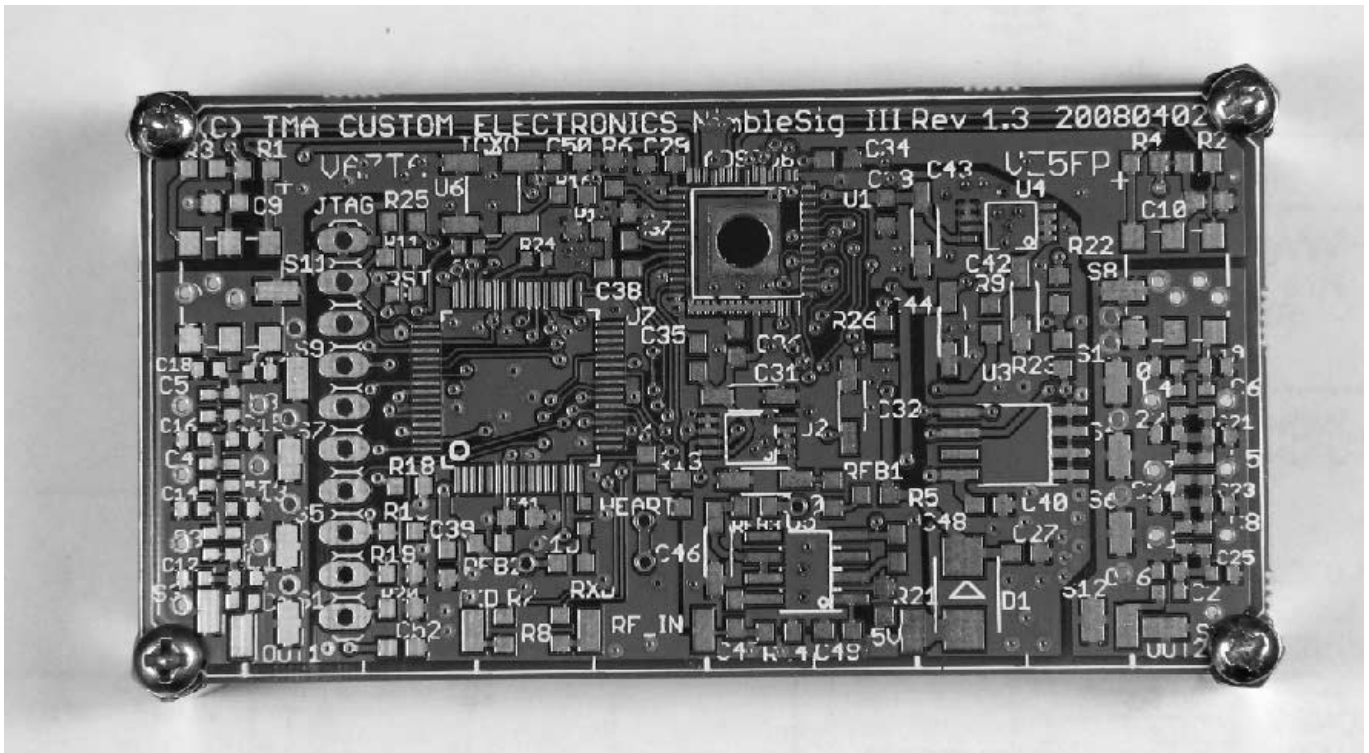


Figure 12 — Part A shows the no. 2-56 machine screws for mounting the circuit board. Part B shows the no. 2-56 tapped mounting standoffs. — Note: use nylon standoffs to preserve the grounding design.

PLL disabled. Photos C2 and C3 are a similar comparison with the output set to 146 MHz.

The photos in row 3 are relatively narrow, higher resolution displays intended to show modulation and phase noise. The DDS output carrier frequency was set to 103.333 MHz. From left to right the spans are 5 kHz, 10 kHz, 20 kHz and 200 kHz with resolution bandwidths of 30 Hz, 300 Hz, 300 Hz and 3 kHz respectively. Thanks mainly to the grounding scheme and the use of multiple power regulators these photos illustrate that the DDS signal is free of any significant periodic noise modulation, which would otherwise appear as symmetrical sidebands.

The lower, straight baseline in photo C3 illustrates the spectrum analyzer noise floor with the input disconnected. This test was a somewhat inconclusive attempt to illustrate the phase noise whilst running from an external 500 MHz reference. The external 500 MHz reference source was provided by a signal generator based on a PLL synthesizer as opposed to a low phase noise source, which would have been a better choice. The contribution to the phase noise from the signal generator to the measurement done here was not determined. I hope to pursue the phase noise testing using a known low noise 500 MHz signal source for the reference and a filter to prevent analyzer overload in the future. I think it is fair to say that the noise performance of this DDS design looks good enough to justify pursuing a wider dynamic range measurement.

Modulation

Both AM and FM, variable rate, sinusoidal audio modulation modes are provided within NimbleSig III. Either RF output may be modulated but simultaneous modulation of both outputs is not supported. The modulation rate can be varied from 1 Hz to 20 kHz. The amplitude modulation depth can be varied from 1% to 99%. The power-on-reset defaults are set at 400 Hz and 30%. The FM deviation can be set in 1 Hz steps from 10 Hz to 100 kHz, with defaults set at a rate of 400 Hz with 3 kHz deviation. In the case of the AM mode, the RF output amplitude is dropped by 6 dB to provide headroom for the

modulation envelope peaks. Thus, during the AM mode, the calibrated average RF output level from the generator drops from -10 to -16 dBm.

The modulation process increments and decrements the amplitude or frequency in discrete, sinusoidally defined steps that simulate a pure sine wave modulation tone. The step definitions, either amplitude or frequency, are calculated in advance after the user enters the desired modulation frequency, along with either the amplitude modulation percentage or frequency modulation deviation values. For modulation frequencies below 1.5 kHz the step definition data is stored within the MPU RAM. The MPU sends this data on a repetitive basis to the DDS, step-by-step, during modulation to shift either the DDS output amplitude or frequency depending on the mode. For higher modulation rates (above 1.5 kHz) the pre-calculated step data is stored in advance within internal DDS registers (called profile registers). The internal modulation capability of the DDS is then used under the control of the MPU to impose the higher rate RF carrier modulation.

The modulation scheme used provides finer resolution as the modulation rate decreases. The number of steps used for modulation frequencies below 1.5 kHz is limited by the total time it takes to send the data for defining the next step to the DDS plus the execution time of the modulation interrupt service routine (ISR). Table 1 illustrates how the audio spectrum is broken up into seven segments, in which the number of steps per cycle varies from 180 down to 30 as the modulation frequency is increased.

For modulation frequencies of 1.5 kHz and lower a timer interrupt that is assigned a high priority in the MPU vector interrupt controller (VIC) is used to update the DDS registers with new step definition data. This data is sent just prior to each modulation step via the high speed (25 Mb/s) SPI interface. As previously mentioned modulation frequencies above 1.5 kHz use the internal modulation mode of the AD9958 DDS. This mode, which is limited to a maximum 30 steps per cycle resolution, offers a higher modulation rate capability as the data for each step is preloaded into internal DDS reg-

isters. This eliminates the need for sending definition data for each step on a real time basis when the modulation is running. The steps are selected via the dedicated, parallel-address-style profile register selection bus, which the MPU can update with just a single general-purpose IO operation. The fast interrupt (FIQ) mode of the LPC2138 MPU along with a short (13 machine instructions), assembler code interrupt service routine (ISR) work together when triggered by the modulation rate timer to update the profile register selection address. The MPU achieves very fast speed in FIQ mode by marching in and out of the very short ISR with minimal overhead. The minimal overhead is facilitated by dedicated FIQ mode registers provided within the MPU, which eliminate the traditional need for doing push/pops to/from the stack during entry/exit to/from an ISR.

Amplitude Modulation

Figure 14 is a photo array that illustrates the amplitude modulation characteristics of NimbleSig III. Row 1 illustrates how the number of amplitude steps per cycle vary inversely with the modulation rate. This technique provides very fine steps for the lower modulation rates, which optimizes the shape of the modulation envelope for the commonly used THD test frequencies. Additionally it minimizes the amplitude of the sampling spurs and helps keep the sampling frequencies well above the audio band for all but very low modulation rates. The sampling resolution is divided into seven bands. Table 1 lists the seven audio band segments with the associated step resolution and rates.

Row 2 consists of the frequency domain spectrum displays of the time domain modulation envelopes in the photos directly above.

Photos E1, E2 and E3 in Figure 14 illustrate the performance of the internal modulation feature of the AD9958. Although the DDS internal modulation is limited to a resolution of 30 steps per cycle, the modulation envelope remains well defined and also very low in distortion. The in-band spurs are more than 50 dB down from the carrier.

Figure 14, photos A3 and B3 are photos

Table 1
NimbleSig III Modulation Resolution for Different Modulation Rate Bands

Lower Band Edge (Hz)	Upper Band Edge (Hz)	Steps/Cycle	Degrees/Step	Minimum Step Rate (Hz)	Maximum Step Rate (Hz)
1	250	180	2	180	45,000
251	400	120	3	30,000	48,000
401	500	90	4	36,090	45,000
501	800	72	5	36,072	57,600
801	1000	60	6	48,060	60,000
1001	1500	36	10	36,036	54,000
1501	20,000	30	12	45,030	600000

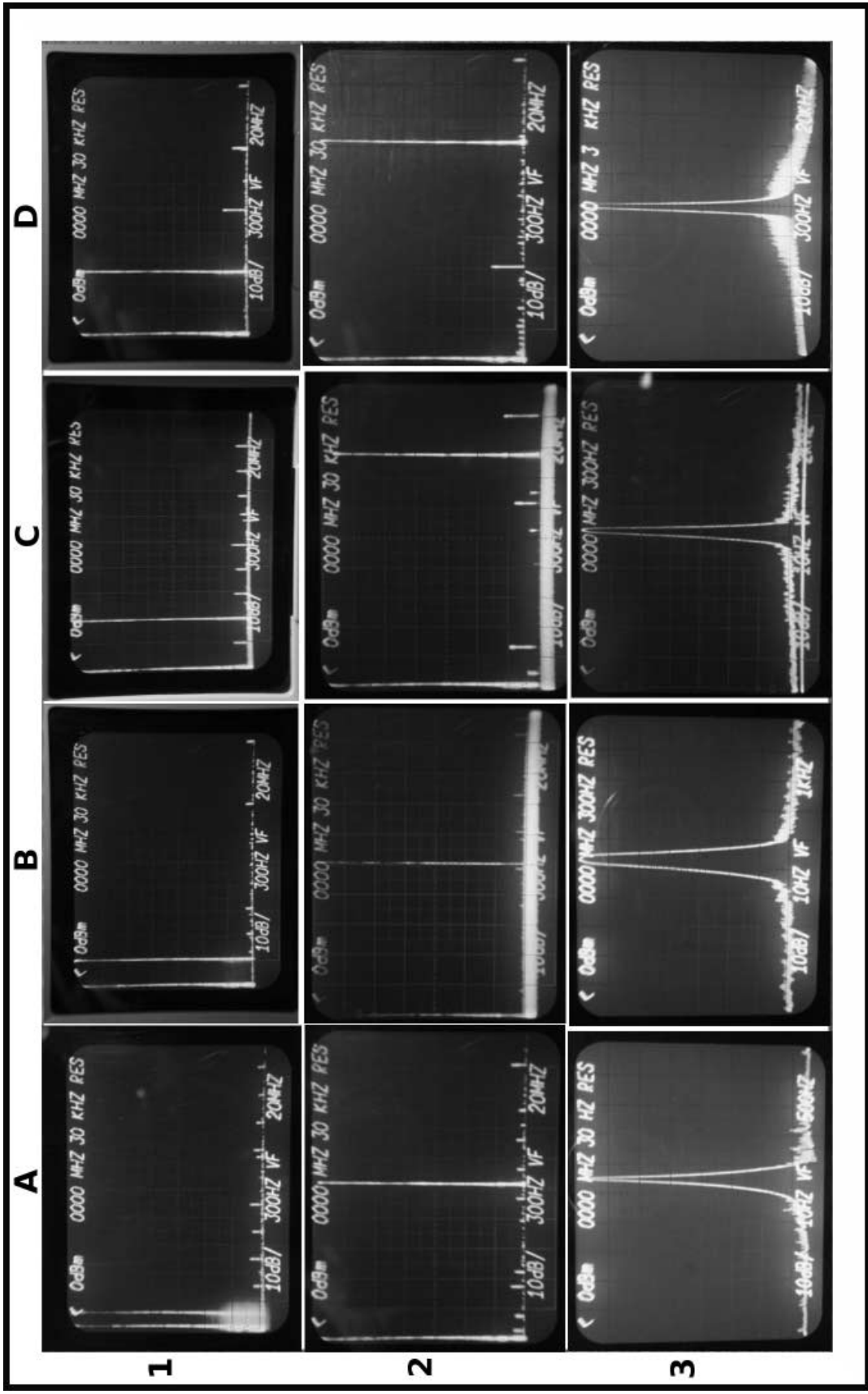
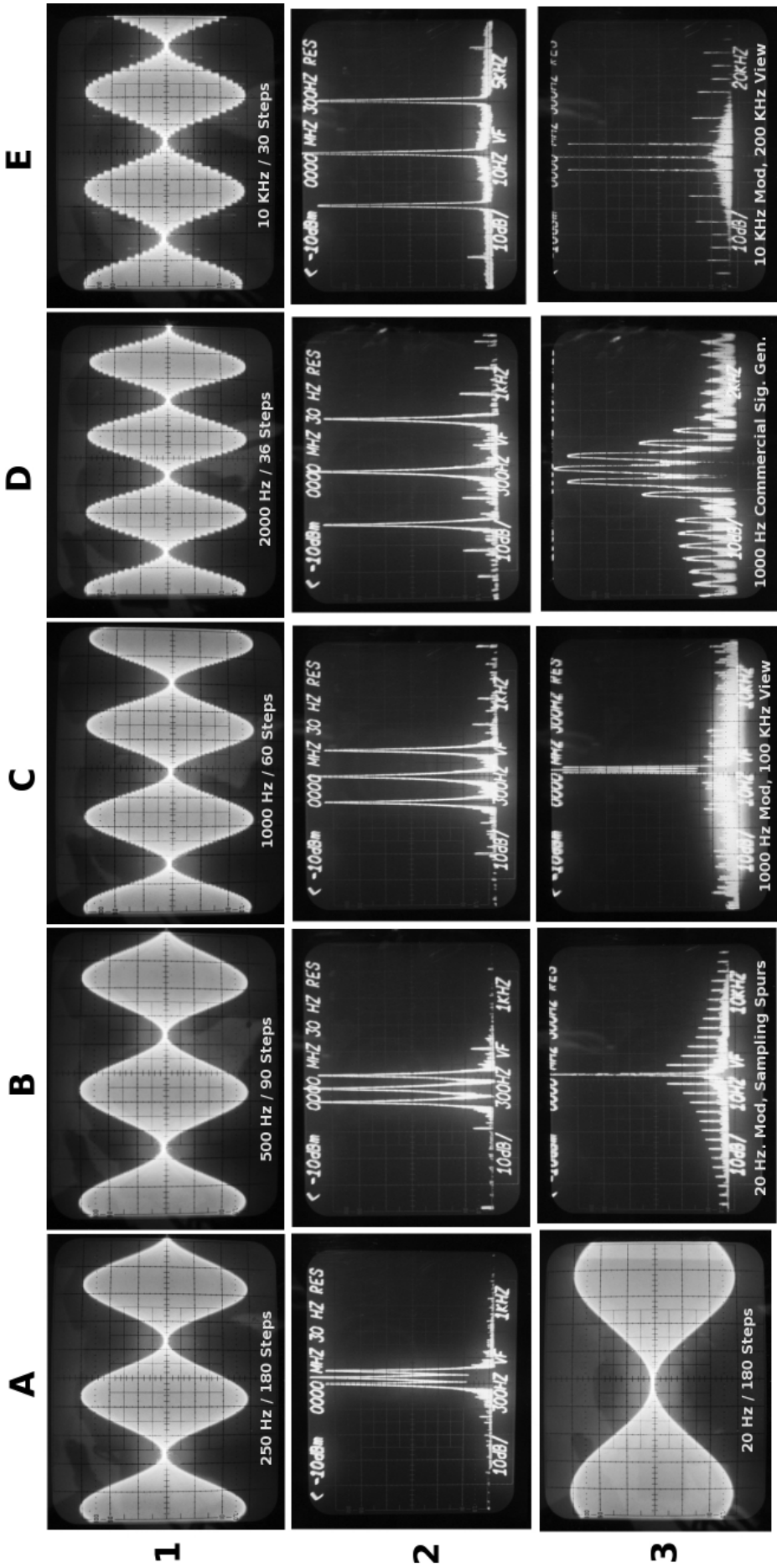


Figure 13 — NimbleSig III spectrum purity tests.



NimbleSig III Amplitude Modulation

Figure 14 — NimbleSig III amplitude modulation envelope and frequency spectrum displays.

of the 20 Hz modulation envelope. These photos are noteworthy because the step rate of 3,600 Hz falls well within the audio spectrum. As shown, the step rate sidebands are about 46 dB below carrier, which would be about 40 dB below the 20 Hz sidebands (not visible here). Although it is unlikely that this characteristic would affect typical receiver testing, operators performing very low modulation frequency tests should expect the presence of very low amplitude (-40 dB or lower) step rate frequency related tones within the audio spectrum.

Figure 14, photos C3 and E3 show wider views of the spectrum during modulation. As shown the splatter level is about -55 dBc at the 1 kHz rate and -42 dBc at the 10 kHz rate. I believe the microprocessor IO transient delays are responsible for the higher splatter at 10 kHz. The transients are just barely visible in photo E1.

I provided photo D3 in Figure 14 to provide some perspective to the quality of the NimbleSig III modulation performance. D3 is the spectrum photo from my late 1990s technology, high end (about \$8000 new), industrial quality, commercial signal generator. As shown the second harmonic modulation sidebands are about 30 dB below the fundamental sidebands. This converts to a total harmonic distortion of a little more than 3%, which is within the generator specification of maximum 4% THD.¹⁴ As shown by Photo C3, the NimbleSign III AM distortion sidebands are about 20 dB lower than the second order sidebands of my commercial signal generator. It is apparent from this that the THD performance of the digital modulation method used here should be less than 0.5% considering the bandwidth restrictions

of a typical AM receiver.

A downside of the digital modulation used by NS3, which is usually of no consequence for receiver testing, is that there are relatively high frequency, moderate level sampling rate sidebands generated by the encoding step transitions. These sidebands appear in the frequency spectrum at multiples of the sample rate around the carrier as shown in Figure 14 photo B3 for 20 Hz modulation (discussed above regarding audible spurs for very low frequency modulation rates). The amplitudes of these spurious sidebands decrease as the order of the sidebands increase and also decrease as the modulation steps are made finer. The closest, most significant, first order sideband pair will be at least 30 kHz away from the carrier (except in the case of very low modulation rates, where the amplitude of the spurs would be relatively low because of the finer steps). The spurs are usually of no concern, because they are well beyond the bandwidth of the typical communications receiver, which normally would not pass these sampling rate sidebands. If the device under test happens to have more than 30 kHz of bandwidth, such as receivers used for video or high speed data, the digital modulation spurs could appear within the baseband spectrum after the detector at a worst case amplitude of about 5% of the voltage of the modulation signal. Thus, those who wish to use NS3 for modulation related applications should be aware that modulation spurs could be present in broadband applications.

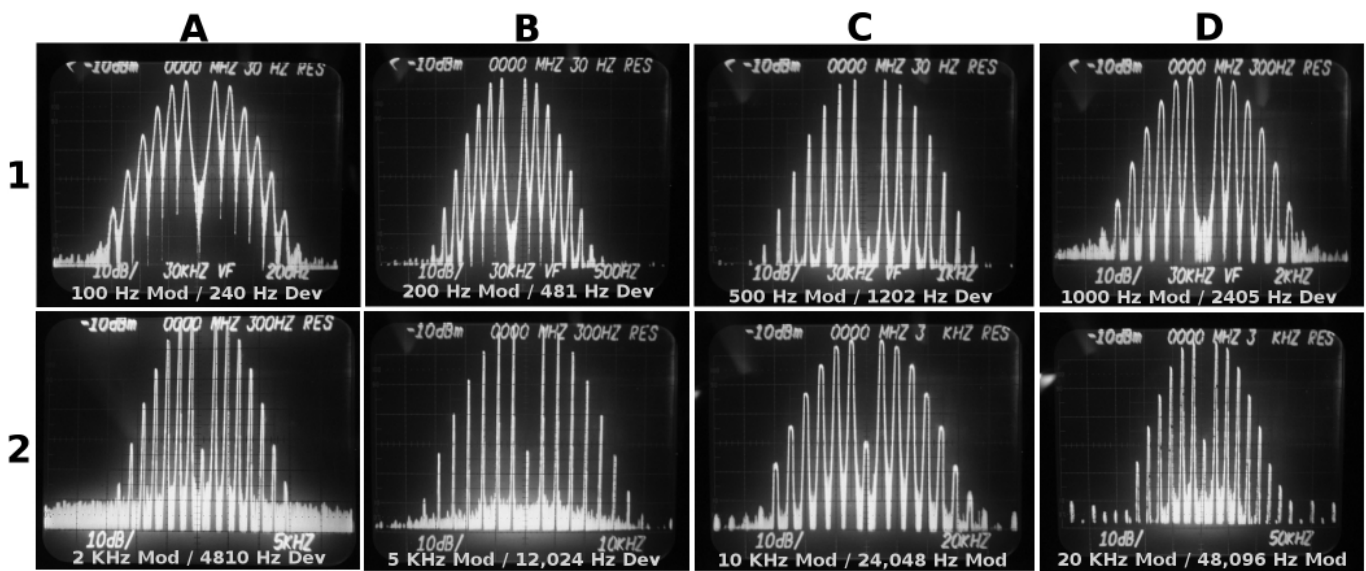
The amplitude of the modulation sampling rate sidebands could be greatly reduced if the modulation steps could be sloped to approximate the sine wave shape. The AD9958 does provide a feature for shap-

ing the step transitions for digital modulation where the step sizes are all the same. Unfortunately, I was unable to adapt this feature for sinusoidal modulation, as the step sizes vary.

Frequency Modulation

The frequency spectrum display of an FM signal is useful for viewing the transfer of carrier power into the sidebands as the deviation is increased from zero. When the peak deviation is set to approximately 2.4 times the modulation frequency (modulation index = 2.4028) all the signal power is shifted into the sidebands and the carrier power literally drops to near zero. This carrier drop out phenomenon commonly referred to as 1st Bessel zero is very useful for checking deviation accuracy and purity of modulation.¹⁵

Figure 15 is a photo array of first Bessel zero nulls (modulation index of 2.4048) obtained for modulation rates between 100 Hz and 20 kHz in a 1-2-5 sequence. This provides insight to the NS3 FM modulation performance and deviation setting accuracy. The deep Bessel function carrier nulls are shown near the center of the photos. The depth of these nulls, which are very deep considering the logarithmic display, is a good indicator of quality of tone, tone frequency and deviation accuracy. A degradation of any of these qualities would prevent a deep Bessel zero carrier dropout. Since the NS3 DDS frequency step resolution is 0.116 Hz (500 MHz / 2³²) both the the relative frequency of the modulation steps and the peak deviation are accurately controlled. This level of accuracy could be useful for checking the calibration of deviation meters.



NimbleSig III - FM Modulation

Figure 15 — Bessel zero FM modulation frequency spectrum displays at various modulation rates

The symmetry of the significant sidebands is also an indicator of good modulation linearity. The tonal quality of the FM should be similar to AM as the same approach is used for generating the modulation signal.

Dual Output Relative Phase Offset

The AD9958 provides 14 bit resolution control of the output phase of the two output signals. This results in a phase step resolution of approximately 0.02197° . The NimbleSig III phase command values are entered in millidegrees. This provides a reasonably human-friendly data entry method that effectively harnesses the fine resolution steps with minimal rounding error. The commands will be described in more detail in Part 3 of this article.

A unique command is provided that loads the same frequency simultaneously into both generators, and in the process locks the output signals together with a defineable phase offset. Oscilloscope photo A1 of Figure 16 shows the waveforms from the two RF outputs operating in phase while photo B1 illustrates the cancellation of the two signals when added together with one oscilloscope channel inverted. The Figure 16, A2 and B2 photos show the two signals with a 180,000 and 90,000 millidegree offsets respectively.

Power Detector Modes

The NS3 design permits RF level measurement from a single sample, or the average level from either 128 or 1024 consecutive samples.

Additional commands permit the detection of the maximum or minimum level detected during 1024 consecutive samples. The sample rate is currently set for once every 56.3 μ s, thus a 1024 sample sequence takes about 58 ms. Consequently, a 1024 sample sequence spans sufficient time to capture the maximums and minimums of an AM signal modulated at a 20 Hz rate. This feature can be used to measure peak envelope power or percentage of modulation.

Parts 2 and 3 to Follow

Part 2 of this article will describe the software, programming and initial testing of the NimbleSig III module. Part 3 of this article will describe the NS3 command set in detail, calibration procedures and a mouse button control program.

Acknowledgments

I wish to acknowledge many discussions with Jim Koehler, VE5FP, who deserves much credit. Jim is currently developing a signal generator that is based on the NS3 module.

I wish to thank Analog Devices Inc for their development of the fine RF integrated circuits on which NimbleSig III is based. I

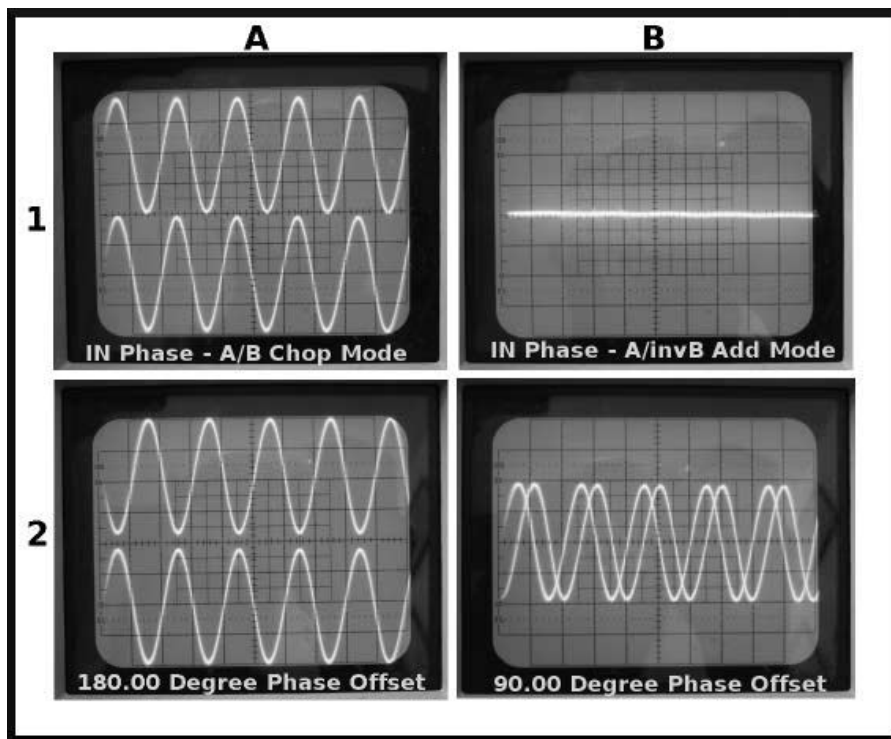


Figure 16 — Relative generator A / B controlled phase offset time domain oscilloscope views.

wish to thank Rowley Associates (in particular Mr. Paul Curtis) for their excellent *CrossWorks for ARM* development tools product and for their solid support, which enabled me to bring the development of the NS3 firmware to a successful conclusion.

I would also like to thank the ARRL QEX editorial staff and Technical Advisors for their assistance in the finalization and publishing of this article.

Notes

¹NimbleSig winning entry URL: www.circuitcellar.com/designstellaris2006/winners/1648.html.

²ADI AD9958 data sheet URL: www.analog.com/static/imported-files/data_sheets/AD9958.pdf.

³ADI DDS application notes: www.analog.com/en/DcList/0,3090,770%255F%255F43,00.html.

⁴SPI Bus: en.wikipedia.org/wiki/Serial_Peripheral_Interface_Bus.

⁵LPC2138 User's Manual: www.standardsic.nxp.com/support/documents/microcontrollers/pdf/user.manual.lpc2131.lpc2132.lpc2134.lpc2136.lpc2138.pdf.

⁶I2C Bus: en.wikipedia.org/wiki/I2c.

⁷Microchip 24LC512 datasheet: ww1.microchip.com/downloads/en/DeviceDoc/21754E.pdf.

⁸Rowley *CrossWorks for ARM*: www.rowley.co.uk/arm/.

⁹DDS Nyquist Images: www.analog.com/en/rfif-components/direct-digital-synthesis-dds/products/application-notes/resources/index.html.

¹⁰LPF Design Reference: www.analog.com/UploadedFiles/Application_Notes/351016224AN_837.pdf.

¹¹Filter Design Software: www.tonnesoftware.com/.

¹²LTSpice Simulation Software: www.linear.com/designtools/software/switchercad.jsp.

¹³NimbleSig III Web page: www3.telus.net/ta/NimbleSig%20III/.

¹⁴THD Measurement and Conversion: www.dogstar.dantimax.dk/tubestuf/thdconv.htm.

¹⁵Frequency Modulation: en.wikipedia.org/wiki/Frequency_modulation.

Tom Allread, VA7TA, became interested in electronics when still in grade school, repaired radio and television sets in his teens, obtained his Amateur Radio ticket at the age of 19, and went on to obtain commercial radio operator certification a year later. He subsequently graduated from the Capitol Radio Engineering Institute Engineering Technology program. His career was in the telecommunications industry where he worked in microwave and VHF radio equipment maintenance, training, engineering standards and design, and long distance network operations management.

Tom is now retired and lives on Vancouver Island with his wife Sylvia, VA7SA. Tom has a history in repeater building and emergency communications, and he enjoys operating mobile CW, building equipment and is currently the net manager for the 20 meter Trans Canada Net. His other interests include microcontroller programming, circuit design, computing, hobby farming, digital photography, bicycling and sailing.

QEX

Experimental Determination of Ground System Performance for HF Verticals

Part I

Test Setup and Instrumentation

This description of the test setup used by the author for a series of experiments sets the stage for a series of articles describing his results.

HF verticals located on or near ground are a perennial topic among amateurs. Over the past several years this discussion has been illuminated (and in some cases obscured!) by the advent of really good modeling software based on NEC (numerical electromagnetic code). This has resulted in a vast literature on antennas using the results of modeling. However, these results are not without some controversy. In particular the relative merits of a large number of buried radials versus a few elevated radials has been especially contentious. What has been missing from the discussion are careful field measurements done with good instrumentation and technique to see if the NEC predictions actually hold up in the real world. To address this problem I performed a series of field experiments, over a period of a year, to examine how different ground system arrangements affected the behavior of a vertical antenna and to see if field measurements on a real antenna would correlate with NEC modeling.

The results of these experiments will be presented in a series of *QEX* articles. There is no pretence that these experiments will answer all questions or even definitively settle some of the arguments, but at least they should give us something to think about.

In Part 1, I will discuss the test range, test instrumentation and test procedures used for all the experiments. Part 2, which is included in this issue of *QEX*, discusses an earlier and apparently overlooked prediction from NEC,

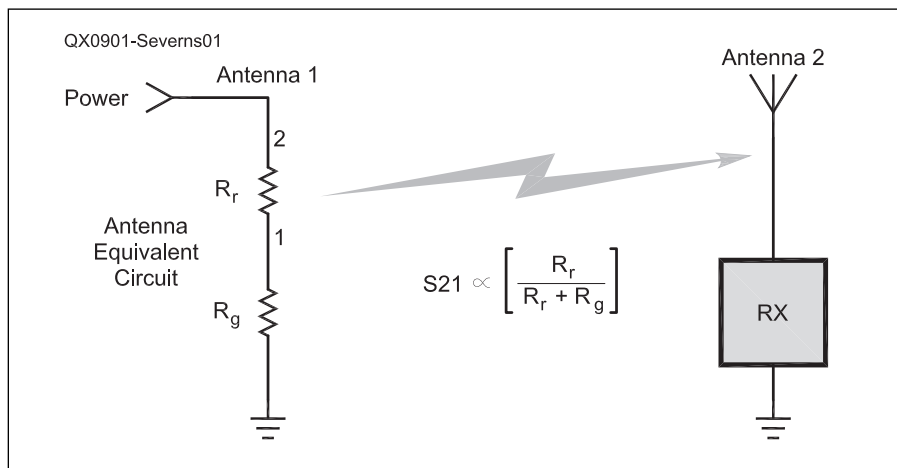


Figure 1—This drawing illustrates the traditional measurement scheme.

that in sparse (<10 radials) radial systems lying close to ground, there can be a substantial increase in ground loss when the radials are made much longer than $\frac{1}{8}$ wavelength. This is a case of more copper = more loss, which is not at all intuitive! Part 3 will compare verticals with a large number of ground surface radials to verticals with four elevated radials. This part will directly address the elevated radial controversy. Part 3 will also have comparisons between several different elevated radial configurations. Part 4 will

look at the effect of radial numbers on the characteristics of $\frac{1}{4}$ wavelength and several shorter loaded antennas. Part 5 will take a look at the problems of ground systems for multiband verticals, where a range of 7 to 30 MHz must be accommodated. Finally in Part 6, I will report on some experiments with a full size $\frac{1}{4}$ wavelength vertical on 160 m. In addition, because this series will take many months to be published, there will be lots of time for feedback. I plan to include some of this in Part 6.

Test Setup

The physical layout of the test range, the instrumentation employed and the test procedures were all key elements in obtaining reliable results. The following discussion provides descriptions of these elements which remained essentially constant for the experiments. The majority of measurements were done at 7.2 MHz although there was some work at 160, 30, 20, 17, 15 and 10 meters. The information given here is intended to provide information common to all the experiments.

Test Concept

The traditional test procedure for these kinds of measurements is well known. As shown in Figure 1, a test antenna is excited with a known power, and the resulting signal is measured at a remote point. A change is then made in the test antenna and the measurement is repeated. The difference between the two measurements is a measure of the effect of the change in the antenna and/or ground system on performance. The signal transmission to antenna 2 from the excitation of antenna 1 (S_{21}) will be proportional to the radiation efficiency of the antenna. In other words, $S_{21} \sim \text{input power} \times R_r / (R_r + R_g)$ where R_r is the radiation resistance and R_g is the ground loss. For our purposes we can assume that losses due to conductors are small. Both R_r and R_g will vary as we change the ground system but the final goal is to see the effect on the transmitted signal.¹

The standard way to make these measurements is to use a transmitter combined with forward and reflected power meters to excite the test antenna (antenna 1) with a known power. A calibrated receiver is connected to a remote receiving antenna (antenna 2) to measure the resulting signal. In my initial tests I used both an HP3586C and an HP3585A spectrum analyzer for the receiver. I wished to measure the performance differences between configurations to within 0.1 dB if possible, and these instruments were capable of that. However, the limiting factor turned out to be my ability to measure the excitation power; 0.1 dB corresponds to about 2%. To make repeatable measurements to 0.1 dB you would need to measure power to better than 1%.

To get around that problem I decided to use the instrumentation scheme illustrated in Figure 2. I chose to make the measurements with a vector network analyzer (VNA) in the transmission mode (S_{21} is the response at port 2 due to the excitation at port 1). The transmission path was from the VNA output port, out to the test antenna via a transmission line, from there to the receive antenna and back to the VNA input port via

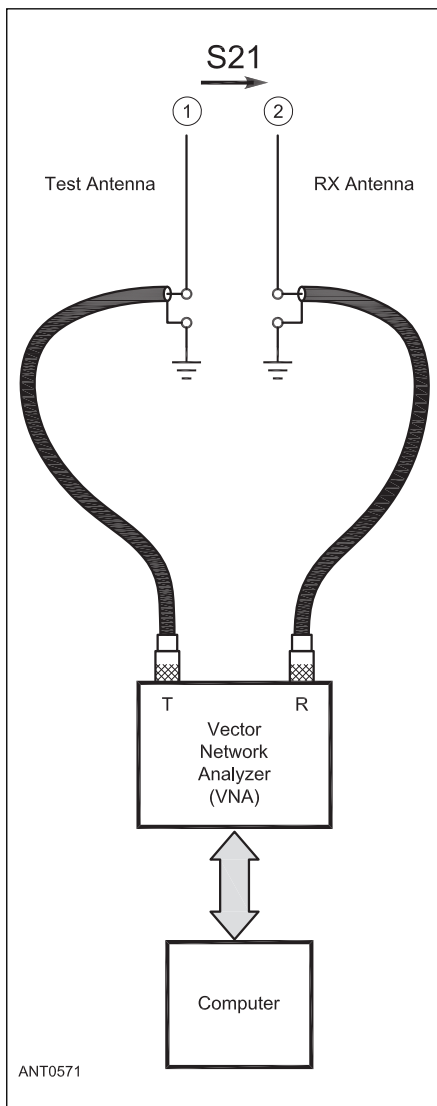


Figure 2 — This diagram shows the vector network analyzer approach for measuring antenna performance.



Figure 3— A view of the test antenna area and test equipment shelter. The receiving antenna is at the far end of the pasture.

¹Notes appear on page 25.

another transmission line.

Amplitude measurements with a professional VNA are typically displayed to 0.001 dB, but of course nothing else in the system is stable to that level. In practice I found that measurements made over a short period of time (2-3 hours) were repeatable to within 0.05 dB. That is more than adequate for these experiments. A weakness of this measurement method is that as the separation between the test antenna and the receiving antenna is increased, the attenuation around the transmission loop becomes quite large, -40 to -60 dB. For instrumentation and a physical setup with a noise floor and stray coupling below -110 dBm, this is acceptable but it did limit the separation distance on 40 m to about 2.25 wavelengths for the particular receiving antenna employed. This is in the far field but not by much. Another limitation was that ± 0.05 dB repeatability was possible only when the antenna under test and the receive antennas were actually stable to that level. This usually meant that measurements had to be made in early morning when the test range was in the shade or late in the day when things had reached thermal equilibrium. It was very easy to detect a cloud passing over by the small changes due to temperature changes in the antennas. I could readily detect the effect of the wind on the vertical, causing it to move slightly. In the end the A-B comparison measurements were probably within a few tenths of a dB but only when I carefully attended to all the details.

This brings us to an important point. The purpose of the experiments was to determine the effect of different ground system arrangements from their effect on S_{21} . All the measurements were relative A-B comparisons. In other words, they were comparisons between two different configurations. There was no



Figure 4 — This photo shows a typical test antenna and center post support.

attempt to measure absolute signal strengths or radiation patterns. The separation distance between the test antenna and the receiving antenna was sufficient to place the receiving antenna outside the reactive near field but the groundwave was still significant. This was not a problem for the type of measurements being made. The presence of a metal pump house and a travel trailer, both of which are small in terms of a wavelength might have had an impact on pattern measurements but should not have affected the type of A-B measurements being made in this series of experiments.

Physical Arrangement

The test range was set up in a field as shown in Figure 3, with an area for the test antennas (including ground systems), a remote receiving antenna (in the far distance) and a small travel trailer to provide shelter for the instrumentation.

The eight poles, in an 80 foot diameter circle around the test antenna, were used to support elevated radials as needed. When more than eight elevated radials were needed, a ½ inch Dacron line was stretched around the posts at the desired height and tightened with a turn-buckle. Each post has a backstay to a buried deadman anchor so the radials could be well tensioned. Radial heights on each post were located using a laser level to keep the radial fan flat around the circle.

In the center of the circle there is a support post (PVC pipe) as shown in Figure 4, with Dacron support lines attached to the top. This post is intended to hold the antenna under test and allow it to move up and down to vary the height for elevated radial tests. An example



Figure 5 — Here is the test antenna base at ground level, with 64 radials.



Figure 6 — The base plate is in position for elevated radials.

of the base plate at ground level with 64 radials attached is shown in Figure 5.

The base plate is isolated from ground but there are three ground stakes (4 foot copper-clad steel rods) close to the plate for those tests where grounding is desired. The ground stakes have short pig-tail leads to connect to the base plate when desired.

Figure 6 shows an example of the base plate positioned for elevated radial tests. The base plate, the radials and the entire test antenna are elevated by sliding them along the support pipe. This arrangement made it very easy to change the height of the radials in small increments up to 4½ feet above

ground. The radials lying on the ground in Figure 6 were *not* present during elevated radial tests!

As shown in Figures 5 and 6, a coaxial common mode choke (balun) was used to isolate the transmission line from the test antenna. This was done for all measurements whether or not ground stakes were engaged. The choke has an impedance of >3 kΩ at 7.2 MHz. For those tests in which the SteppIR vertical was employed, the balun that comes with that antenna was used in lieu of the choke shown in the photos.

The receiving antenna was a 3-turn diamond loop with a diagonal dimension of

24 inches, as shown in Figure 7. The loop was resonant at 8.2 MHz. This loop was installed at the top of a 40 foot mast, as shown in Figure 8.

The distance from the base of the test antenna to the receiving loop is a little over 300 feet, about $2\frac{1}{4}$ wavelengths at 7.2 MHz. The elevation angle from the base of the test vertical is about 8° .

The coax from the VNA output port to the base of the test antenna was $\frac{1}{2}$ inch Andrews Heliac with N connectors. The coax from the receiving antenna back to the VNA was LMR400. Low loss coax was used because it provided better shield attenuation to reduce coupling and in the case of the heliac running out to the test antenna, the very low loss removed the need for an additional correction



Figure 7 — This photo shows the loop receiving antenna.



Figure 8 — Here is the receiving antenna atop a 40 foot mast. N7MQ assisting!

factor for the change in cable loss with variations in SWR.

Test Instrumentation

Feed point impedance, transmission gain (S21) and radial current measurements were all made using a VNA. Two analyzers were available: an HP3577A with an HP35677A S-parameter test box and an N2PK analyzer with dual fast detectors. Figures 9 and 10 are photos of these instruments.

Note the organic automatic heating unit

on top! Critical for maximum accuracy! The common mode choke in the photo is undergoing characterization for transmission loss and series impedance at 7.2 MHz. It turned out however, that the impedance of the choke was much greater than the 50Ω reference impedance of the VNA. Above about $2 \text{ k}\Omega$ even an HP VNA becomes inaccurate for a direct measurement. For choke measurements, I used an HP4815 analyzer, which is well suited for high-impedance measurements.

After careful comparisons between the HP and N2PK VNAs, the N2PK was selected for



Figure 9 — HP3577A with an HP35677A S-parameter test box.



Figure 10 — Here is my test bench, showing the N2PK VNA with the associated laptop computer and HP calibration loads.



Figure 11 — This photo shows a typical shielded current transformer.

most of the measurements because its performance was very close to the HP and had the advantage of direct readout to a computer, which made data reduction much easier. The N2PK VNA was also much lighter than the HP (70+ pounds!) and much more suitable for field measurements.

On several occasions it was necessary to measure the current division ratios between the radials and in some cases, the relative current distribution along a radial. To make these measurements a set of shielded current transformers, like the one shown in Figure 11 were used.

To make a current measurement, a radial wire was passed through the current transformer, as shown in Figure 12. Current transformers were placed in the same location simultaneously on all the radials during a measurement. The transformer being used to sense current was terminated in $50\ \Omega$ by the instrumentation, so all of the dormant current transformers were also terminated in $50\ \Omega$. This was done to compensate for any interaction introduced by the current transformer. At the very least, the effect of the current transformer would be the same on all radials. The active current transformer was isolated with a choke as shown in Figure 12.

Even with this degree of care, the current measurements were still a bit tricky because of the residual interaction between the cable from the current transformer and nearby radials. In some cases I actually used four identical cables in a symmetrical layout to try to minimize imbalance due to this interaction. I believe the resulting measurements were reasonable and useful but not especially precise!

The relative value of the current was determined by using the VNA in the transmission mode, measuring S21 for the loop from the VNA output port to the base of the antenna, out along the radial to the current transformer and back to the VNA input port. This was a convenient way to measure the

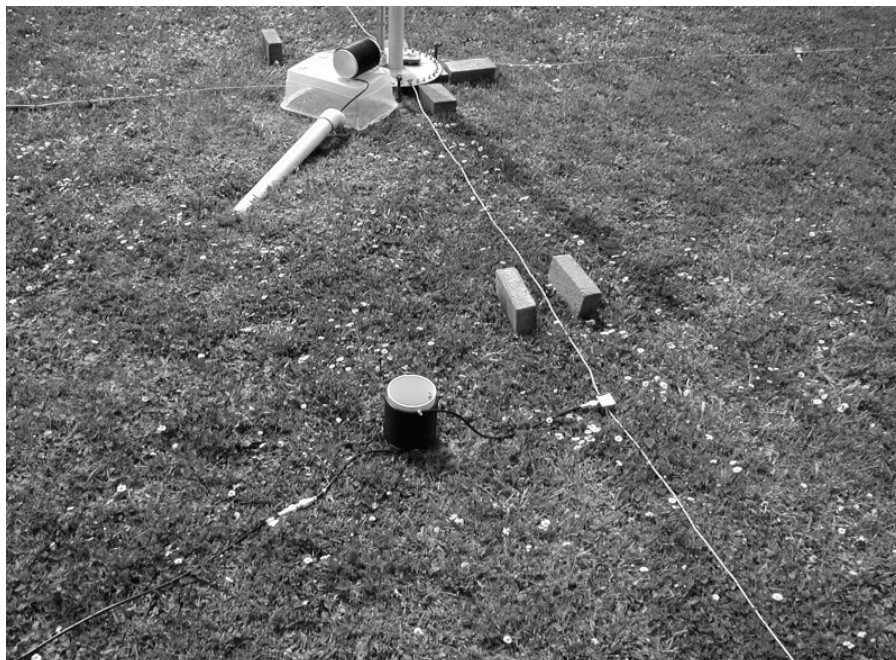


Figure 12 — Here is the test setup for a typical radial current measurement.

current division between radials and the relative current distribution along a radial.

Comments on test procedures

A good physical setup and professional instrumentation are a very good start, but to obtain reliable data great care must be exercised in using and calibrating this equipment. For feed point impedance measurements, at the beginning and end of every test run an OSL (open, short, reference load) calibration was performed with the calibration plane at the test antenna feed point. At the beginning and end of each test run a transmission calibration was also performed.

In addition, before beginning a series of measurements a measurement of stray coupling and possible interference was performed. The procedure was to disconnect the feed line from the base of the test antenna, terminate the feed line with a $50\ \Omega$ load and then measure the transmission gain of the entire system in this state. Throughout the series of experiments, this transmission level was never higher than $-110\ \text{dBm}$ and usually $-115\ \text{dBm}$ or lower, at 7.2 MHz. As a further check on results, most experiments were run several times to verify consistency and repeatability. All of this was very time consuming but absolutely necessary to assure the best possible measurements. I did not delude myself, however, into thinking the measurements were perfect and cannot be improved on. I do believe the results make sense, fit well with NEC modeling predictions, give useful insights into vertical antenna/ground system behavior, and potentially can be of practical help in optimizing a given antenna installation.

Acknowledgement

This experimental work was inspired by the earlier work of Jerry Sevick and Arch Doty.^{2,3} Some of my experiments were a repeat of their earlier work with more advanced instrumentation. I would also like to thank Mark Perrin, N7MQ and Paul Thompson, W8IEB for the many hours of help they provided during the experiments. Without their help, I would still be out in the field taking measurements!

Notes

¹R. Severns, N6LF, "Radiation Resistance Variation With Radial System Design," Sep 2008. Available at: antennasbyn6lf.com.

²J. Sevick, W2FMI, *The Short Vertical Antenna and Ground Radial*, CQ Communications, Inc, 2003. Jerry's work also has appeared in a number of QST articles.

³A. Doty, K8CFU, "Improving Vertical Antenna Efficiency, A Study of Radial Wire Ground Systems," *CQ Magazine*, April 1984, pp 24-31. This article also has a very nice list of earlier references related to ground systems for verticals.

Rudy Severns, N6LF, was first licensed as WN7WAG in 1954 and has held an Extra class license since 1959. He is a consultant in the design of power electronics, magnetic components and power-conversion equipment. Rudy holds a BSE degree from the University of California at Los Angeles. He is the author of two books and over 80 technical papers. Rudy is an ARRL Life Member, and also an IEEE Fellow.



Unusual Terrain Influence on VHF/UHF Propagation

Students at Idaho State University climb mountains to explore an interesting propagation phenomenon.

In our studies of RF propagation, we have been investigating an interesting phenomenon that involves mountainous terrain. Vance Hawley, WA7FDR, our instructor at Idaho State University (ISU), has measured VHF/UHF signal strengths at a number of vehicle-accessible mountain locations and has found that as he drives down the mountains from their summits, the signal strengths increase. As he continues, however, the signal strengths decrease. We wondered what propagation mechanism might be at work.

The Idaho State Radio Frequency (RF) class consulted with several engineers and technicians working in the propagation field. Their responses varied, as each individual seemed to have a different explanation based on their personal experience and research. It appears that the propagation phenomenon we will be discussing is not well understood.

In all of the professional documents read for this project, we found only one possible mention of this phenomenon, in the 21st edition of *The ARRL Antenna Book*, page 23-6, with an illustration reproduced here in Figure 1. Unfortunately, the original author, who has since passed away, doesn't describe the illustration in great detail. *Antenna Book* editor Dean Straw, N6BV, was unable to locate the original notes that might have explained the author's intent.

The Investigation Begins

Our initial test site was an unnamed, minor, somewhat rolling peak southwest of Pocatello, Idaho. The first test we performed was with a vertically polarized Yagi antenna connected to a spectrum analyzer monitoring the 162.55 MHz signal from the NOAA (National Oceanic and Atmospheric Administration) weather radio station on East Butte. Using this setup, we measured signal strengths at various elevations. See the results in Table 1.

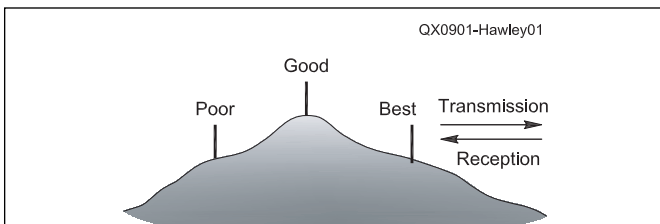


Figure 1 — According to the caption from this illustration from the *ARRL Antenna Book*, propagation conditions are generally best when the antenna is located slightly below the top of a hill on the side facing the distant station. Communication is poor when there is a sharp rise immediately in front of the antenna in the direction of communication.

Figure 2 provides a graphic illustration of the measurement variations compared to elevation. At the left side of the chart you will note that the elevation at the first point is at 6427 feet, about 99 feet down from the 6526-foot summit (the left of the chart shows the signal strength in dBm). The decreasing signal strength is clearly shown. In the middle of the chart you will notice a sudden dip in overall strength, which was caused by interference in the Fresnel Zone of the antenna. (The slope angle decreased for a short distance before increasing once again.)

Table 1
Signal Strength Measurements at Our Un-named Peak Test Location

Grid	Elevation (Feet)	Signal Strength (dBm)
12T UN 76866 42527	6526	-74
12T UN 76856 42537	6505	-75.3
12T UN 76849 42548	6495	-78.4
12T UN 76842 42567	6485	-80
12T UN 76835 42593	6475	-78
12T UN 76792 42686	6460	-74.3
12T UN 76784 42693	6451	-69.6
12T UN 76775 42701	6438	-65
12T UN 76775 42701	6438	-64.6
12T UN 76769 42712	6430	-65
12T UN 76770 42728	6427	-60.8

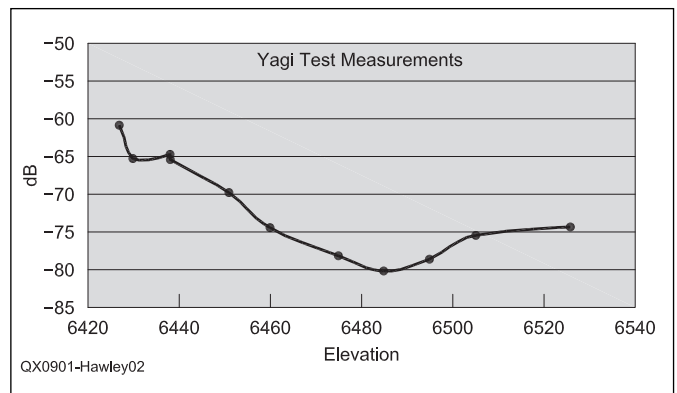
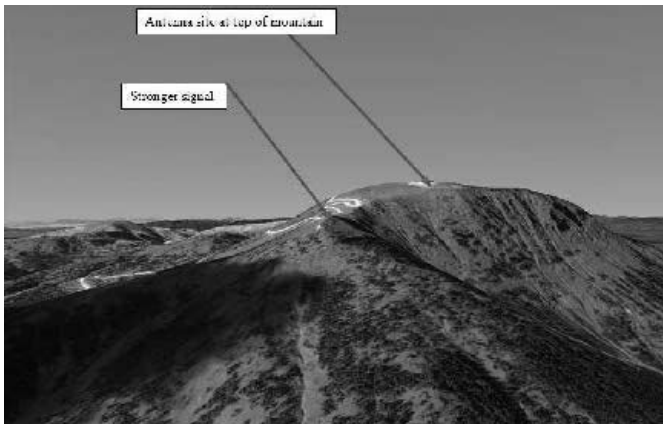
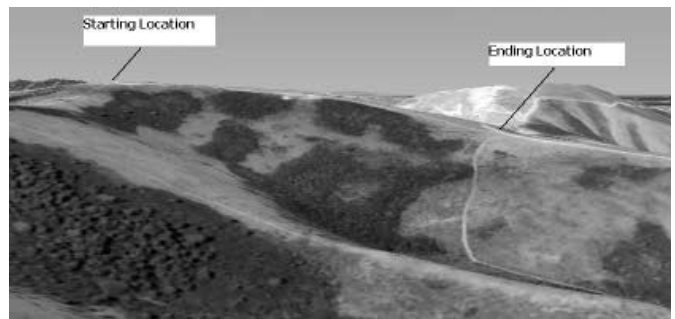


Figure 2 — Variations in signal strength during the tests.



A photo of Sawtell Peak.



A view of the test site from the side.

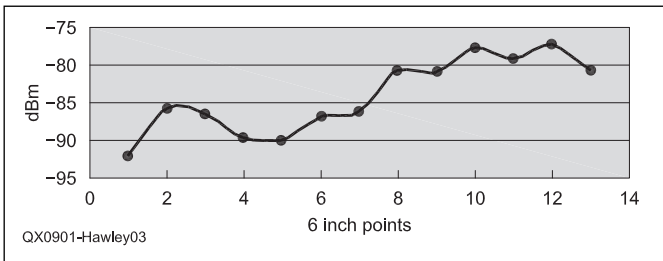


Figure 3 — Increasing signal strength as the test points moved down the face of the mountain with the antenna 6 inches above the ground.



Two of our students positioning the Yagi antenna for best reception.

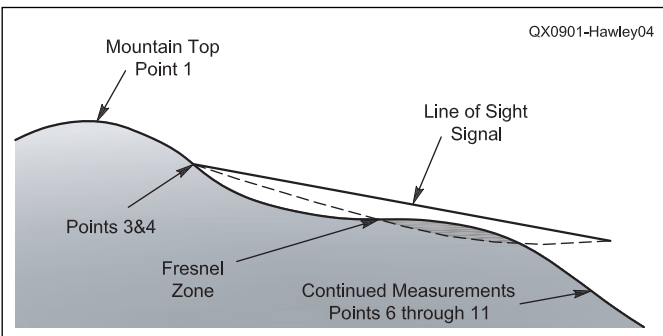


Figure 4 — Fresnel Zone attenuation during our tests.

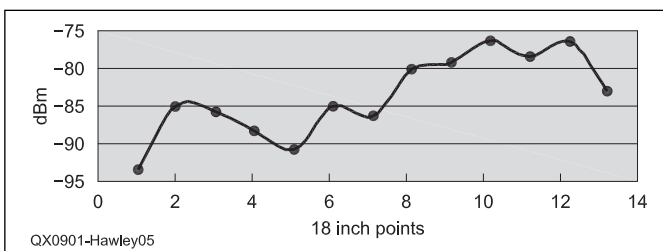


Figure 5 — Signal strength results as the test points moved down the face of the mountain with the antenna 18 inches above the ground.

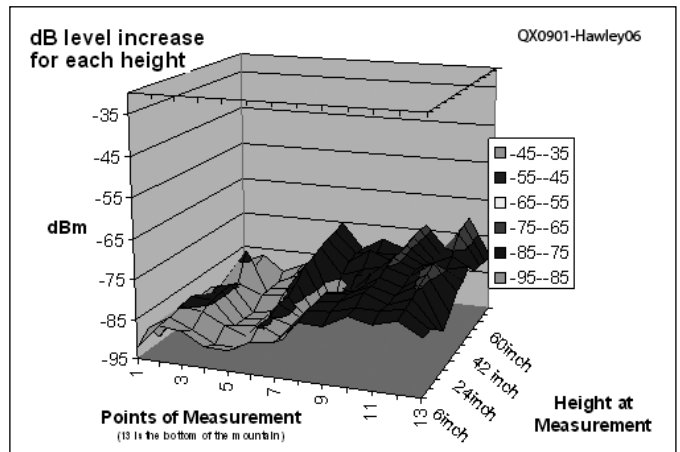


Figure 6 — A 3D graph of the dipole data.

For our next set of measurements we used a 1/2-wavelength dipole mounted horizontally on a graduated pole. These measurements were taken from the original test site. Again we monitored the 162.55 MHz NOAA station on East Butte, 47 miles distant.

Measurements were made with every 20 foot elevation change as we progressed down the face of the mountain. At each measurement point we also raised the antenna 6 inches, beginning from its ground-level starting point. Measurements

were taken with a Tektronix 2712 spectrum analyzer.

Figure 3 shows the signal increasing as we progressed downward with the antenna 6 inches above the ground. You'll notice that Figure 3 also shows signal degradation from points 4 through 6. This is because there was a hill between the receive antenna and the transmitting tower. This hill crossed into the first Fresnel Zone, reducing the signal strength (Figure 4). Signal strengths changed according to variations in terrain as we moved down the mountain (Figure 5). Tables 2 and 3 contain the entire data set.

Figure 6 provides a 3D graph of the dipole data. Looking at the graph, it shows the signal level increasing as the measurement points shift down the mountain. It also illustrates that signal levels rose as the antenna height above ground level increased.

Inconclusive Results

While we were able to observe the phenomena first hand, our tests provided no concrete explanations.

The location that was chosen for the Yagi test had some problems that may have plagued the measurements. The aiming accuracy of the Yagi was hard to measure because the wind was blowing at about 50 MPH and

it was snowing. Directly in front of where the measurements were taken there was another mountain with many commercial broadcast stations. Their signals were clearly overloading the spectrum analyzer.

To correct these problems, some meticulous measurements will need to be taken. Shifting the tests to the UHF range would permit the use of a smaller, easier-to-manage Yagi. Regardless of the frequency, the Yagi

pattern will need to be carefully plotted.

We had planned to perform further tests, but this was not possible due to weather conditions. It would have been better if we had been able to spend a few days on top of multiple mountains with more time to take measurements under better circumstances.

Table 2
Signal Strength Measurements According to Dipole Height

Elevation (feet) Height (inches)	6520	6512	6511	6467	6460	6455	6452
		Signal Strength (dBm)					
6	-85.8	-92.2	-86.5	-89.9	-89.6	-86.2	-79.1
12	-85.8	-89.2	-88.2	-91.2	-91.2	-87.5	-77.7
18	-84.8	-93.5	-85.5	-90.6	-88.2	-86.2	-78.1
24	-84.1	-92.2	-84.5	-89.6	-90.6	-86.2	-77.7
30	-85.8	-95.9	-84.1	-89.9	-90.6	-88.6	-77.7
36	-85.5	-94.5	-84.1	-89.9	-90.9	-90.6	-76.7
42	-86.9	-93.5	-85.9	-87.2	-88.2	-89.2	-76.7
48	-89.6	-91.5	-93.8	-87.5	-88.2	-90.9	-77.1
54	-89.6	-92.2	-93.5	-85.5	-87.9	-84.2	-78.7
60	-82.2	-90.2	-93.5	-85.8	-90.2	-82.4	-79.7
66	-88.9	-91.2	-95.5	-85.2	-89.6	-81.7	Noise
72	-86.9	-89.6	-91.2	-85.5	-88.6	-82.1	Noise

Table 3
Signal Strength Measurements According to Dipole Height

Elevation (feet) Height (inches)	6450	6446	6444	6443	6438	6425
		Signal Strength (dBm)				
6	-86.9	-80.7	-81	-77.7	-80.7	-77.4
12	-84.5	-79.7	-79.4	-77.7	-80.7	-76.7
18	-84.8	-79.7	-78.7	-75.7	-82.7	-76
24	-83.4	-79.1	-78.7	-76	-85.2	-74.3
30	-83.4	-81	-79.7	-75.7	-82.7	-73.6
36	-81.7	-86.9	-80.7	-75	-79.1	-72.6
42	-79.1	-85.2	-79.1	-74.3	-78.4	-75.3
48	-78.4	-82.1	-80.7	-74.3	-76.4	-77.7
54	-77.1	-82.1	-80.7	-74.3	-79.4	-76
60	-76.7	-78.4	Noise	-73.6	-79.4	-71.6
66	-76	-81	Noise	-73.3	-80.4	-70.9
72	-75.3	-78.7	Noise	-73.6	Noise	-70.6

Possible Explanations

One of the possible explanations for this phenomenon is multipath reflection. When two transmitted signals are reflected from different points, they can recombine in or out of phase as they arrive at the receiver. If they are in phase, they will add to each other, resulting in a stronger signal. If they are out of phase, they will subtract from each other, producing a weaker result. Figure 7 illustrates this concept.

The problem with this hypothesis is that there was no supporting evidence that would allow us to determine if this mechanism was in play. According to Vance Hawley, there was no measurable signal on the valley floor when this phenomenon was observed at Jumpoff Peak and Sawtell Mountain, high mountain sites in the area. However, Russ Andrews, an electrical engineer at BMG Engineering, stated:

“I would expect the signal to be weak on valley floor. But multi-path could be coming from other mountains off the direct path. It could be coming from the valley floor much farther away than where you took valley measurements. It can also occur over a much smaller scale, even a few meters.

“Multipath conditions are easily detected. The process is to carefully measure the signal strength at a location. Then slowly move to other locations, noting the signal strength variations as you move. There should be little or no variation if there is little or no multipath. Lots of variation = lots of multipath. Remember to keep your and other peoples bodies away from the sense antenna. Do not use an unbalanced antenna or feed line for the sense antenna. An unbalanced antenna will introduce its own multipath even where there is none in free space. The feed line of an unbalanced system is part of the antenna, and will contribute a multi-path component. Use a dipole and feed it with a 1:1 balun. You don't have to worry about impedance matching.”

Although we were unable to return to the mountains, it would have been interesting to test this theory.

Larry D. Ellis with SoftWright LLC, a company that produces the *Terrain Analysis Package (TAP)*, had this to say:

“I imagine what you are seeing in this case is reflected signal. This is virtually impossible to predict. It (multipath) can be much greater than incident signal at times. Where I have seen it the most is when you have a site not

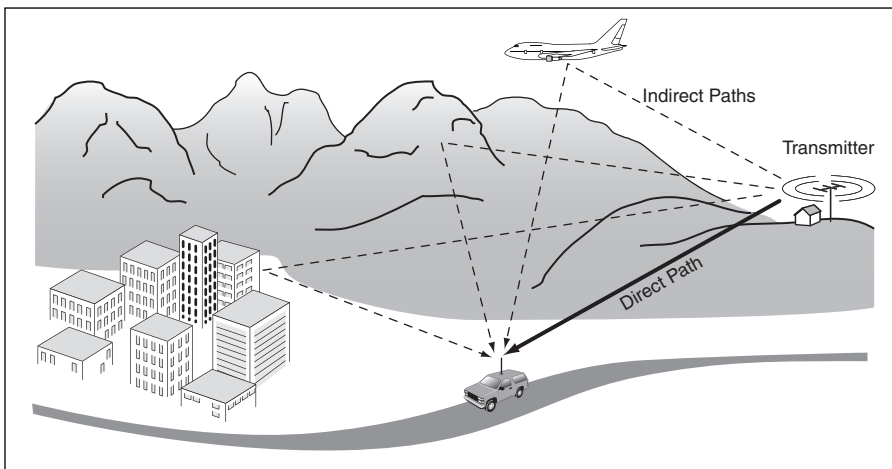
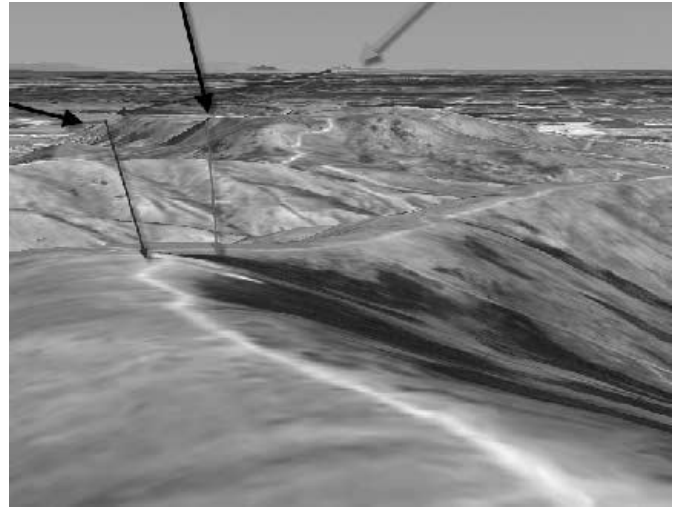


Figure 7 — An example of multipath propagation.



Todd Romriell reading the signal strength on the spectrum analyzer.



Potential diffraction areas around the mountain.

at the top of the mountain and the backside of an omni is feeding huge levels of signal into the mountain, which then bounces back in an uncontrolled phase delay. This causes multi-path interference and is a bear to solve. The way one treats that is by suppression of radiation toward the offending reflector (of which rock is particularly effectual). I can envision it being similar along the path along the surface up the mountain, but to compare levels you would have to be at the same azimuth in the plane orthogonal to the center of radiation from the antenna. That generally is considerably in the air. If you are receiving at a location and find more inbound signal from a direction (using a Yagi as a sniffing antenna) other than toward the transmitting antenna, it can be from many sources. Common ones are reflection (as above) and also re-radiation. That is when an element picks up the signal and then re-transmits it. I have seen that from tin roofs, metal fencing wire, and very often high-voltage power towers. Certain AM broadcast antennas can cause this as well, although not often above VHF.

“Sadly, there are not many good texts on this subject. We have a great library here and yet most of these thoughts have come from extensive experience in the field-testing antenna patterns.”

Another suggestion we received was that we were experiencing knife-edge diffraction from mountains between the transmitter and receiver. Knife-edge diffraction occurs when a radio wave crests the top of a mountain. The sharp terrain at the summit causes the signal energy to effectively spill over the other side at a downward angle. Although this could be a possibility in some instances, it would not always be the case during our tests.

Knife-edge diffraction is best explained by Huygens’ Principle, which states that

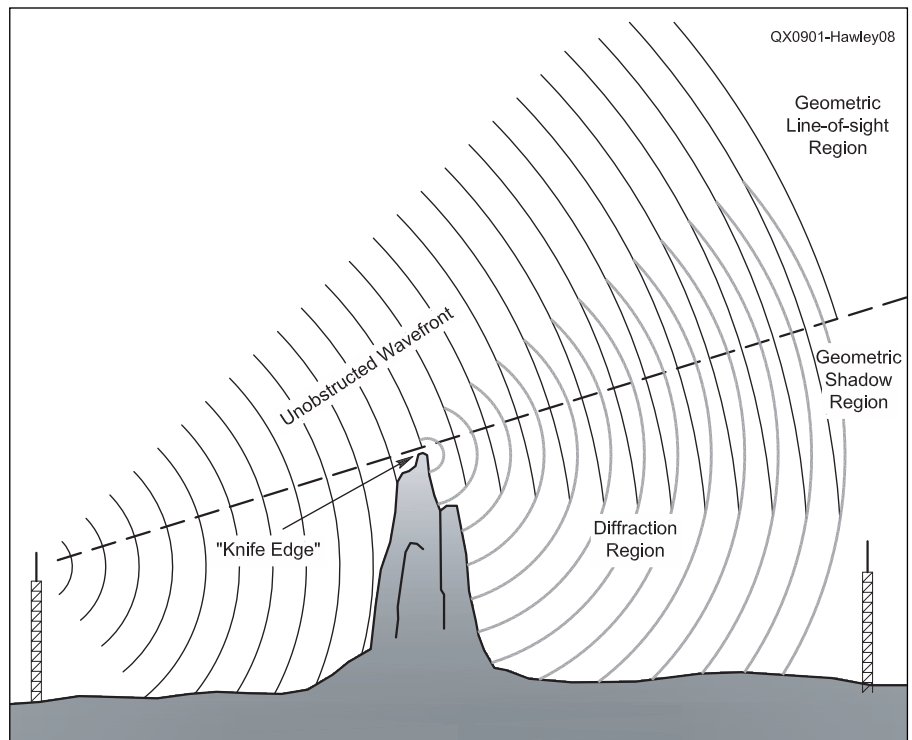


Figure 8 — Knife-edge diffraction.

every point of an advancing wavefront can be considered as a new source of *secondary waves*. The wave amplitude at any point ahead can be obtained by superposition of these new *wavelets*. So, when an incident wave collides with an obstacle, it can create new wavelets that can meet to add and subtract from each other, resulting in a pattern in which some places have greater strength than the incident wave, and other places can have reduced strength (Figure 8). Of course, this would happen multiple times as each wave collides with the obstacle. As multiple

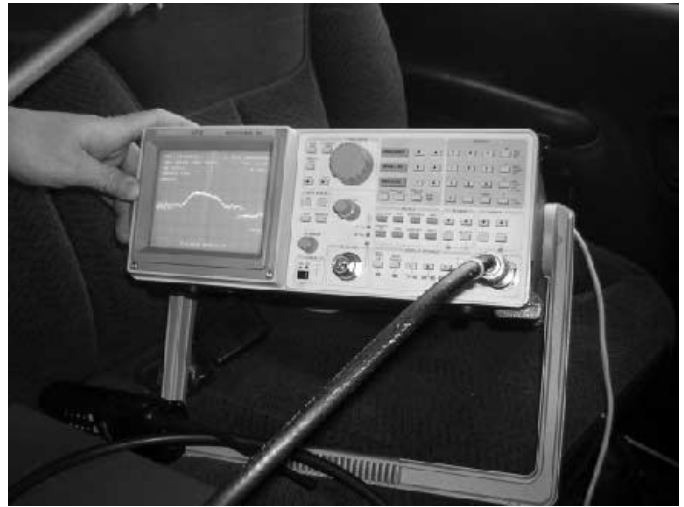
waves collide with multiple objects, they create new signal wave fronts that will have greater strength along the points where the new wavelets are adding in phase.

We certainly had sufficient jagged terrain for diffraction to occur at the location where we took our test measurements. It is difficult to say, however, that knife-edge diffraction offers an adequate explanation since the phenomena we are investigating has also been observed in situations where diffracting terrain was unavailable.

Another factor that affects line-of-sight



Ryan Kolar positioning the dipole antenna for measurement.



The spectrum analyzer showing signal strength.

propagation is the Fresnel Zone effect. The Fresnel Zone is a circular shaped zone (Figure 9) between the transmitter and the receiver, with different regions that affect the signal path. These regions, as shown in Figure 10, can be calculated to show the more crucial paths. The first and second regions are the most critical because they are the most direct paths to the receiver. If an object is conflicting within the first or second region, the signal will change direction, taking multiple paths to the receiver that can add or subtract depending on phase (see Figure 11). The equations for the Fresnel Zone can calculate for interference between the transmitter and receiver, but for our test measurements there were too many unknowns for the calculations to be relevant. The best scenario for no interference between the transmitter and the receiver is to have a smooth valley floor with other earth structures as far from the signal as possible. Otherwise, the signals will reflect and could cause a loss in signal strength at the receiver.

We asked Tom Eckles PE, of Hatfield & Dawson Consulting Engineering, to enter the Sawtell and Jump-Off locations into *Pathloss 4.0* to model the local and distant terrain diffraction characteristics. He determined that diffraction obstructions are in the line of sight to the high mountain sites of Jumpoff Peak and Sawtell Mountain as observed from the distant locations where they have provided communication, and this could account for variations in signal strength as the diffracted-path signal is received.

The diffraction variations were also plotted for both paths (Figures 12 and 13). The figures show a huge signal strength gain as the receive points are moved down the faces of the mountains (about 30 dB within 400 meters of the top). At the top of the mountains, the receive points are flat and within the first Fresnel Zones. As the receive

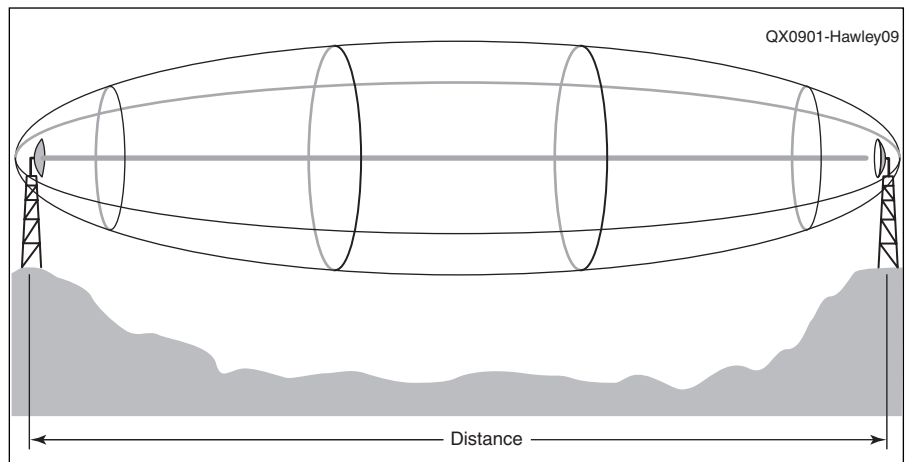


Figure 9 — The Fresnel Zone is a somewhat circular zone between the transmitter and the receiver with different regions that affect the signal path.

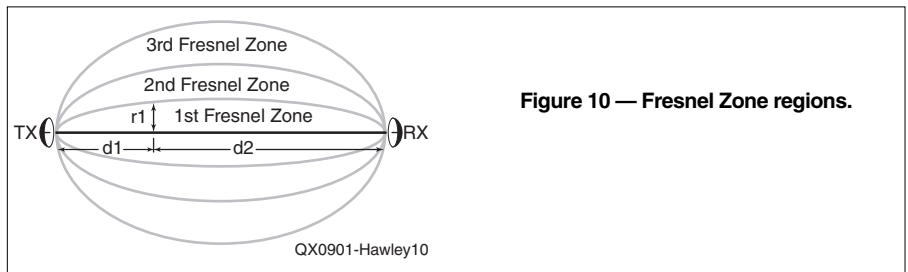


Figure 10 — Fresnel Zone regions.

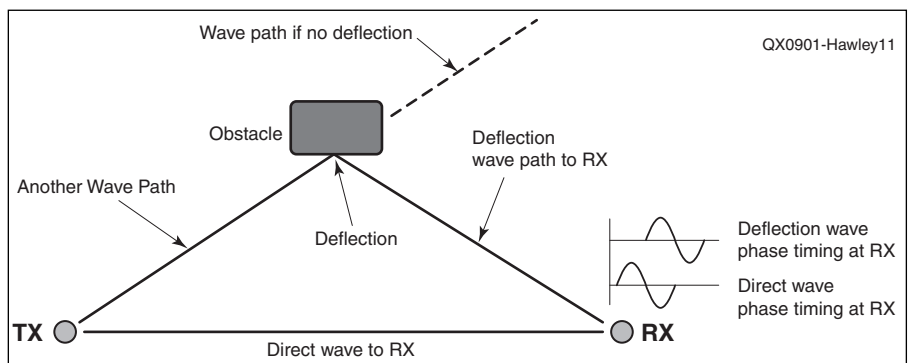


Figure 11 — Direct and indirect signal paths between transmitter and receiver.

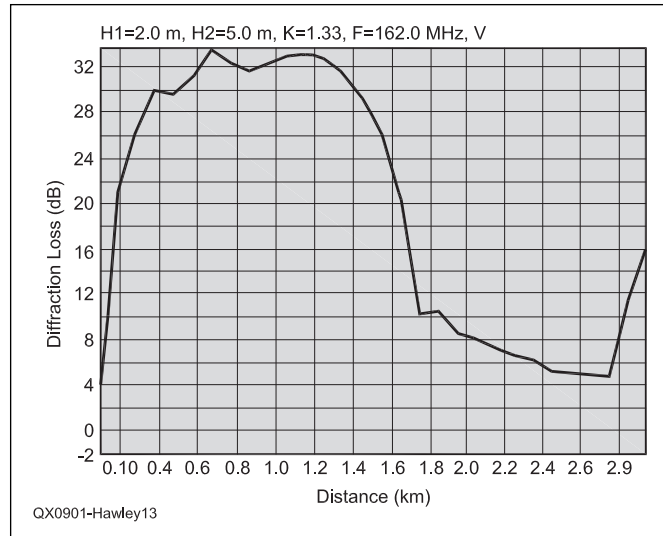
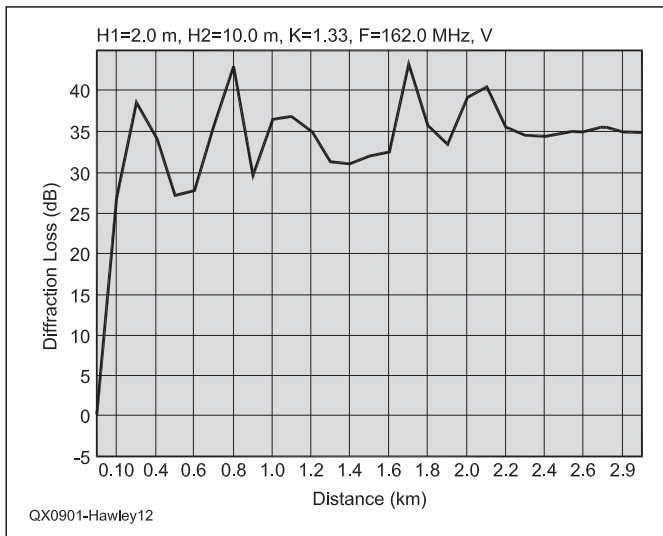


Figure 12 — Calculated loss variations to Jumpoff Peak from Nevada.

Figure 13 — Calculated loss variations to Sawtell Peak from Powell, Wyoming.

points are moved down the mountains, the signal strengths improve because the terrain is sloping and not protruding into the Fresnel Zones to the same degree as before. This causes the Fresnel Zone loss to decline by about 6 dB. With regard to the signal strengths improving on the side of the mountains, Tom Eckles wrote, “Both paths show this effect, so one reason for the difference in signal strength between the tops of the peaks and the lower elevations may be the difference in the overall diffraction path characteristics between the two locations.”


The diffraction variations and the Fresnel Zone effects could potentially explain the propagation phenomenon. If there is less Fresnel Zone protrusion on the side of the mountain and the diffracting signal is improving, the overall result could be greatly enhanced signal strength, which would only occur on the side of the mountain. This scenario only works, however, when the transmitter and receiver are separated by a diffracting path. If there is no diffracting path, the signal is flat and does not give the same results as the position changes. The Fresnel Zone effect could still be a factor, however, if there is no diffraction path.

Conclusion

We believe we have confirmed the signal-strengthening phenomenon, but our tests did not determine the exact means by which this is occurring. We were unable to describe precisely how the signals arrived at our test receivers, which is a critical piece of information. The signals may arrive by multipath propagation, diffraction or by some other undetermined factor. To be able to fully explain this phenomenon, we need to perform more extensive and accurate measurements.

References

Andrews, Russ. “Re: Mountain-top Mystery.” bmgei@earthlink.net. 22 Mar. 2007.
 Brown, Gary. “Re: Propagation.” randem@vt.edu. 17 Feb. 2007.
 Eckles, Thomas, P.E. “Personal Communication.” teckels@hatdaw.com. 12 April 2007.
 Ellis, Larry D. “RE: Propagation.” E-mail to the author. 24 Jan. 2007.
 Fendt, Walter. “Reflection and Refraction of Waves.” Science Joy Wagon. 16 Jan. 1999. Mississippi State University. 23 Mar. 2007. www.sciencejoywagon.com/physicszone/lesson/otherpub/wfendt/huygens.htm.
 “Fresnel Zone.” Wikipedia. 17 March 2007. Wikipedia. 3 May 2007. en.wikipedia.org/wiki/Fresnel_zone.

Hawley, Vance. “Personal Communication.” 8 Jan 2007.
 Lawrey, Eric. “Chapter 1.” OFDM as a modulation for wireless communication. 28 June 2002. Sky DSP. 27 Apr 2007. www.skydsp.com/publications/4thyrthesis/chapter1.htm.
 “Telecom Dictionary.” Telecom Dictionary J.: Higgins International. 25 Apr. www.faxswitch.com/Definitions/telecom_dictionary_k.html.
 Straw, R Dean, N6BV, *The ARRL Antenna Book*. 20th ed. Newington, CT: ARRL, 2005. 23-5 — 23-6.
 “Wireless - Fresnel Zones and their Effect.” 07 February 2006. 07 April 2007 www.zytrax.com/tech/wireless/fresnel.htm. 

Phase Lock With Lower Noise

JWM Engineering Group

Model 1152-ALN

1152MHz

Model 2556-ALN

2556MHz

Model 1152-A

1152, 1268, 1296.8, 1080,

1128, 1104, 1123.2,



Visit our website for complete details, application notes and our other products.



www.jwmeng.com

the left channel of the computer sound card line-in. The CMOS switch multiplexes this Reflect signal with the Through measurement signal originating from mixer M3 and its following amplifier. The multiplexing is necessary, as standard sound cards have only a stereo line-in channel, which can capture just two signals simultaneously. But a third signal, the Reference signal, is required to determine the signal phases. The Reference signal is obtained by mixing the LO and RF DDS signals with M2 and amplifying the output signal with the following operational amplifier. It is then fed into the right channel of the sound card line-in. Note that the VNWA works with an IF of about 1 kHz. The sound card is used as an IF amplifier, so the computer realizes a digital IF filter.

If a Device Under Test (DUT) with two ports is placed between the TX and RX terminals of the VNWA, its scattering parameters S_{11} and S_{21} can be derived from the three measurement signals (Through, Reflect, Reference). By manually turning the device, also S_{12} and S_{22} can be measured.

In the current design, both the CMOS switch and the DDSs are digitally controlled with the computer parallel printer port. Software integration of a USB interface is under development.⁴

Hardware

Figure 2 shows the VNWA2.1 board mounted into a small metal sheet box as seen from top. The left SMA connector is the TX port output. It is directly connected to the internal SWR bridge. The bridge is surrounded by the mixers M1, M2 (left) and the RF-DDS (right). The right SMA connector is the RX port input. Above, the mixer M3 and to the left the LO DDS are found.

The SubD9 connector on the upper side of Figure 2 is the digital control port, which is directly connected to the computer parallel printer port. Also, the power supply is provided through this connector.

The 3.5 mm audio connector on the upper right of Figure 2 is the stereo audio output to be connected to the computer sound card line-in.

The digital part of the board runs on 1.8 V dc and 3.3 V dc. These voltages can directly be obtained with low drop regulators by tapping 5 V dc from a computer USB port. The analog circuitry requires a low noise 6 V dc power supply. Fortunately, it only consumes 10 mA of current. In order to power the whole board from 5 V dc, a low power step up switching regulator was added on the upper left corner of the board. It translates 5 V input voltage to 8.5 V on output, which is then reduced to 6 V dc with a dissipative voltage regulator. This way, a very low noise 6 V power supply could be obtained and no

interference from the switching regulator could be observed. The whole board consumes 350 mA from a 4.5 V supply when overclocked to the limit. A USB port can deliver up to 500 mA and thus is able to power the board.

The printed circuit board is a simple two layer design. Thanks to a lot of brainwork and the terrific layout work of Dan, MØDFI, almost all components and connections could be placed on the top side. Only one semi rigid coax line had to go to the bottom, connecting the TX section mixers with the LO DDS. The

bottom side of the board is almost completely covered with a metal ground plane. The latter is crucial to obtain good isolation between the TX and RX section up into the GHz range. The board size is 100 × 60 mm² and the passive components are mostly 0603 size.

Test results

Figure 3 shows the frequency dependent available signal amplitudes under various operating conditions and the isolation level.

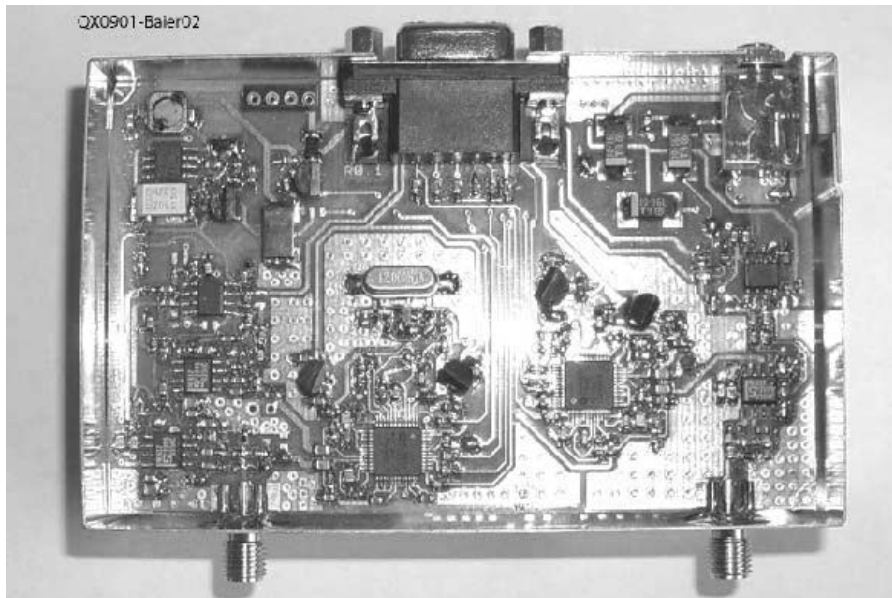


Figure 2 — Top view of the VNWA2.1 board. Board size is 100 × 60 mm².

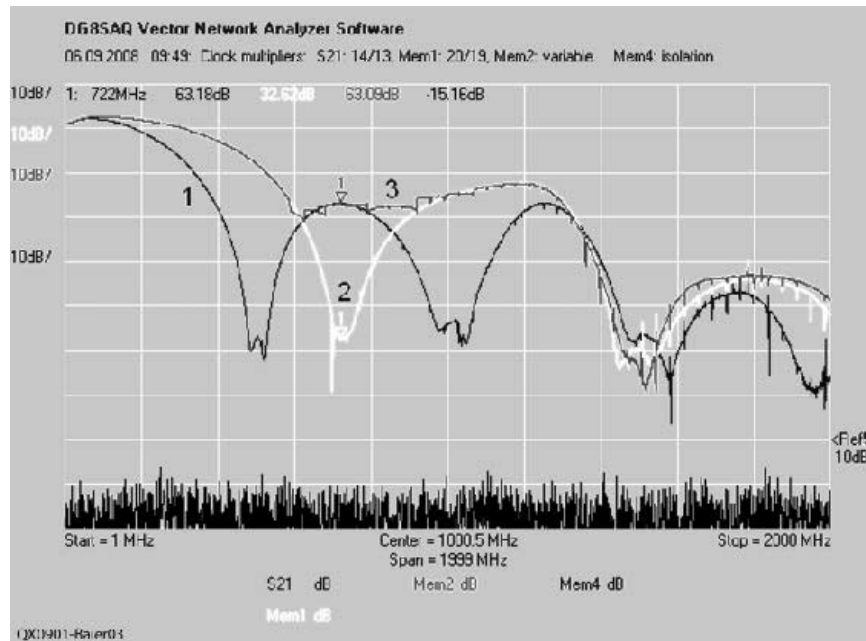


Figure 3 — Frequency dependent available signal amplitudes: Trace 1/S21: clock multipliers are 14/13; trace 2/Mem1: clock multipliers are 20/19; trace 3/Mem2: clock multipliers are dynamically switched during the frequency sweep. Also shown is the noise floor of the system with TX output and RX input isolated (bottom trace, Mem4). Note that traces 2 and 3 exactly match from the starting point up to their first crossing of trace 1.

The isolation trace on the bottom shows, that there is no crosstalk between TX output and RX input measurable within the available dynamic range.

It can be seen from traces 1 and 2, that there are strong alias signals up to 1.3 GHz, which become increasingly noisy with increasing frequency, though. Also, there are distinct notches visible, which result from the fact that the output levels of DDSs drop to zero near integer multiples of their core clock frequency, which is around 500 MHz for trace 1 and 700 MHz for trace 2. The notches are in fact double notches, as the two DDSs run on slightly different clocks and the product of both DDS output powers enters into the signal amplitude. Observe that trace 1 rather nicely fills the first notch of trace 2 and vice versa. This leads to the idea of dynamically switching the DDS clock multipliers during the frequency sweep — in other words, measuring at different frequencies with different clock multipliers. Trace 3 was obtained in this way. Here, the notches are gone altogether and sufficient signal amplitude is obtained for a continuous frequency sweep from audio frequencies up to 1.3 GHz. This idea is also nicely described by Sam Wetterlin.⁵

Figure 4 shows a wideband transmission response of a through calibration standard (traces 1 and 2) and an isolation measurement (trace 3) from 1 MHz to 1.3 GHz obtained with dynamic clock multiplier adaptation during the sweep as described above. Note, that by virtue of a through calibration prior to measurement, all amplitude discontinuities from Figure 3 have vanished. An amplitude accuracy of a few hundredths of a dB and a phase accuracy of a few tenths of a degree are achieved up to 1.3 GHz. Obviously the uncertainties increase and the dynamic range decreases from 500 MHz upwards because of a decreasing signal amplitude. Up to the 70 cm amateur radio band a dynamic range of about 90 dB is achieved. Above that, the dynamic range drops, but still remains around a remarkable 70 dB.

Figure 5 shows a reflection measurement on a 1 m long open ended coaxial cable over the same frequency range as in Figure 4. A SOL (short, open, load) calibration has been performed prior to the measurement. The amplitude plot nicely shows the cable attenuation, which increases with frequency. The amplitude ripple is not a hardware error, but it is caused by port mismatch. This describes the fact that the reflection coefficients of the calibration standards (open, short, load) are not exactly known to the correction algorithm. The Smith chart shows the expected spiral, which has corners due to the rather small number of frequency points (200) used here.

It is quite remarkable, that the instrument works up to 1.3 GHz, as the mixers I used are only specified up to 500 MHz. The latter originally was the targeted upper frequency limit. The degradation of the mixer performance leads to measurement errors beyond 500 MHz, though. Still, the instrument is sufficient for most ham purposes up into the

23 cm range, as hams usually don't require extremely high precision results.

It is to be noted that there are also measurement errors due to interference at some integer multiples of the DDS input clock frequencies. Remember that the design contains no signal shaping RF filters whatsoever. The interferences were mostly avoided so far by

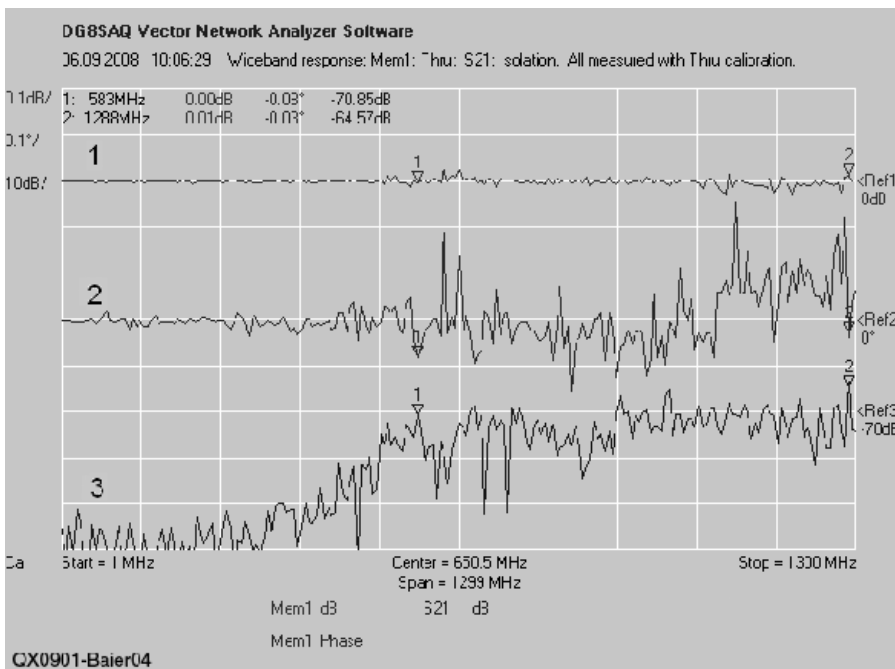


Figure 4 — Wideband transmission response of a through calibration standard from 1 MHz to 1.3 GHz obtained with dynamic clock multiplier adaptation during the sweep (trace 1 / Mem1-dB: amplitude response; trace 2 / Mem1-Phase: phase response) and wideband isolation (trace 3 / S21-dB). A through calibration has been performed prior to measurement.

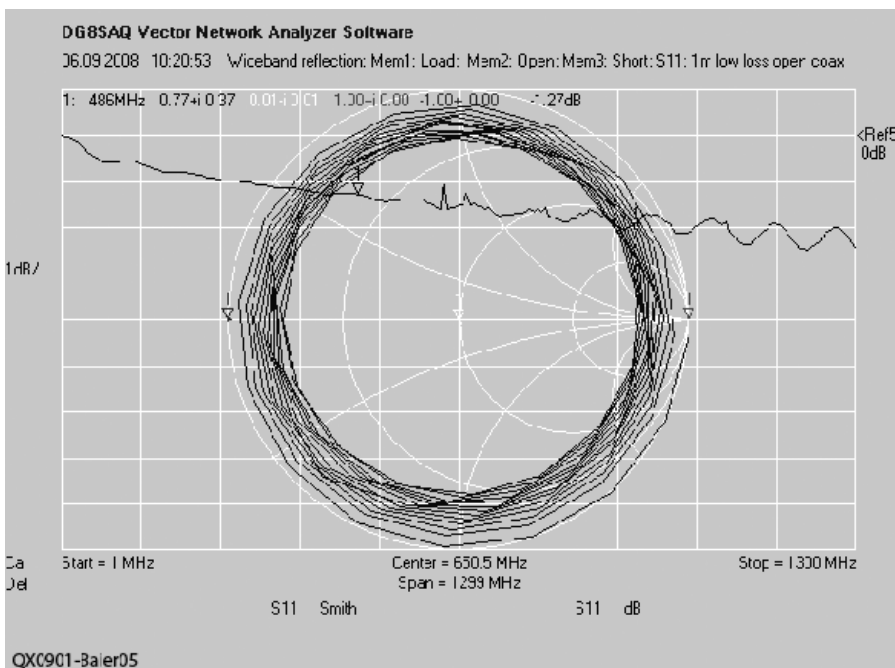


Figure 5 — Reflection measurement on a 1 m open ended coaxial cable from 1 MHz to 1.3 GHz. A SOL (short, open, load) calibration has been performed prior to measurement.

selection of the measurement frequency grid. One such interference can be seen in Figure 6, where it manifests itself as a peak with about 0.15 dB amplitude in trace 2 at about 360 MHz (= half of the DDS core clock frequency). It is caused by interference of two aliases, which happen to cross there, when the DDSs are swept.

Figure 6 shows a high precision comparison of reflection coefficients between VNWA2.1 and Rohde & Schwarz ZVM measurements on a 30 cm open ended low loss semi rigid coaxial cable in the fundamental VNWA frequency range up to 600 MHz. In the Smith chart, only the VNWA2.1 data is shown, since the data of both instruments are so similar, that they cannot be distinguished there. This is also seen from the amplitude traces 1 and 2. Note, that their scales are only 0.02 dB per division, demonstrating, that the VNWA2.1 works very accurately up to 500 MHz. Note, that it is most challenging to precisely measure reflection coefficients near magnitude 1.

Figure 7 shows the wideband measurement of a “real” device, namely a 1 GHz SAW filter. Also, this measurement has been obtained by dynamically switching the clock multipliers during the sweep. Obviously, the dynamic range of the instrument is still good enough to measure such a device at 1.3 GHz.

Due to the huge usable continuous frequency range from 1 kHz to 1.3 GHz, it makes sense to perform measurements on a logarithmic frequency grid with the VNWA2.1, in order to obtain Bode plots. A simple example is shown in Figure 8. It shows a Bode plot of the transmission through an SMA T, terminated with a 120 nH SMD inductor at the base of the T (S_{21} , trace 2) compared to the transmission of the through calibration standard (Mem4, trace 1) from 1 kHz to 1.3 GHz. In the lower frequency region, the ohmic resistance of the inductor limits the attenuation to about 40 dB. The mid frequency region shows the expected linear decrease of the attenuation on the doubly logarithmic scale, due to the increasing ac resistance of the inductor with increasing frequency. Traces 3 and 4 (Cus2 and Cus4) show two different simulations of the transmission through the T. Trace 3 uses the actually measured reflection coefficient of the inductor, which is stored in Mem1, to calculate the T transmission. Trace 4 uses a simple model of an ideal 120 nH inductor connected in series with a resistor of 0.26 Ω to simulate the T transmission. Trace 5 (Mem1) actually shows the measured series resistance of the inductor. Note, that all simulations have been performed within the VNWA measurement software, which includes a parser and compiler for complex mathematical expressions.

So, measurement results can be manipulated in real-time during the sweep or simulation traces can be calculated and displayed in customized ways. Figure 9 shows the input mask of the mathematical expression parser containing the impedance formula of the lossy 120 nH inductor normalized to 50 Ω

used in the simulation trace 4 in Figure 8.

Summary and outlook

I have described a very simple computer-based vector network analyzer, which operates on a continuous frequency band from

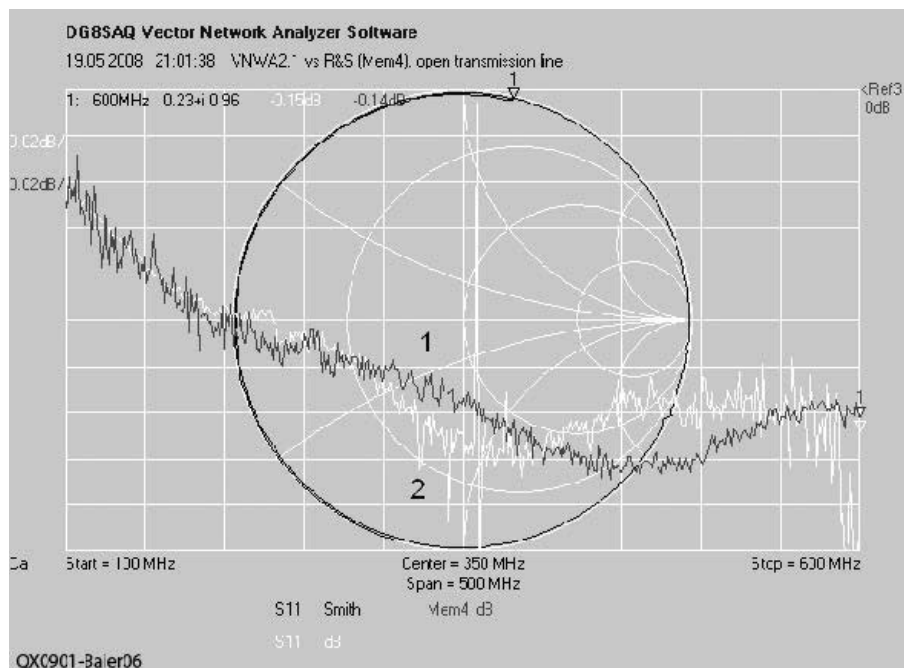


Figure 6 — High precision comparison of reflection coefficients between VNWA2.1 and Rohde & Schwarz ZVM measurements on a 30 cm open ended low loss semi rigid coaxial cable in the fundamental VNWA frequency range up to 600 MHz. Trace 1 / Mem4: ZVM; Trace 2 / S11: VNWA2.1.

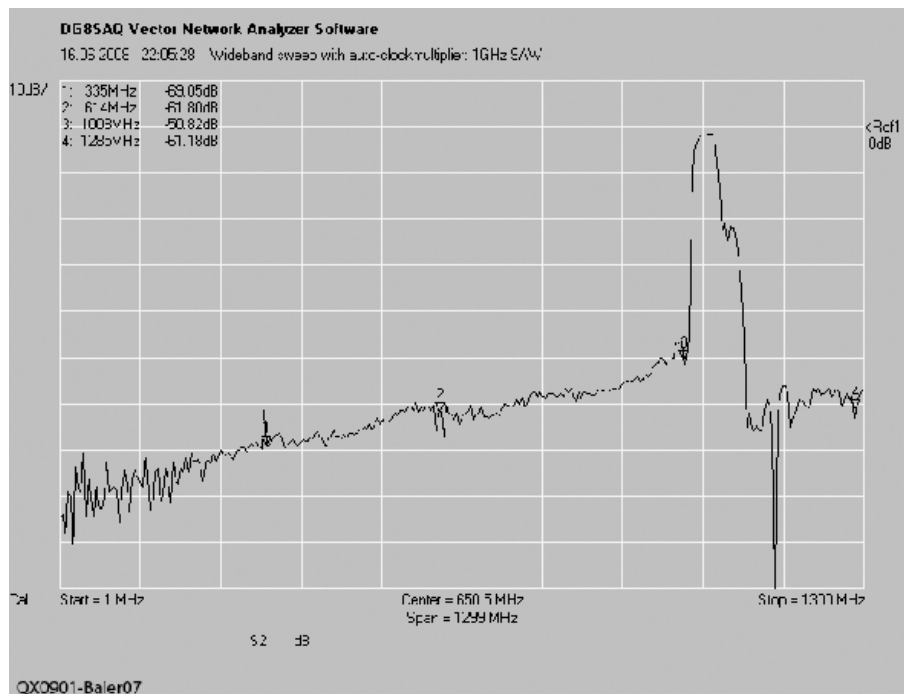


Figure 7 — Wideband measurement of a 1 GHz SAW filter. The filter isolation of 60 dB at 1.3 GHz can still be measured.

1 kHz to 1.3 GHz, thus still covering the 23 cm Amateur Radio band. The wide operating frequency range was obtained by deliberately using aliasing frequencies of the built-in direct digital synthesizers and by dynamically switching their clock frequencies during the measurement sweep. The design is implemented on a single two layer printed circuit board with all components placed on the top layer. The board is powered by a single non-stabilized 4.5 V to 5.5 V dc source consuming a current of 350 mA.

The design is very experimental, as the DDS chips and the mixers are operated well outside their specification limits. Therefore, I do not intend to provide preassembled boards. Nevertheless, I would like to give experimenters the possibility to work with such an instrument by providing unassembled printed circuit boards. Good experience, steady hands and an excellent eye sight are required for manual assembly. Look at my Web site for details and for my most recent VNWA software.^{6,7}

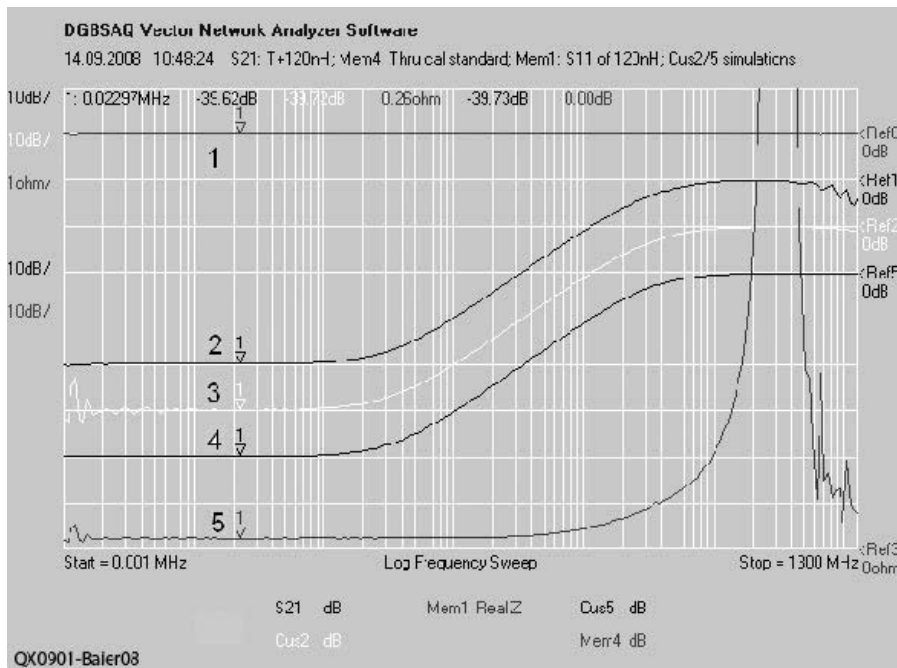


Figure 8 — Bode plot of the transmission through an SMA connector, terminated with a 120 nH SMD inductor at the base of the T (S21, trace 2) from 1 kHz to 1.3 GHz. Also shown are two simulations of the transmission (Cus2, trace 3, calculated from measured S11 of the inductor), (Cus5, trace 4, calculated with model inductor 120 nH in series with 0.26 Ω) and the transmission of the through calibration standard (Mem4, trace 1). Note that all mentioned traces have been shifted in reference level positions for better visibility. Mem1, trace 5 shows the measured real part of the inductor impedance.

A picture is worth a thousand words...

With the
ANTENNA MODEL™
wire antenna analysis program for Windows you get true 3D far field patterns that are far more informative than conventional 2D patterns or wire-frame pseudo-3D patterns.

Describe the antenna to the program in an easy-to-use spreadsheet-style format, and then with one mouse-click the program shows you the antenna pattern, front/back ratio, front/rear ratio, input impedance, efficiency, SWR, and more.

An optional **Symbols** window with formula evaluation capability can do your computations for you. A **Match Wizard** designs Gamma, T, or Hairpin matches for Yagi antennas. A **Clamp Wizard** calculates the equivalent diameter of Yagi element clamps. **Yagi Optimization** finds Yagi dimensions that satisfy performance objectives you specify. Major antenna properties can be graphed as a function of frequency.

There is **no built-in segment limit**. Your models can be as large and complicated as your system permits.

ANTENNA MODEL is only \$90US. This includes a Web site download **and** a permanent backup copy on CD-ROM. Visit our Web site for more information about **ANTENNA MODEL**.

Teri Software
P.O. Box 277
Lincoln, TX 78948

www.antennamodel.com
e-mail sales@antennamodel.com
phone 979-542-7952

I want to thank Dan, M0DFI, for a great job laying out the circuit board. I also want to thank Hermann, DF2DR, Andreas, DL1TT, and Ferdinand, DB2SG for great support on board production and for beta-testing the project and Stefan Fuchs for his support with the ZVM reference measurements.

Notes

¹Professor Dr. Thomas C. Baier, DG8SAQ, "A Low Budget Vector Network Analyzer for AF to UHF," *QEX*, Mar/Apr 2007, ARRL. See

also www.mydarc.de/DG8SAQ/VNWA/

²Professor Dr. Thomas C. Baier, DG8SAQ, "Letters to the Editor," *QEX*, Jul/Aug 2007, ARRL.

³www.analog.com/en/rfif-components/direct-digital-synthesis-dds/ad9859/products/product.html

⁴Professor Dr. Thomas C. Baier, DG8SAQ, "A Low-Cost, Flexible USB Interface," *QEX*, Jan/Feb 2008, ARRL, pp 11-15.

⁵Sam Wetterlin, "Using DDS Aliases to Extend the Frequency Range," www.wetterlin.org/sam/AD9952/MultipleClockAliases.pdf

⁶www.mydarc.de/DG8SAQ/NWA.html

⁷Please see www.SDR-kits.net or contact sdrkits@gmail.com for information about the availability of circuit boards and kits. Details are being worked out at press time.



Figure 9 — VNWA software input mask showing the impedance formula of the lossy 120 nH inductor normalized to 50 Ω used in the simulation trace 4 of Figure 8.

Professor Dr. Thomas Baier, MA, teaches physics, mathematics and electronics at the University of Applied Sciences in Ulm, Germany. Before his teaching assignment, he spent 10 years of work on research and development of surface acoustic wave filters for mobile communication with Siemens and EPCOS. He holds 10 patents.

Tom, DG8SAQ, has been a licensed radio amateur since 1980. He prefers the soldering iron to the microphone, though. His interests span from microwave technology to microcontrollers. Lately, he has started Windows programming with Delphi. Tom spent one year in Oregon USA rock climbing and working on his master's degree.



Octave for SWR

Let Octave perform the calculations for SWR and line loss, to verify an equation and graph.

We can often use a tool like *GNU Octave* to refute, validate, or just study various published formulas and assertions.¹ *The ARRL Antenna Book* asserts, for instance, that Equation 16 and Figure 14 on Page 24-10 give the additional loss that must be added to the matched line loss of a transmission line to determine the total line loss of the transmission line, when the load (antenna) connected to the line is not matched to the impedance of the line.² The graph also appears in *The 2009 ARRL Handbook* and in older ARRL publications at least as early as 1952.^{3,4,5} Equation 1, below is Equation 16 and Figure 1 in this article is a reproduction of the graph.

$$\text{Total Loss (dB)} = 10 \log \left(\frac{a^2 - |\rho|^2}{a(1 - |\rho|^2)} \right) \quad [\text{Eq 1}]$$

where $a = 10^{ML/10}$ = matched-line loss ratio.

Keep in mind that we can calculate the reflection coefficient, ρ , from the SWR.

$$|\rho| = \frac{\text{SWR} - 1}{\text{SWR} + 1} \quad [\text{Eq 2}]$$

First, we can use *Octave* to verify that the graph accurately represents Equation 1. Although we could write a script file, this is a good application for use of *Octave's* interactive mode. We'll simply type the equations from the *Octave* command line as:

```
octave:1> m_loss_dB = 2;
octave:2> SWR = 4;
octave:3> a = 10 ^ (m_loss_dB / 10);
octave:4> rho = (SWR - 1) / (SWR + 1);
octave:5> total_loss_dB = 10 * log10((a ^ 2 - rho ^ 2) / (a * (1 - rho ^ 2)))
total_loss_dB = 3.2664
```

¹Notes appear on page 40.

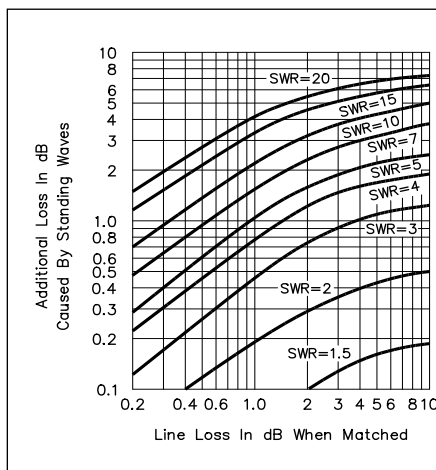


Figure 1 — Additional line loss due to standing waves (SWR, measured at the load). To determine the total loss, in dB, add the matched-line loss to the value from this graph.

The semicolons at the ends of most of the lines suppress outputs from those calculations. We'll omit the semicolon from the expression for *total_loss_dB*, and its value will be printed as soon as we execute that expression by pressing ENTER. By using the command line editor feature of *Octave*, we can scroll back to expressions for *m_loss_dB*, *SWR*, *a*, and ρ , change them and re-execute their code, and then execute the code for *total_loss_dB* again for different values. Doing this for several values of loss and SWR demonstrates that Figure 1 does represent Equation 1 very well.

Technically, we should have considered the fact that the absolute value of ρ is used in Equation 1. If we restrict our SWR values to positive real numbers greater than or equal to 1, though, we can assume that taking the absolute value of ρ — *abs(rho)* in *Octave* — is unnecessary.

What about the mismatch between the transmitter and the line, though? Won't that determine how much power is redirected

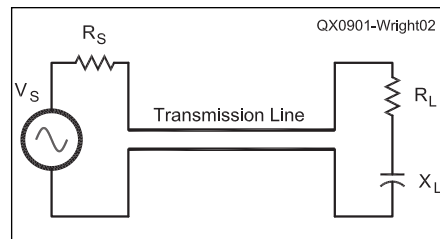


Figure 2 — Generator (transmitter), transmission line, and load (antenna).

toward the load? Let's assume that we have a transmitter with a source impedance of 50 Ω (*RS* in Figure 2) connected to an antenna through a 50 Ω transmission line. There is, therefore, no mismatch between the transmitter and the line. If there is a mismatch at the load end of the line, the power reflected from the load will pass back along the line to the transmitter and will all be absorbed by the source impedance. None of the returned power will therefore be re-reflected back toward the load.

Now let's change *RS* in Figure 2 to 0 Ω . There will, of course, be more power transmitted toward the load, but we can reduce *VS* by half and cause the same power to be transmitted toward the load as was transmitted by the 50 Ω transmitter. This mismatch between the load and the transmitter will provide complete re-reflection of the reflected wave and more power will reach the load than was the case when the source and line were matched.

Our concern is bolstered by the fact that a procedure and equations in *Reference Data for Radio Engineers* make provision for different losses depending on whether there are mismatches at one end only or at both ends of a transmission line.⁶ So how can Equation 16 and Figure 14 of *The ARRL Antenna Book* ignore the interaction between mismatches? Have we found a flaw in a concept that has been around for decades?

We can look into this matter by using a *GNU Octave* script from one of our previ-

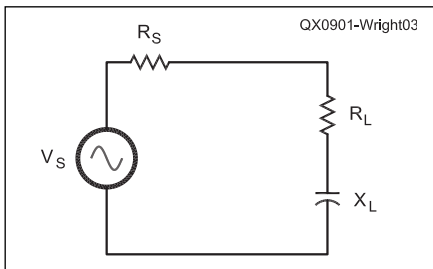


Figure 3 — Generator (transmitter) connected directly to load (antenna)

ous studies.⁷ The code in this script treats the transmission line as a T-equivalent network, and we'll modify the code a bit to produce the outputs we would like to see for this study. See Table 1. We can calculate the power transmitted through any point in the circuit, if we know the current at that point and the resistive component of the "downstream" impedance, by applying the formula $P = I^2R$.

Since there are various measures of loss available, we'll use several of them. We'll calculate the insertion loss by first calculating the power transferred to the antenna without a transmission line, as shown in Figure 3, and then the power transferred to the antenna with the transmission line interposed between the transmitter and the antenna.⁸ The insertion loss is expressed in dB as $10 * \log_{10} (P1 / P2)$ where $P1$ is the power in the antenna with no line and $P2$ is the power in the antenna with the line in place. The insertion loss is intended to measure the performance degradation caused by inserting a particular network, circuit or, as in our case, transmission line in between a source and a load.

We'll calculate the transducer loss by first calculating the maximum available power (See Note 8.): $P_m = VS^2 / 4RS$. We'll then compare the maximum available power with the actual power as $10 * \log_{10} (P_m / P2)$. The transducer loss is intended to compare the power in the load in a circuit under actual operating conditions with the power that the same source could provide to an ideal load.

We'll also use the line loss, sometimes called "power loss" or "transmission loss."^{9,10} This loss is of interest because it's the one specified in Figure 14 of *The ARRL Antenna Book*. The *Antenna Book* differentiates between the matched line loss of the transmission line and the total loss, which includes the line loss of the line including additional losses imposed by mismatches. This loss is the difference in powers, expressed in dB, transmitted in a single direction at two different points along a line or in a circuit or network. The line loss of the transmission line in Figure 2 is calculated as $10 * \log_{10} (P3 / P2)$ where $P3$ is the power transmitted into the line by the transmitter and $P2$ is, as

**Table 1
Octave Code for Additional Transmission Line Loss Calculations**

```

#!/usr/bin/octave -qf
#
# Print header

printf("\n\n      *** TRANSMISSION LINE CALCULATIONS ***\n\n");

# Characteristics of transmission line

f = 7.01; # FREQUENCY IN MHz
d = 30; # LENGTH OF LINE IN FEET
a = 2.0; # LINE LOSS IN dB PER 100 FEET
v = 83; # VELOCITY FACTOR AS A PERCENTAGE
Zo = 50; # CHARACTERISTIC IMPEDANCE IN OHMS

# Specify source (transmitter) and load (antenna)

VS = 2.0;
RS = 50.0;
Rt = 25; # REAL PART OF TERMINATING IMPEDANCE IN OHMS
Xt = -37.0; # IMAGINARY PART OF TERMINATING IMPEDANCE IN OHMS

# Convert inputs as required

a = a ./ 1e2; # convert dB per 100 feet to dB per foot
adB = a; # Save a in dB for further use
a = 0.1151 * a; # convert dB to nepers
c = 9.836e8; # speed of light in feet per second
lambda = c / (1e6 * f); # wavelength of signal in vacuum
lambda = (v / 1e2) * lambda; # adjust lambda for velocity
B = (2 * pi) / lambda; # calculate Beta
ZL = Rt + j * Xt; # calculate complex terminating impedance

# Calculate elements of T-equivalent network

# ZA = input series element
# ZB = output series element
# ZC = shunt element

ZA = Zo * tanh((a + j * B) * d / 2.);
ZB = ZA;
ZC = Zo / sinh((a + j * B) * d);

# Prepare matrices for solution of currents

right_side = [RS + ZA + ZC, -ZC; -ZC, ZB + ZC + ZL];
left_side = [VS; 0];

# Solve for currents

denom = det(right_side);
for m = 1: rows(right_side)
    numerator = right_side;
    for n = 1: rows(right_side)
        numerator(n, m) = left_side(n);
    endfor
    current(m) = det(numerator) / denom;
endfor

```



```

# Calculate SWR and reflection coefficient at antenna terminals

refl_coef = (ZL - Zo) / (ZL + Zo);
SWR = (1 + abs(refl_coef)) / (1 - abs(refl_coef));
printf("\n SWR = %-8.5g", SWR);

# Calculate input impedance

Zd = Zo * ((ZL * cosh((a + j * B) * d) + Zo * ...
sinh((a + j * B) * d)) / (ZL * sinh((a + j * B) * d) ...
+ Zo * cosh((a + j * B) * d)));
for k = 1:columns(Zd)
    if imag(Zd(1,k)) < 0
        printf("\n INPUT IMPEDANCE = %8.5g - j%-8.5g", ...
            real(Zd(1,k)), abs(imag(Zd(1,k))));
    else
        printf("\n INPUT IMPEDANCE = %8.5g + j%-8.5g", ...
            real(Zd(1,k)), imag(Zd(1,k)));
    endif
endfor

# Calculate input power to line from source

Pwr_in = abs(current(1)) ^ 2 * real(Zd);

# Calculate power delivered to load

Pwr_load = abs(current(rows(right_side))) ^ 2 * real(ZL);

# Calculate power that would be delivered to the load
# if the transmission line were omitted

I_no_line = VS / (RS + Rt + j * Xt);
Pwr_load_no_line = abs(I_no_line) ^ 2 * Rt;

# Calculate power delivered by source voltage

Pwr_source_v = abs(VS / (RS + Zd)) ^ 2 * real(RS + Zd);

# Calculate total line loss

Line_loss = 10 * log10(Pwr_in / Pwr_load);
printf("\n T-NETWORK TOTAL LINE LOSS (in dB) = %-8.5g", Line_
loss);

# Calculate ARRL Antenna Book Total Loss (Eq. 16)

mllr = 10 ^ (d * adB / 10);
Total_loss = 10 * log10((mllr ^ 2 - abs(refl_coef) ^ 2) / ...
(mllr * (1 - abs(refl_coef) ^ 2)));
printf("\n ARRL EQ. 16 TOTAL LOSS (in dB) = %-8.5g", Total_loss);

# Calculate insertion loss

Insert_loss = 10 * log10(Pwr_load_no_line / Pwr_load);
printf("\n INSERTION LOSS (in dB) = %-8.5g", Insert_loss);

# Calculate transducer loss

max_avail_pwr = VS ^ 2 / (4 * RS);
Transducer_loss = 10 * log10(max_avail_pwr / Pwr_load);
printf("\n TRANSDUCER LOSS (in dB) = %-8.5g\n\n", Transducer_
loss);

# end SWR_1.m script

```

above, the power transferred to the antenna by the line. We'll call this "total line loss" in our code to be explicit.

The *Octave* code for calculating these measures of a transmission line appears in Table 1. Table 2 tabulates various inputs to and outputs from the code. As we found when we worked with *The ARRL Antenna Book* equation from the *Octave* command line, we get really good agreement between calculations of line loss using the T-network and using Equation 16 from *The ARRL Antenna Book*. Since we aren't anticipating using the code to operate on matrices, we'll omit the matrix dot operators that we've used in some of the previous versions of this code.

Note from Table 2 that, for electrically long lines, the insertion loss and the transducer tend to converge toward the line loss. For short lines, the insertion loss will generally be lower than the line loss and the transducer loss will be higher than the line loss when the load end of the line is mismatched.

Does all this shoot down our logical deductions about the interactions between the source and the load with respect to an increase in loss with SWR? Well, sort of: by experimenting with various source and load impedances, we can observe that there are changes in transducer loss and insertion loss with changes in the mismatch at either end of the transmission line. The line loss, though, responds only to changes at the load end. This verifies, along with the numeric results, Equation 16 and Figure 14 of *The ARRL Antenna Book*. The line loss "cares" nothing about the source impedance because it sees energy flowing from the source, but doesn't care about the internal details of that source. The line has no way to "know" whether the source is transmitting all the energy for the first time or is re-reflecting energy returned from the load end mismatch.

What about, though, the treatment of mismatches at both the source and the load in *Reference Data for Radio Engineers*? The loss being compared there is the transducer loss so there is no conflict with our conclusions.

Note that it is difficult to directly measure insertion loss when the "circuit" is such that connecting the source directly to the load is difficult, or impossible, as is often the case with a transmitter and an antenna connected via a transmission line. It would be possible to measure transducer loss, but not very convenient since a relatively precise conjugate load capable of dissipating the output power of the transmitter would have to be provided. For practical work, then, the line loss, which can readily be measured if instrumentation can be brought to the appropriate points along the line, would seem to be the most appropriate measure of loss for radio trans-

mission line work. In many cases, where the SWR is not high, the total line loss can be approximated well by the matched loss of the transmission line.

Notes

- ¹John W. Eaton, *GNU Octave Manual*, Network Theory Limited, 1997 (see www.octave.org).
- ²R. Dean Straw, N6BV, Ed, *The ARRL Antenna Book*, 21st Edition, The American Radio Relay League, Inc, 2007, p 24-10.
- ³Mark Wilson, K1RO, Ed, *The ARRL Handbook for Radio Communications*, 2009, 86th Edition, The American Radio Relay League, Inc, 2008, pp 21.6-21.8.
- ⁴*The Radio Amateur's Handbook*, 29th Edition, The American Radio Relay League, Inc, 1952, page 316.
- ⁵Jerry Hall, K1TD, Ed, *The ARRL Antenna Book*, 13th Edition, The American Radio Relay League, Inc, 1974, page 82.
- ⁶*Reference Data for Radio Engineers*, Fourth Edition, International Telephone and Telegraph Corporation, 1956, pages 569 through 573.
- ⁷Maynard Wright, W6PAP, "More Octave for Transmission Lines," *QEX*, Jan/Feb 2008, pp 26-31.
- ⁸Technical Personnel, American Telephone and Telegraph Company, Bell Telephone Companies, and Bell Telephone Laboratories, *Telecommunications Transmission Engineering, Volume 1 - Principles*, Western Electric, 1974, pages 45-47: the definitions here are actually of

Table 2

SWR	1:1	1:1	3.2914	3.2914
Frequency (MHz)	7.01	7.01	7.01	7.01
Length of line (feet)	400	400	100	30
Attenuation of line (dB/100 feet)	2.0	2.0	2.0	2.0
Velocity (%)	83	83	83	83
Z ₀ (Ω)	50	50	50	50
VS (V)	2.0	2.0	2.0	2.0
RS (Ω)	50	0.05	50	50
Rt (Ω)	50	50	25	25
Xt (Ω)	0	0	-j37	-j37
T-net total line loss (dB)	7.998	7.998	2.9337	0.99898
ARRL total loss (dB)	8	8	2.9343	0.99921
Insertion loss (dB)	7.998	7.998	1.9995	0.59985
Transducer loss (dB)	7.998	31.986	3.457	2.0574

gains, not losses. If they are taken to be definitions of transfer functions, they can be applied to losses as well, and the explanations in this reference are particularly clear.

- ⁹IEEE Std 100-1988, *Standard Dictionary of Electrical and Electronics Terms*, Fourth Edition, The Institute of Electrical and Electronics Engineers, Inc., 1988.
- ¹⁰Lawrence A. Ware, EE, PhD, Henry R. Reed, EE, PhD, *Communication Circuits*, Third Edition, John Wiley & Sons, 1942, page 123.

Maynard Wright, W6PAP, was first licensed in 1957 as WN6PAP. He holds an FCC

General Radiotelephone Operator's License with Ship Radar Endorsement, is a Registered Professional Electrical Engineer in California, is an ARRL Member, and is a Life Senior Member of IEEE. Maynard has been involved in the telecommunications industry for over 44 years. He has served as technical editor of several telecommunications standards and holds several patents. He is a Past Chairman of the Sacramento Section of IEEE. Maynard is a member of the North Hills Radio Club in Sacramento, California, where he currently serves as Secretary/Treasurer.

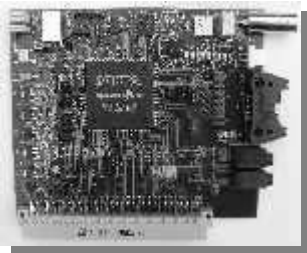
QEX



HPSDR is an open source hardware and software project intended to be a "next generation" Software Defined Radio (SDR). It is being designed and developed by a group of enthusiasts with representation from interested experimenters worldwide. The group hosts a web page, e-mail reflector, and a comprehensive Wiki. Visit www.hpsdr.org for more information.

TAPR is a non-profit amateur radio organization that develops new communications technology, provides useful/affordable hardware, and promotes the advancement of the amateur art through publications, meetings, and standards. Membership includes an e-subscription to the *TAPR Packet Status Register* quarterly newsletter, which provides up-to-date news and user/technical information. Annual membership costs \$20 worldwide. Visit www.tapr.org for more information.

NEW!

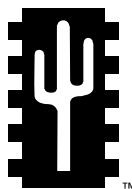


MERCURY
100kHz-55MHz Direct Sampling Receiver

TAPR is proud to support the HPSDR project. TAPR offers two HPSDR kits and four fully assembled HPSDR boards. The assembled boards use SMT and are manufactured in quantity by machine. They are individually tested by TAPR volunteers to keep costs as low as possible. A completely assembled and tested board from TAPR costs about the same as what a kit of parts and a bare board would cost in single unit quantities. TAPR is non-profit, and the proceeds help fund new projects.

HPSDR Kits and Boards

- **PINOCCHIO** passive extender kit
- **ATLAS** backplane kit
- **OZYMANDIAS** USB 2.0 interface
- **JANUS** A/D - D/A converter
- **PENELOPE** 1/2 W transmitter



TAPR

PO BOX 852754 • Richardson, Texas • 75085-2754

Office: (972) 671-8277 • Fax: (972) 671-8716 • e-mail: taproffice@tapr.org

Internet: www.tapr.org • Non-Profit Research and Development Corporation

A Protocol for Multicast Weather Data Distribution Over AX.25

This article is reprinted with the author's permission from The 27th ARRL and TAPR Digital Communications Conference Proceedings. The DCC was held in Chicago, Illinois, Sep 26-28, 2008.

Abstract

A protocol is described for use on top of AX.25 in order to form multicast, push-architecture, regulatory compliant, radio weather data links. This protocol is especially suited to disseminating NEXRAD weather surveillance radar data over 1200 baud AFSK VHF radio links. Further, a larger scale system for distributing weather data using various means, among them radio links using this protocol, is discussed along with the current status of its implementation. Using the defined protocol over a radio link along with other system components, it is possible to ingest NEXRAD data from fast, operational data sources and to relay that data to severe weather spotter resources in a timely fashion, even when those resources have no access to the Internet or other data network infrastructure.

Key Words

NEXRAD, AX.25, RDTP, NOAAPORT, SKYWARN

Introduction

In the United States many Amateur Radio hobbyists participate in the National

Weather Service's SKYWARN™ program. Nationwide, this program has nearly 280,000 trained severe weather spotters.¹ While not all of these are Amateur Radio volunteers, it is evident that a large group of them, in fact, are amateurs. When considering the future direction of amateur digital communications, technologies supporting volunteer severe weather spotters should be seriously considered.

An architecture for a system which uses amateur packet radio as a physical link to disseminate real time NEXRAD weather surveillance radar data, as well as other relevant products, in support of SKYWARN operations was previously presented in the Sep 2004 issue of *QST*.² Implementation challenges have since been resolved and detailed design has been completed. A protocol is now presented for use above AX.25 to support this data dissemination system. The protocol, called Radar data Datagram Transport Protocol over AX.25 (hereafter RDTP/AX.25), supports multicast or point-to-point

topology, allows data to be pushed asynchronously as it is received from upstream sources, and maintains two-way communication for compliance with 47CFR97. Further, the status of this project is discussed with a focus on new developments since the publication of my Sep 2004 *QST* article.

Design Inputs

AFSK and FSK modems with typical data rates of 1200 and 9600 baud are readily available in amateur equipment, especially when integrated into hardware Terminal Node Controllers (TNCs) or software AX.25 protocol implementations. Making use of this equipment simplifies the constructions of an RDTP/AX.25 station. However, the requirement that this protocol be used over AX.25 is introduced. Further, the maximum frame length is constrained.

The RDTP/AX.25 protocol then must meet these requirements:

- Be implemented on top of AX.25.
- Operate at frame sizes less than 256 bytes.
- Viably relay at least two 5 kB messages

¹Notes appear on page 47.

Table 1
RDTP Call Sign Field Format

Bytes		Bits	Description	Value	Notes
First	Last				
0	6	All	Call sign ASCII text	ASCII string, unused bytes filled with 0x00.	Left (byte 0) justified.
7	7	7-4	Reserved	0 bits	Always fill with zeroes.
		3-0	Station SSID	16-bit unsigned integer SSID value.	

Table 2
RDTP Frame Layer Header and Payload

Bytes		Bits	Description	Value	Notes
First	Last				
0	3	All	Protocol identifier sequence	Literal ASCII 'R' 'D' 'T' 'P'	
4	4	All	Protocol version code	Literal 0x00	This field is intended to ease protocol version changes.
5	5	7	From call/SSID present flag	1: From/Transmitting station call sign present 0: From call sign not present	
		6	N+1 parity data flag	1: This frame is N+1 parity data 0: This frame is not N+1 parity data (a normal frame)	
		5-4	Reserved	0	Always fill with zeroes
		3-0	From station SSID	4-bit unsigned integer SSID value	Used only if byte 5, bit 7 is set
6	11	All	From call sign without SSID	Call sign as specified in Table 1 without SSID	Used only if byte 5, bit 7 is set
N-5 6/12	N-5 6/12	All	Message sequence number	Increments per message from 0x00 through 0xFF, then rolls around back to 0x00.	
N-4 7/13	N-4 7/13	All	Frame sequence number	Increments per frame from 0x00	Reset at 0x00 for each message
N-3 8/14	N-3 8/14	All	Frames in message	Total number of frames in this message minus one	Subtracting one makes use of the value 0x00 and slightly expands the maximum data length RDTP is capable of handling
N-2 9/15	N-2 9/15	All	Compression code	0: No compression 2: Bzip2	Use of libbz2 is recommended. Compression applies only to the payload.
N-1 10/16	N-1 10/16	All	Frame layer payload length	The length in bytes of the payload section of this RDTP frame	For example, 0x00 would indicate no data section present, but would likely never be used.
N	N + data length		Frame layer payload (data section)	A segment of a sequence of RDTP logical entities. These segments will be concatenated by the receiver in the order of frame sequence number, lowest sequence number first.	This is the content of the RDTP message. It must consist of RDTP logical entity blocks.

received every five minutes.

- Support multicast operation to multiple receivers
- Maintain two-way communications
- Be designed to simplify implementation on both *Windows* and *Linux* operating systems^{3,4}

The protocol should be able to handle various types of weather data, as long as the individual message data lengths are reasonable. This should include radar and text data. The data flow is generally unidirectional, with a clear upstream and downstream side to any link. RDTP should recognize a server side, upstream with respect to data flow, and a client side, which is downstream with respect to data flow. The server will likely be a fixed radio station, and the client could be a fixed or mobile station. In a multicast situation, there could exist an arbitrarily large number of clients in a link.

Some additional discussion supporting these requirements is available in my *QST* article. See Note 2.

Protocol Overview

The previously stated requirements drive significant design decisions, which are discussed in this section.

The requirement to operate on top of AX.25 is established, however, the functional capabilities of AX.25 are not necessarily required, nor even desired. Thus the RDTP protocol is designed to make use of only AX.25 Unnumbered Information (UI) frames. Every frame transmitted includes the transmitting station call sign in the appropriate AX.25 field. This meets 47CFR97 requirements, but may generally be ignored by receiving software. The recipient call sign in the AX.25 frame is always stated as ASCII "RDTPC" for server-to-client frames and "RDTPS" for client-to-server frames. This convention resolves certain issues identified during implementation. The only other AX.25 feature functionally used by RDTP is the Frame Check Sequence (FCS). The current RDTP implementation assumes that the AX.25 stack will have dropped any corrupted data, and thus all data ingested by the RDTP software may be considered error-free. To increase compatibility with available AX.25 stacks, the AX.25 PID is always set to text, though it would ideally be set to a unique identifier for this protocol. For reference, the AX.25 protocol is specified in a document available on the TAPR Web site.⁵

To realize maximum utility from low data rates, such as 1200 baud, compression is specified at the RDTP frame level, and is also available at the weather data level. The bzip2 algorithm was chosen, as its freely available implantation, libbz2, was shown to perform very well in informal engineering confidence

testing and is easily integrated into an RDTP software package on multiple operating systems. Additional compression details are presented in a later section of this paper. For more information on bzip2, see Note 6.

With these fundamental design details explained, the discussion may proceed to protocol semantics. To organize the available data on the server side, the concept of a named data stream is defined. Now posit there exists an RDTP server sourcing weather data from unknown upstream sources, and there further exist one or more RDTP clients, and that all of these stations share the same physical link. In other words, they are all tuned to the same frequency. The server organizes incoming data into logical data streams. The clients all desire data product which are members of one or more of these data streams. At the high level, the client server exchanges will follow this procedure:

- The client waits to be polled, as it shall not speak until spoken to. However, if an unspecified dead air timer elapses, as in initial link establishment, it immediately contacts a known RDTP server requesting one or more data streams.

- The server acknowledges and accepts or denies the client's request for data. Other clients on the channel hear the acknowledgement and realize that it is unnecessary to transmit their own request, unless said clients desire to request additional data streams for which no acknowledgement has yet been received.

- When new data becomes available from upstream, the server classifies this data into a data stream, checks for an active request for that data stream, and if one is found then transmits the data in a manner such that all clients sharing the same physical channel may receive it.

- After transmitting data from a data stream, the server initializes a timer, which once elapsed, will purge the active request for any new data from that data stream. This will cause the channel to shut down until another client request is received.

- To keep channel access organized for the next round of data stream requests, the server will poll clients in an orderly manner. Clients will only speak after being spoken to, as previously stated, and will transmit any pending data stream requests in response to the poll. The process then repeats.

In practice, when data is not flowing, neither the client nor server will transmit. This allows for multiplexed access to the physical channel, and more specifically allows someone else to use the frequency. To establish a link, a client detects dead air and transmits its request. When the last client in a group is taken off air, the server will eventually lose all active data stream requests, and will then

stop transmitting. This is the ideal behavior for operation in the Amateur Radio Service, and is most polite to all band users.

Detailed Protocol Specifications

The requirements and high-level design of the RDTP protocol have been discussed to the greatest extent reasonable within the scope of this paper. The low level details of the protocol will now be presented.

Conventions

These conventions are followed in this section:

- All indices are zero-based.
- Bits are numbered by order, with the most significant bit assigned the highest order number, and the least significant bit the lowest order number. The most significant bit is transmitted first. A numerical value for a byte should be represented over the physical channel following this convention.
- A string of bytes is numbered beginning with the first byte in the string, which is the first byte transmitted. This same notion for strings is used for data structures of numbered bytes.

Call Signs

RDTP call sign fields are filled as shown in Table 1, except for a deviation in the RDTP Frame Layer Header.

Frame Layer

The RDTP Frame Layer exists directly on top of the AX.25 UI frame. It functionally replaces AX.25 connected mode framing with special framing designed for the RDTP application. The most important function of this layer is to allow messages to be broken into frames and then reassembled. To support this, a message sequence number and frame sequence number are defined. Each individual message is numbered and broken into frames. Each frame within that message is then numbered sequentially. These two numbers allow receiving software to group frames into their respective messages, and then to reassemble them in order, even if they were transmitted out of order or repeated later.

Also notable is that this is the level of RDTP that supports data compression and forward error correction. A compression code identifies the data as compressed or not compressed, and indicates the compression algorithm used. When the compression code indicates that compression is in use, only the data section of the frame is compressed, to exclude all of the headers. For forward error correction, simple N+1 parity of the data section only is specified. Setting the N+1 parity flag indicates that a frame is the parity frame for the message indicated by its message sequence number.

The RDTP Frame Layer specification is presented in Table 2.

Logical Entity Layer

The RDTP Frame Layer replaces certain AX.25 functionality to meet the requirements of this protocol. With this layer specified, it is now possible to split and frame messages for radio transmission, so the discussion can continue to the content of those messages. The RDTP Frame Layer's payload is one or more concatenated RDTP Logical Entity Blocks (LEB). The Logical Entity Blocks are the meaningful content of a message. In this section, critical blocks will be discussed and

specified one at a time.

Table 3 presents the specification for the Data LEB. This LEB is used to transmit new weather data from a server to a client. The payload is the data message itself, in original format from its source or compliant to the same specifications if keeping the original format is not possible.

As previously discussed, a server cannot transmit data unless a client requests the data stream and the request is accepted. A client may send to a server a Data Request LEB to

perform this function. This LEB is specified in Table 4.

A server may accept and acknowledge or deny a Data Request LEB received from a client. The Request Ack LEB and Request Denied LEB are used for this purpose, respectively. They are defined in Table 5 and Table 6.

It has been previously stated that RDTP clients shall not speak unless spoken to, unless an exception applies. In normal operation, polling is required. A Poll LEB is

Table 3
Data LEB

Bytes		Bits	Description	Value	Notes
First	Last				
0	0	All	LEB ID	Literal 0x00	Identifier for this type of LEB
1	7	All	Data stream name	Free ASCII text, defined at the implementation or system level	System administrators will specify data stream names
8	8	All	Compression code	0: No compression 2: Bzip2	Use of libbz2 is recommended. Compression applies only to the payload.
9	10	All	Length of data	16-bit unsigned big-endian integer indicating the length of the data payload in bytes	
11	N = 11 + data length	All	Data payload	This is the actual weather data received from the information source	

Table 4
Data Request LEB

Bytes		Bits	Description	Value	Notes
First	Last				
0	0	All	LEB ID	Literal 0x01	Identifier for this type of LEB
1	7	All	Server call sign	RDTP formatted call sign of the server which the data stream(s) are being requested from	The AX.25 address fields are not used due to implementation complications
8	8	All	Number of data stream names	Length of the array of data stream names in the payload	
9	9 + 7N	All	Data stream names	Array of 7-byte data stream names. Each is left justified and right-filled with 0x00 bytes as necessary.	This is a simple C array

defined for an RDTP server to poll clients. Clients shall only respond when a Poll LEB is received giving the specific client permission to transmit. The Poll LEB is specified in Table 7.

The Poll LEB introduces the concept of an access level. Certain systems may have multiple clients of different priorities. An example would be a system with a client station at an Emergency Operations Center, a station at another communications facility, one or more mobile stations for severe weather spotters, and one or more stations operated by general interest Amateur Radio hobbyists that provide little or no operational benefit. The access level feature allows the requests of these stations to be prioritized.

Ideally, each client would be properly programmed with its access level, assigned by a system administrator. In practice, many

erroneous configurations are anticipated, so a special LEB, called the Access Level Is LEB, is defined to advise clients of their access level. A client must comply with the assigned access level if it is capable of responding to level polls. This LEB is specified in Table 8.

Presentation of additional LEB specifications is beyond the scope of this paper. The LEB specifications presented herein establish the minimum functionality for an operational system. Additional LEB types are specified in a draft RDTP specification.⁷ Readers are cautioned that this is a draft specification and will be revised in the future.

System Integration and Testing

The RDTP protocol was designed for integration into a system for ingesting weather data and distributing it to users who can real-

ize benefits from that data. As such, some discussion of an integrated system is appropriate for this paper. With much assistance, I have established a weather data distribution system that is capable of:⁸

- Ingesting real-time NEXRAD, GOES, text, and other data from the US National Weather Service's NOAAPort distribution network. For more information on NOAAPort, see Note 9.
- Relaying that data over connections on top of TCP/IP or AX.25 (the subject of this paper).
- Building relay networks which may have multiple upstream data sources for redundancy.
- Processing that data and presenting it in a meaningful way, displaying it to end users in a Graphical User Interface.

Table 5
Request Ack LEB

Bytes		Bits	Description	Value	Notes
First	Last				
0	0	All	LEB ID	Literal 0x07	Identifier for this type of LEB
1	7	All	Call sign of client being acknowledged	RDTP formatted call sign	
8	8	All	Number of data stream names	Length of the array of data stream names in the payload	
9	9 + 7N	All	Requested data stream names being acknowledged	Array of 7-byte data stream names. Each is left justified and right-filled with 0x00 bytes as necessary.	This is a simple C array

Table 6
Request Denied LEB

Bytes		Bits	Description	Value	Notes
First	Last				
0	0	All	LEB ID	Literal 0x0C	Identifier for this type of LEB
1	7	All	Call sign of client being denied	RDTP formatted call sign	
8	8	All	Number of data stream names	Length of the array of data stream names in the payload	
9	9 + 7N	All	Requested data stream names being denied	Array of 7-byte data stream names. Each is left justified and right-filled with 0x00 bytes as necessary.	This is a simple C array

- Performing various other useful tasks such as: archiving received data, automatically generating mobile phone text message and other alerts from received National Weather Service statements, and driving Internet web sites with real time weather data.

RDTP has been used intermittently in this weather data distribution system for many years. Users have provided feedback that RDTP performance has been excellent. With reasonable processing, it has been found that a

frame of NEXRAD data can be ingested from NOAAPort, stripped to the quarter of the frame which is of interest, relayed via a 1200 baud RDTP link, and processed all before that same frame of NEXRAD data is available on Internet web sites. As more Internet weather sources are developed and the current sources advance this statement will likely no longer be true, but it has been informally tested and found to be true as recent as two years prior to the writing of this paper. See Note 2 for more information.

Project Status and Future Work

The RDTP protocol is one small part of an ongoing project to ingest, distribute, and process weather data in real time, with special interest to NEXRAD data. My colleagues and I originally referred to this project simply as the “Radar Project,” but it has since outgrown that term. As previously discussed, a weather data distribution system has been established which is capable of ingesting many different types of weather data and

Table 7
Poll LEB

Bytes		Bits	Description	Value	Notes
First	Last				
0	0	All	LEB ID	Literal 0x06	Identifier for this type of LEB
1	1	7-4	Poll type	0: Level poll 1: Call sign poll 2: Wide open poll	Any client may respond to a wide-open poll or level 0 poll. Level and call sign poll discussions are located with their respective data fields.
		3-0	Level	Unsigned 4-bit integer 0 for call sign or wide-open polls. Otherwise, an unsigned 4-bit integer level for a level poll. Only clients with this access level or higher may respond.	In practice, multiple level polls may be used, with the server stepping down from 15 to 0, likely skipping many steps at a time.
2	8	All	Call sign being polled	Call sign poll: RDTP formatted call sign. Other polls: This field does not exist, and the LEB will only be two bytes long.	A call sign poll is used to poll a specific client. This functionality is useful to isolate clients that have been heard recently and prevent interference.

Table 8
Access Level Is LEB

Bytes		Bits	Description	Value	Notes
First	Last				
0	0	All	LEB ID	Literal 0x09	Identifier for this type of LEB
1	7	All	Client call sign	RDTP formatted call sign	
8	8	7-4	Reserved	0	Always fill with zeroes. This is a 4-bit unsigned integer.
		3-0	Access level	4-bit access level of the client being addressed	

relaying that data through complex networks consisting of Internet and AX.25 links to end users. To ease implementation, all of the software tools that compose this network are available for both the *Windows* and *Linux* operating systems. Indeed, this is a stated goal for the RDTP design. To the end user, a simply graphical application handles connections to Internet and AX.25 data sources and automates data processing. Deployment of this system to end users is nontrivial, it is also not very difficult.

As of this writing, two NOAAPort satellite receive sites are in operation and are redundantly linked via the Internet through a backbone node. Additional fan-out Internet distribution nodes are available to remove loading from the backbone. An RDTP server is operated in my hometown every summer during critical time periods, where excellent system performance has been observed.

Most relevant to this paper, future work on this project will further define the RDTP protocol and add useful features. Many additional LEBs have been defined for anticipated features but resources have not yet become available to implement and experiment with those envisioned features. Among the highest priority desired RDTP features is a more advanced forward error correction scheme, such as Reed Solomon coding. Additional work will focus on weather data processing software to expand the types of data capable of being processed beyond simple text, radar, and satellite data into graphical depiction of model output, radiosonde observations, additional types of radar and satellite data, and any other data types of interest. Further, future work will yield additional features for various components of the system to perform useful tasks. Severe weather alerting has been identified as a specific area where additional features would be valuable.

Most importantly it must be stated that all of the core development on this project has been completed, and that a much larger, more reliable weather data distribution system may be created without any further development work. The future work of the highest priority is recruiting new volunteers to implement NOAAPort satellite receive sites and RDTP servers to grow the network infrastructure. This provides substantial benefits to the project, notably including a large body of troubleshooting resources for future development, and increasing morale and providing greater value to volunteer software developers.

Acknowledgements

I would like to extend special gratitude to Aaron Heise, KB9QWC, for his extensive contributions over the life of this project. These contributions include, among other things, assistance developing the specification of the RDTP protocol, development of

software tools for integration into the larger scale weather data distribution system, troubleshooting of every weather software tool I have developed, and in general providing extensive engineering insight concerning all aspects of this project.

I would also like to thank Stephen Williams, KB9RLF, and Gerry Parks, N9OEW, for their dedicated contributions of equipment and time to the mission of building a weather data distribution system and also for substantial software troubleshooting assistance, including especially my RDTP implementation software package.

Conclusions

The RDTP protocol and other system components my colleagues and I developed present a complete weather data delivery solution for severe weather spotters and other weather enthusiasts. This solution overcomes the limits of the reach of the Internet and may be implemented at minimal cost. Indeed, a network already exists implementing the concepts discussed. As the software tools in use support redundant operation, the network reliability will increase as new volunteers establish and link new infrastructure. Therefore, interested parties are strongly encouraged to follow references in this paper and contact me for further discussion. With network growth and continued development effort a private, volunteer-operated weather distribution network is possible which will rival not only gratis but also costly commercial solutions that are currently available. This is the ultimate goal and future vision of the long-standing project to develop weather data distribution tools.

A GPL-licensed implementation of the RDTP/AX.25 protocol is available from me.

© 2008 Nicholas Luther

Notes

- ¹NOAA: National Weather Service, Office of Climate, Water, and Weather Services, "What is SKYWARN?", National Weather Service web site: www.weather.gov/skywarn/, Accessed 28 Jul 2008.
- ²N. Luther, "Disseminating NEXRAD Data via Packet," *QST*, Sep 2004, p 81.
- ³*Windows* is a registered trademark of Microsoft Corporation in the United States and/or other countries.
- ⁴*Linux* is the registered trademark of Linus Torvalds in the United States and other countries.
- ⁵W.A. Beech, D.E. Nielsen, and J. Taylor, "AX.25 Link Access Protocol for Amateur Packet Radio," Tucson Amateur Packet Radio Corporation Web site, version 2.2, Jul 1998. This article is available at www.tapr.org/pdf/AX25.2.2.pdf. Accessed 29 Jul 2008.
- ⁶J. Seward, bzip2 Web site, see www.bzip.org/.
- ⁷N. Luther and A. Heise, "RDTP/AX.25 Protocol Specification," DRAFT version 0.3, released Apr 2006. Available from

Winnebago County, Wisconsin ARES®/RACES Web site. Follow the link from www.ecwec.org/noaaport.shtml. ARES is a registered trademark and a program of the American Radio Relay League, Incorporated.

⁸N. Luther, "NOAAPort Dissemination Network," Winnebago County, Wisconsin ARES®/RACES Web site. Available at www.ecwec.org/noaaport.shtml.

⁹NOAA: National Weather Service, Office of Operational Systems, "NOAAPort User's Page," National Weather Service Web site. Available at www.weather.gov/noaaport/html/noaaport.shtml.

Nick Luther has been a licensed Amateur Radio operator in the United States since 1995 and a weather enthusiast for almost as long. He holds a BS in Electrical Engineering with a minor in Mathematics from the Milwaukee School of Engineering, conferred in 2007. He also holds a Wisconsin Engineer-in-Training certificate. Mr. Luther is employed as a design engineer in the Digital Systems Group at Plexus Technology Group in Neenah, Wisconsin, where he is currently participating in the development of a surgical instrument system. He is a member of the Institute of Electrical and Electronics Engineers and the American Radio Relay League.



NATIONAL RF, INC.



VECTOR-FINDER
Handheld VHF direction finder. Uses any FM xcvr. Audible & LED display
VF-142Q, 130-300 MHz
\$239.95
VF-142QM, 130-500 MHz
\$289.95



ATTENUATOR
Switchable, T-Pad Attenuator, 100 dB max - 10 dB min BNC connectors
AT-100,
\$89.95



**TYPE NLF-2
LOW FREQUENCY
ACTIVE ANTENNA
AND AMPLIFIER**
A Hot, Active, Noise Reducing Antenna System that will sit on your desk and copy 2200, 1700, and 600 through 160 Meter Experimental and Amateur Radio Signals!
Type NLF-2 System:
\$369.95



DIAL SCALES
The perfect finishing touch for your homebrew projects. 1/4-inch shaft couplings.
NPD-1, 3 1/4 x 2 3/4,
7:1 drive
\$34.95
NPD-2, 5 1/8 x 3 5/8,
8:1 drive
\$44.95
NPD-3, 5 1/8 x 3 5/8,
6:1 drive
\$49.95

NATIONAL RF, INC
7969 ENGINEER ROAD, #102
SAN DIEGO, CA 92111

858.565.1319 FAX 858.571.5909
www.NationalRF.com

Experimental Determination of Ground System Performance for HF Verticals Part 2 Excessive Loss in Sparse Radial Screens

These experimental results may surprise you, and might turn "conventional wisdom" upside down.

In 1998, Jack Belrose, VE2CV, used *NEC* modeling to show the effect of resonant and non-resonant radials placed very close to the ground surface on the behavior of a $\frac{1}{4}$ wavelength vertical.¹ One of the observations in that article was that the use of a small number of $\frac{1}{4}$ wavelength (free space) radials, lying on the ground surface, could lead to much higher losses than expected, and that shortening the radials could actually reduce ground loss. This seems counter to more classical analyses which show that making radials too long may be a waste of wire but does no harm. The classic analysis, however, does not take into account the possibility of resonances in the radial screen that might amplify the radial current, increasing ground loss.

The purpose of this experiment was to see if a real antenna would actually demonstrate the predicted behavior, and validate the *NEC* predictions experimentally.

Description of the Experiment

The experiment was done in six parts spread over a three week period:

- 1) The antenna for part 1 was a telescoping

aluminum-tubing vertical, averaging 1 inch in diameter, with a fixed height of 34 feet. The test frequency was 7.2 MHz. I used four no. 18 insulated wire radials lying on the ground surface. All four radials were of equal length, which was varied from 33 feet down to 18 feet. The impedance at the feed point, the transmission gain (S21) and the current division ratios between the radials were measured and recorded. The antenna and radials were isolated from ground and the feed line with a common mode choke.

2) For part 2, part 1 was repeated, first isolated from ground and then with one or more ground stakes connected, to evaluate the effect of using ground stakes at the base of the antenna. Tests were also done without any radials, and with just 1, 2 or 3 ground stakes connected to the base plate.

3) Part 3 of the experiment was the same as part 1 except with 8 radials (no ground stakes).

4) For part 4, the antenna was changed from the fixed tubing vertical to a remotely adjustable SteppIR vertical. In parts 1, 2 and 3, the antenna height was kept constant at 34 feet, but in this part of the experiment the height was changed to re-resonate the antenna as the radial number and radial lengths were changed.

The test frequency was 7.2 MHz.

5) After completing the first four parts of the experiment it was clear that shortening the radials from the standard free space $\frac{1}{4}$ wavelength value did indeed improve the signal, at least in the case of 4 and 8 radials, so I wanted to see what the effect was for 16 and 32 radials. Trimming that many radials to gradually shorten them, however, was a bit more work and wasted wire than I was prepared for. Instead, I ran this part of the experiment first with 4, 8, 16 and 32, thirty-three foot radials, which I had on hand, and then with 4, 8, 16 and 32, twenty-one foot radials, which were also on hand. This gave me two data points for each number of radials. Again, the test frequency was 7.2 MHz, with measurements of S21 and feed-point impedance.

6) Part 6 of the experiment was a check to see if the same kind of improvement would be seen at 30, 20 and 15 m by shortening the radials from $\frac{1}{4}$ wavelength (free space). This part of the experiment was not nearly as thorough as the first five parts but did confirm that the same basic behavior was present at the higher frequencies as that seen on 40 m. The test frequencies were 10.120 MHz, 14.200 MHz and 21.200 MHz.

¹Notes appear on page 52.

Experimental Results

Part 1

Figure 1 shows the variation in $|S_{21}|$ (magnitude of the transmission gain) as a function of radial length. The amplitude scale is normalized to 0 dB for a radial length of 33 feet, which is approximately a $\frac{1}{4}$ wavelength in free space at 7.2 MHz. The Y-axis shows the improvement in dB as the radials are shortened.

The improvement is quite large, about 2.8 dB, which would have a noticeable effect on signal strength. In Belrose's paper the improvement was about 3.5 dB but that was for average soil. My average ground characteristics are approximately $\sigma = 0.015$ S/m and $\epsilon_r = 30$, which is quite a bit better than average ground. These values were derived from ground probe measurements.² One would expect more improvement for poorer soil.

An earlier experiment in which the current distribution on a 33 foot radial, at 7.2 MHz, was measured, gave the results shown in Figure 2.

A quick check was made during the present experiment, and the current distribution appeared to be essentially the same. From the current distribution we can see that the radial in Figure 2 is resonant well below 7.2 MHz. To move the current maxima back to the base of the vertical we would have to reduce the radial length by about 10 feet. Looking back at Figure 1, we see that we are very close to the maximum $|S_{21}|$ when the length has been reduced by 10 feet to 23 feet. What appears to be happening is that we are tuning the radials to resonance (or at least close to it) at 7.2 MHz to compensate for the loading effect of the soil in close proximity to the radial wire.

The division of current between the radials was measured for 18 foot and 33 foot

Table 1

Current Division Between Radials Normalized to 1 A of Total Base Current.

Radial Number	I_n , 33-Foot Radials (A)	I_n , 18-Foot Radials (A)
1	0.24	0.26
2	0.24	0.25
3	0.25	0.25
4	0.27	0.24

Table 2

Measured Feed Point Impedances

Radial length (ft)	Feed Point Impedance (Ω)
33	$135 + j28$
30	$108 + j55$
27	$83 + j51$
24	$67 + j37$
21	$60 + j22$
18	$57 + j8$

lengths. Table 1 shows the results. The current division was quite uniform and the differences too small to have significant effect on the observed gain changes.

The variation of feed-point impedance as the radial lengths were shortened (with the vertical height constant at 34 feet) is shown in Table 2.

Parts 2 and 3

Part 1 was done during a week of heavy rain. Parts 2 and 3 were performed 8 days after part 1, when the soil had drained and dried out significantly so the ground characteristics may have changed somewhat.

The next step in the experiment was to expand the radial count from 4 to 8 radials and also to investigate the effect of using grounding stakes (4 foot copper clad steel

rods) connected at the base of the antenna. Measurements with 4 and 8 radials were repeated in each run. This run was with a fixed height for the vertical (34 feet). The results are shown in Figure 3.

At all lengths, 8 radials are an improvement over 4. With 8 radials, the amount of improvement with radial shortening is smaller but still useful. We can also see that adding a ground stake in the case of 4 radials also makes a substantial improvement but we should keep in mind that my soil would be classified as "very good" so we would expect ground stakes to be more effective than they would be in poorer soil.

The results for the case of no radials and 1, 2 or 3 ground stakes, normalized to the cases of four 33 foot radials and four 21 foot radials, with no ground stakes, are given in Table 3. Vertical height was constant at 34 feet.

Part 4

In part 4 I changed to the SteppIR vertical and adjusted the height to re-resonate the vertical for each radial length. The results are shown in Figure 4, which are very similar to the results for constant height given in Figure 3. No ground stakes were employed.

Part 5

From the earlier test results, I could see that the improvement due to radial shortening decreased as the number of radials increased.

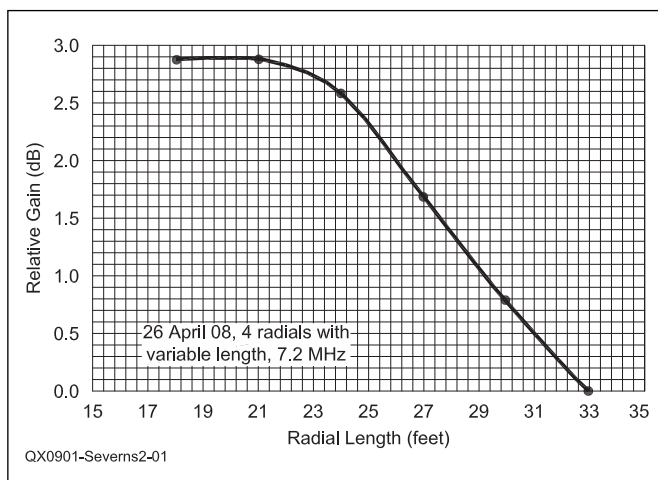


Figure 1 — This graph shows the improvement in $|S_{21}|$ as the radials were shortened. There were four radials lying on the ground surface.

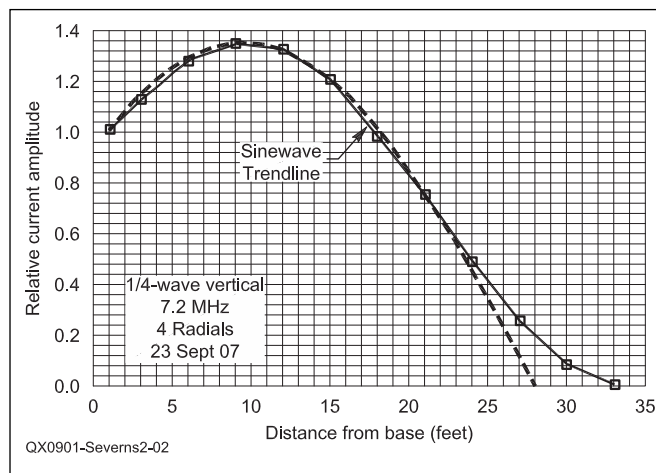


Figure 2 — This graph shows the relative current amplitude along a radial.

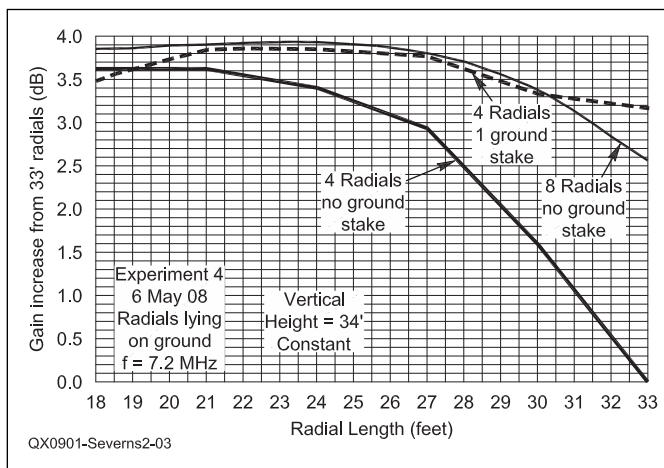


Figure 3 — This graph shows the change in |S21| with radial length. The vertical antenna height was a constant 34 feet.

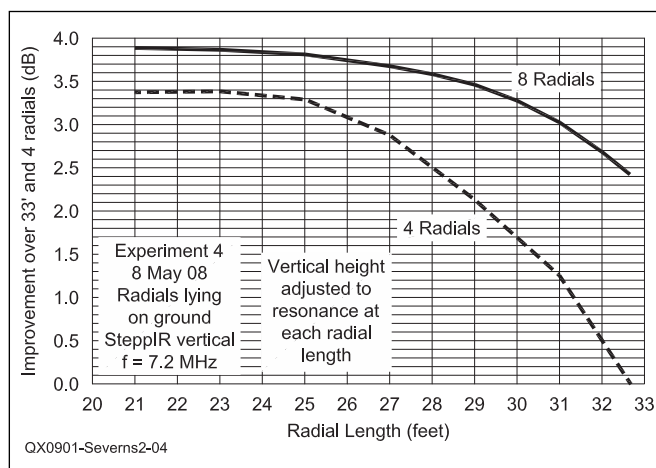


Figure 4 — This graph shows the change in |S21| with radial length. I adjusted the SteppIR antenna height to resonance for each radial length.

Table 3
Test Results for no Radials and 1, 2 or 3 Stakes, Compared to 4 Radials with no Ground Stakes.

Number of Stakes	Feed Point Z (Ω)	Compared to Four 33-Foot Radials, No Ground Stakes (dB)	Compared to Four 21-Foot Radials No Ground Stakes (dB)
1	77 + j 40	2.67	-0.95
2	69 + j 30	3.09	-0.53
3	66 + j 26	3.25	-0.37

Table 4
Results for 4, 8, 16 and 32 Radials, with Lengths of 33 Feet and 21 feet.

Number	33-Foot Radials Feed Point Impedance (Ω)	21-Foot Radials Feed Point Impedance (Ω)	33-Foot Radials S21 Relative to Four 33-Foot Radials (dB)	21-Foot Radials S21 Relative to Four 33-Foot Radials (dB)	Delta Gain Change (dB)
4	89.8	52.5	0	3.08	+3.08
8	51.8	45.6	2.26	3.68	+1.42
16	40.5	42.8	3.76	3.95	+0.19
32	37.7	41.6	4.16	4.04	-0.12

In this part of the experiment the number of radials was extended to include 16 and 32 radials to quantify that difference. The test was conducted with sets of 4, 8, 16 and 32 thirty-three foot radials, and then repeated with the same numbers of 21-foot radials. The SteppIR antenna was used, and its height was adjusted to re-resonate as the radials were altered. The results are tabulated in Table 4. These measurements were made several days after those used in Figure 4, so there are some differences because of small changes in the ground characteristics, radial layout, and other conditions. These day-to-day variations are a major reason for repeating some parts of earlier experiments multiple times and trying to do a complete experiment in a short period of time (a couple of hours).

It should be noted that a ground system consisting of only four radials is really flaky.

Measurements vary significantly with small variations in radial layout, changes in soil moisture, placement of the feed line relative to the radials, and so on. Shortening the radials does seem to reduce this sensitivity, but even so, a four radial system should only be an emergency measure.

As expected, as the number of radials is increased the change due to radial shortening gets much smaller. Over the very good ground on which these measurements were made, shortening the radials gave only a modest advantage when more than 8 radials were used. Over poorer soils, however, radial shortening with 16 radials might be worth doing. The lower value for feed point impedance (Z_f) with 33-foot radials is at least in part due to the shorter height needed to resonate. For 21-foot radials the height had to be increased to re-resonate the antenna.

It is interesting to note that with 32 radials, the 33-foot radials were actually slightly better (0.12 dB) than 21-foot radials. Quite probably there was some optimum length in-between that may have been slightly higher than either, but that is not likely to be very large and I decided it wasn't worth the trouble to cut up a set of 32 radials to find out. The important point is that the changes in gain, input impedance and height variation to re-resonate all get much smaller when more radials are used. I would think that with 32 or more radials you wouldn't worry about resonances in the radial screen. The problem is only important when fewer than 16 radials are deployed.

Table 5 shows the antenna height (h) in inches. This is the reading from the control box. The actual height is about 12 inches longer due to the height above ground of the

Table 5
Indicated Height of the Vertical.

Number of Radials	33-Foot Radials h (inches)	21-Foot Radials h (inches)
4	357	381
8	366	382
16	374	382
32	377	382

reel and the lengths of connecting wires, plus the length of radials from the reel box to ground surface. The columns for h do, however, give an idea of the change in height. In the case of 33-foot radials the change is quite large (20 inches) between 4 and 32 radials. On the other hand with 21-foot radials the change in h with radial number is very small, fractions of an inch. The values in the Table are rounded off to the nearest inch.

Part 6

In the final part of this experiment the effect of radial shortening on 30, 20 and 15 m was examined. This was really just a quick look using radials left over from the earlier parts of the experiment, cut down from them rather than making up a new set of 1/4 wavelength (free space) radials for each band. In all three cases 8 radials were used. The test frequencies were: 10.120 MHz, 14.200 MHz and 21.200 MHz. The corresponding free space 1/4 wavelengths would have been, 24.3 feet, 17.3 feet and 11.6 feet respectively. The results are shown in Tables 6, 7 and 8. The value for |S21| is the actual measurement.

One oddity in this data was that the best radial length on both 30 and 20 m was the same, about 15 feet. There is some dispersion (variation with frequency) in the soil characteristics but I don't think that's a full explanation. In all cases the optimum length was well short of the free space 1/4 wavelength. I think this part of the experiment needs to be rerun cutting down from full length radials. This will be done at some future time.

NEC Modeling

At this point it was clear that Belrose's original work was basically confirmed experimentally, but I was curious to see how closely this data could be replicated using NEC4-D modeling software (EZNEC Pro + MultiNEC). The first trial model employed 4 radials with lengths from 6.4 m (21 feet) to 10 m (33 feet). The wire table for this model is given in Table 9. The radials were placed 5 mm above 0.01/14 soil. The test frequency was 7.2 MHz and the vertical height was adjusted to maintain resonance as the radial number was changed.

We can compare the maximum gain data against the experimental data for 4 radials (from Figure 4) as shown in Figure 5.

The match in gain data is very good, as was the current distribution on the radials. The impedance data was also close. We can also see what NEC predicts about the current distribution on a radial as we change the length. Figure 6 shows the current distribution on a 33-foot radial for NEC model 1.

Figure 6 looks very similar to the experimental measurement shown in Figure 2. When we shorten the radials to 21 feet, we get the current distribution shown in Figure 7. This is very close to resonance.

The match in gain and current distribution, however, is really too good to be believed. First of all, this is not an exact model of the real antenna. The vertical uses a strip of beryllium-copper, not a no. 12 wire, and I believe my ground characteristic is better than the 0.01/14 used in the model. Models with wires very close to the ground sur-

Table 6
30 m, 1/4 Wavelength Free Space = 24.3 Feet.

Radial Length (ft)	Z _i (Ω)	S21 (dB)	h (in)
21	44.4	-62.31	260
20	41.6	-61.12	261
18	41.0	-61.84	264
16	42.6	-61.78	267

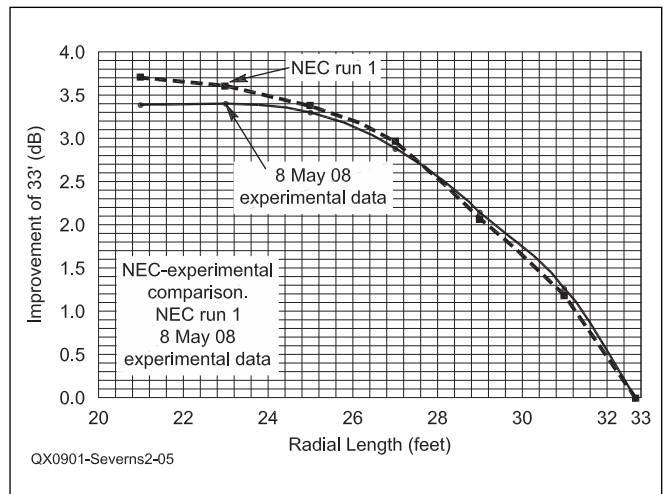


Figure 5 — Here is a comparison between NEC modeling run 1 and the experimental data using 4 radials taken on May 8, 2008.

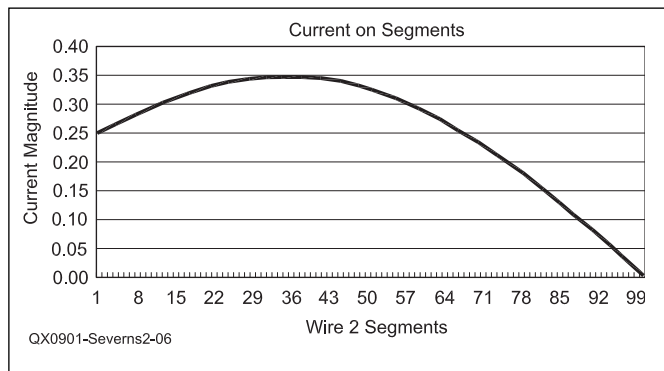


Figure 6 — This graph shows the current distribution on a 33 foot radial (NEC model).

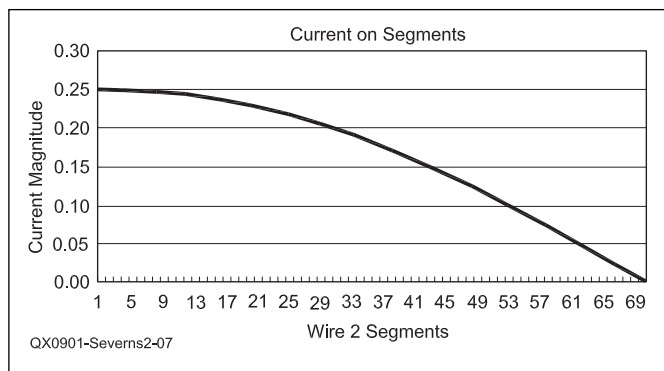


Figure 7 — Here is the current distribution on a 21 foot radial (NEC model).

Table 7**20 m, ¼ Wavelength Free Space = 17.3 Feet.**

Radial Length [ft]	Z _i (Ω)	S21 (dB)	h (in)
16	37.8	-62.03	178
15	36.0	-61.84	179
14	35.0	-61.91	181

Table 8**15 m, ¼ Wavelength Free Space = 11.6 Feet.**

Radial Length [ft]	Z _i (Ω)	S21 (dB)	h (in)
9	27.3	-60.34	60
8	30.0	-60.29	60
7	34.3	-60.11	60
6	41.0	-60.46	60

Table 9**Model Wire Table**

End 1 X (m)	Y (m)	Z (m)	End 2 X (m)	Y (m)	Z (m)	Diameter (mm or #)	Segs (359)	Show Lengths in Wire	• m Length	O w/ Seg Len
40 m gp 4 rad A										
0.000	0.000	0.005	0.000	0.000	10.306	#12	103	W1	10.301	0.100
0.000	0.000	0.005	6.400	0.000	0.005	#12	64	W2	6.400	0.100
0.000	0.000	0.005	0.000	6.400	0.005	#12	64	W3	6.400	0.100
0.000	0.000	0.005	-6.400	0.000	0.005	#12	64			
0.000	0.000	0.005	0.000	-6.400	0.005	#12	64			

Table 10**Z_i and Peak Gain**

Freq (MHz)	L	M	R at Src1	X at Src1	SWR(50 Ω)	Max Gain
7.200	9.056	10	83.15	0.03	1.663	-4.41
7.200	9.275	9.45	65.72	0.01	1.314	-3.22
7.200	9.535	8.84	54.59	0.00	1.092	-2.12
7.200	9.757	8.23	49.83	-0.01	1.003	-1.45
7.200	9.955	7.62	48.23	-0.02	1.037	-1.04
7.200	10.136	7.01	48.48	0.01	1.031	-0.81
7.200	10.306	6.4	49.91	-0.02	1.002	-0.70

Where L is the height of the vertical in meters and M is the length of the radials in meters.

face are very sensitive to small changes in the model and wire segmentation. A change in height as small as 1 mm when the wires are at 5 mm above ground, makes a very substantial change in the results. By diddling the model, I can get the kind of match shown in Figure 5, but when I go the other way and attempt to use the model to predict the behavior of the real antenna, the results could be way off. When it comes to wires very close to ground — distances comparable to the wire diameter — NEC replicates the general behavior but you do not know enough of the details of the real antenna and it's immediate environment to expect exact quantitative results from the model.

In addition, the characteristics of real soil vary widely even at a fixed location: vertically, horizontally and over time. The soil will very likely have grass (weeds?) over it, which varies in length and water content during the year. We will seldom have more than a general idea what our ground characteristics are even with ground probe measurements.

We will also not really know the height above ground to a fraction of mm! The radials will be buried somewhere in the grass, so who knows what the effective height really is.

Final comments

The effect that showed up initially in Belrose's article and in later NEC modeling appears to be real. I think it is clear that in a sparse radial system lying directly on the ground surface, it is possible to incur substantial additional ground losses over what we might expect. The prediction from NEC modeling of this effect appears to be confirmed, at least qualitatively. I have been able to reproduce it experimentally multiple times, on multiple bands, with different antennas.

While NEC predicts the effect, you can't rely on NEC modeling for exact predictions. You will have to do final adjustment in the field. This is not a general indictment of NEC. When the antenna has not been right

down next to the ground surface, I have found NEC predictions to be very good when I went out and built the actual antenna.

We have a couple of ways to attack the problem of radial resonance and excess ground loss: first, cut the radials to be near resonance while lying on the ground. That works if you have the instrumentation, but is hardly a practical approach in general. The second and much more practical approach is to use at least 16, or better yet, 32 radials. As I pointed out earlier, ground systems using only a few radials are a poor idea for many reasons.

Notes

¹J. Belrose, VE2CV, "Elevated Radial Wire Systems For Vertically Polarized Ground-Plane Type Antennas, part 1 — Monopoles," *Communications Quarterly*, Winter 1998, pp 29-40.

²R. Severns, N6LF, "Measurement of Soil Electrical Parameters at HF," ARRL, *QEX*, Nov/Dec 2006, pp 3-9.



TAPR Announces HPSDR Mercury Direct-Sampling Receiver

The Mercury direct-sampling receiver board is the latest addition to the growing family of Software Defined Radio (SDR) components developed by the High Performance Software Defined Radio (HPSDR) group and manufactured by TAPR. The Mercury receiver board interfaces to a PC through its companion USB interface board (Ozy) and backplane (Atlas). More information is available on the Internet at www.hpsdr.org and www.tapr.org.

Mercury Specifications:

ADC overload: -12dBm (preamp on), +8dBm (preamp off)
 MDS (500Hz), 160m - 6m: -138dBm (preamp on), -118dBm (preamp off)
 IP3 equivalent (independent of spacing): +33dBm (preamp on), >+50dBm (preamp off)
 BDR (5kHz, 1dB GC): -119dBm (ADC overload limited, not phase noise limited)
 122.88MHz clock phase noise: -149dBc/Hz at 1kHz spacing



Photo 1 — This is the last of three Mercury prototypes. The TAPR production units will be identical to this hand-built prototype. The voltage regulators are along the left side. The 122.88 MHz low phase-noise oscillator is the large silver can in the upper left corner. The RF front-end circuitry is in the upper right corner; the RF signal flows from the BNC input on the right to the LT2208 ADC (square chip in the middle) where it is digitized and fed to the Altera EP3C25 Cyclone 3 FPGA (large chip in the middle). On the right edge, from bottom to top are headphone and line outputs; SPI interface to the Alex Preselector; and forward and reverse power signals to the analog converter on the Penelope transmitter. The 96-pin DIN connector along the bottom plugs into the Atlas backplane.

Mercury Features:

- 100kHz - 55MHz frequency coverage
- LTC6400-20 20dB LNA (software switchable)
- LTC2208 16-bit ADC sampling at 122.88Msps
- Front-end low-pass filter and ADC anti-aliasing filter
- SSB, AM, C-AM, FM, CW, PSK etc
- Seventeen unbuffered digital I/O from FPGA to header connector
- On board audio CODEC for line and headphone outputs
- Alexiars (RF Preselector) SPI control and power interface
- Clocking options:
 - On board ultra low phase noise 122.88 MHz crystal oscillator phase locked to on board 10MHz TCXO or external 10MHz reference such as Gibraltar.
 - 122.88MHz output available via LVDS
 - Optional external VHF clock input via LVDS
 - 10MHz TCXO available via Atlas bus
- Altera EP3C25 Cyclone 3 FPGA based DDC (digital down-conversion) enabling future code upgrades
- Atlas bus compatible, USB interface to PC via Ozy board (no sound card required)
- I and Q balance adjustment not required due to direct sampling of RF input
- Supported by *PowerSDR* software

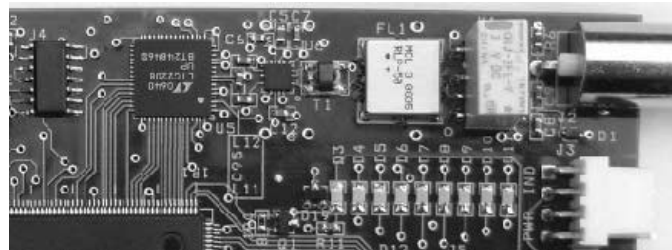


Photo 2 — This is a close-up of the Mercury RF front-end. Signals flow from the BNC on the right to the LTC2208 130 Msps ADC (large square chip) on the left. In order from right to left are: BNC RF input; attenuator relay; 50 MHz low-pass filter; coupling transformer; LTC6400 20 dB LNA; LTC2208 ADC. The components between the LNA and the ADC form an anti-aliasing filter. On the extreme left is an LVDS clock buffer.

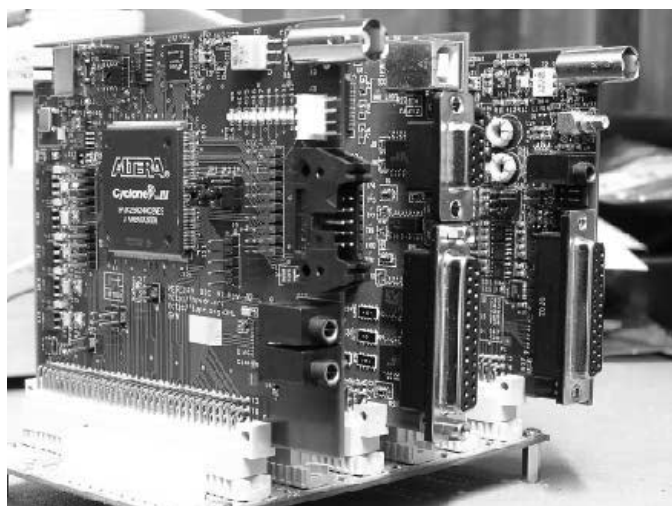


Photo 3 — This is a complete HPSDR transceiver consisting of (front to back) Mercury direct-sampling receiver; Ozy USB interface; Penelope 1/2 W direct up-conversion transmitter. These boards are plugged into the Atlas six-slot backplane. The connector in the foreground on the Atlas backplane is a standard ATX power connector.



SDR: Simplified

This issue begins a new column dedicated to software defined radios and digital signal processing.

Gerald Youngblood, K5SDR, has done a fantastic job of bringing SDR to the reach of many amateurs with his series of *QEX* articles, and the Flex Radio products.¹ Others have implemented designs like the Soft Rock that use simple RF circuits to get the signals down to “audio” for work with a sound card. We will be looking at techniques that move the RF as close as possible to the antenna. The “Holy Grail” of software defined radios is hooking a DAC and an ADC directly to the transmit/receive switch. Components are getting faster and allowing designs to move higher in frequency and closer to the antenna.

We will start with some experiments using the PC sound card as an arbitrary waveform generator (a fancy signal generator) and using some software tools to look at signals.

Intended Audience

I hope you are included in my target audience. I am writing this column for readers who have heard of software defined radios, and who have read about some of the concepts, but who still feel a bit “in the dark” about how this all works. If you are anxious to take your understanding to the next level, then I believe this column will help you. Here are the skills and tools that will make it possible to fully participate in the presentations and the laboratories:

- 1) You will need some exposure to the C language or *Pascal/Delphi*, but the examples can also help you learn these
- 2) Analog RF experience
- 3) A PC with a sound card
- 4) Average high school math ability (trigonometry and algebra)
- 5) Windows media player or other WAV file player
- 6) An oscilloscope is nice to have but not required
- 7) Roxio *Wave Editor* is also nice to have but not required

Most of the folks doing DSP work tend to be math or computer science wizards rather than interested in RF electronics. Usually by the fifth page of most DSP books or articles by those types of authors, my eyes glaze over from the complex math involved. We can't

get away from the math entirely, but we can do almost all of the work with just basic high school trigonometry and algebra. We will use some of that trig in our first lab.

Software and Hardware Resources

We are really lucky that almost all of the software tools we need are free. Here is a list of packages you should download:

- 1) *Visual C++* — www.microsoft.com/express/product/default.aspx
- 2) *Visual Basic* — www.microsoft.com/express/product/default.aspx
- 3) *uCLinux* for the Blackfin DSP IC — [//blackfin.uclinux.org/gf/](http://blackfin.uclinux.org/gf/)
- 4) SDR: Simplified Utilities in the *QEX* files section of the ARRL Web site, www.arrl.org (These files will be updated concurrent with each installment).²
- 5) *Gnuplot* — www.gnuplot.info/

In future installments, we will be doing laboratories with the Analog Devices Blackfin 537 IC. This is a digital signal processor with hardware support for high speed signals and also some regular computer CPU features. This is in contrast to a PC and its sound card, where it is a computer first and signal processor second. The Blackfin BF537 is available from DigiKey on the BF537 Stamp evaluation board, which costs \$212.50. We will also need the AD7476 ADC board (\$32) and we will make a DAC output board. There are boards for various processors in the EZ Kit Lite series, but those are higher priced. The Blackfin family is used by Yaesu and Icom for IF DSP. TenTec uses the Sharc family for IF DSP.

We could have chosen DSP evaluation boards from TI or Freescale, but Analog Devices has “student priced” boards that are readily available from DigiKey, and there are open source tools available for the Analog Devices boards. There are open source tools for the other manufacturers, too. It is good that there are open source tools because buying most of the manufacturers’ proprietary software tools would require a second mortgage!

Paul Decker, KG7HF, is a manager in the Analog Devices DSP software tools group, and he has volunteered to help us to learn DSP. Many thanks to him for his help so far, and for his continued support.

Introduction to I and Q

We need to start with some background on

the basics of signal processing before we get into the nitty gritty of doing the processing digitally. If you have done much reading on DSP or software defined radios, you have seen mention of I and Q. There is significant mention of I and Q in Chapter 16 of the 2009 edition of *The ARRL Handbook*.³ The “I” stands for “in-phase” and the “Q” stands for “quadrature.” *Quadrature* is simply a mathematical term that means 90° out of phase, so our first trig identity is:

$$\cos(A) = \sin(A + 90^\circ)$$

The general convention is backwards to the way most of us think of trigonometry. The cosine wave is considered the “in-phase” reference and the sine wave is the “quadrature” term. By convention, RF folks use *sine wave* to talk about our waveforms, but the math works better when we think in terms of cosine waves. The math reason for using the cosine as the reference is that the cosine is symmetrical about time zero, while the sine is not.

The next identity is the basis for everything related to quadrature analysis:

$$X \cos(A + y) = I \cos A + Q \sin A$$

where $A = 2 \times \pi \times \text{frequency}$

$$X = \sqrt{I^2 + Q^2}$$

X = amplitude of the new waveform

y = $\arctan(Q / I)$ = phase offset from the reference cosine wave

Translated: you can create a new sine wave of any amplitude and any phase relative to the reference cosine wave by adding a sine wave and a cosine wave of the same frequency.

When we modulate a signal, we can vary the phase of the modulated signal (changing A + y) or vary the amplitude (changing X) or vary both at the same time. Varying I and Q simultaneously to modulate a carrier is called Quadrature Amplitude Modulation (QAM). All forms of “traditional” modulation such as SSB, FM, and digital phase modulation can be created by applying the proper I and Q signals to a QAM modulator. When we want to recover the information from a modulated signal, we may only need amplitude information (full carrier AM) or phase information (FM and PM). Some modulation schemes require knowing both the phase and the amplitude to recover the information. Double Sideband-suppressed carrier AM is an example. Many digital modulation methods use complex combina-

¹Notes appear on page 56.

tions of phase and amplitude to transmit multiple bits simultaneously.

We can use the I and Q signals in receivers to recover both the amplitude and the phase of the information of modulated signals in a process that is the mathematical inverse of the modulation process. When we start doing the math using DSP, we can frequently do the inverse operation digitally, where an analog method is either impossible or very expensive.

Using Gnuplot

We can use *Gnuplot* (which is also a part of the *Octave* math package) to see that our quadrature formula is actually true. *Gnuplot* turns your computer into a graphing calculator. Download the *Gnuplot* installation file from the www.gnuplot.info/ Web site and install it on your computer. Search your C: drive for **wgnuplot.ini** after you have installed *Gnuplot*. Save the original **wgnuplot.ini** file in a safe place on your C: drive (or use an alternate name to backup the file). One of the files in the zip file available for download from the ARRL *QEX* Web site is **iq.plt**. After you download the zip file and extract the files, copy the **iq.plt** file to the bin directory of your *Gnuplot* installation. There is also a file named **wgnuplot.ini** in the *QEX* files download zip file. Replace the original version on your computer with this new **wgnuplot.ini** file from the *QEX* files. Launch **wgnuplot.exe**. At the command prompt, type **pwd** and verify that the directory is **C:\gnuplot\bin**. If the path is not **C:\gnuplot\bin**, type the command **cd "c:\gnuplot\bin."** Then type **load "iq.plt."** Note that the quotes around the file names are required for proper operation. This command runs the commands in the batch file **iq.plt** and displays a graph, as shown in Figure 1. These commands take a cosine of amplitude 3 (shown with long dashes) and a sine of amplitude 4 (shown as a solid line) and create a new wave of amplitude 5 (shown as a dotted line). Notice that the dotted-line waveform is shifted with respect to the reference cosine wave by positive 53°, which is (arctan (4/3)).

Gnuplot comes from the *Unix* world, so interactions with the computer may seem unusual. The first place this is true is file paths. You need to use the *Unix/Linux* convention for path names. In *Windows*, you would type **C:\gnuplot\bin**. In *Gnuplot*, the same directory is entered as **C:/gnuplot/bin**. Notice that the **pwd** command produces a path with Microsoft backslashes but you must use the *Unix* style forward slashes for any command options you enter. Fortunately, the designers have added some features from the *Windows* command system, so repeating and modifying commands is easy. The most useful are the command repeat and editing keys. Up arrow and down arrow will cycle

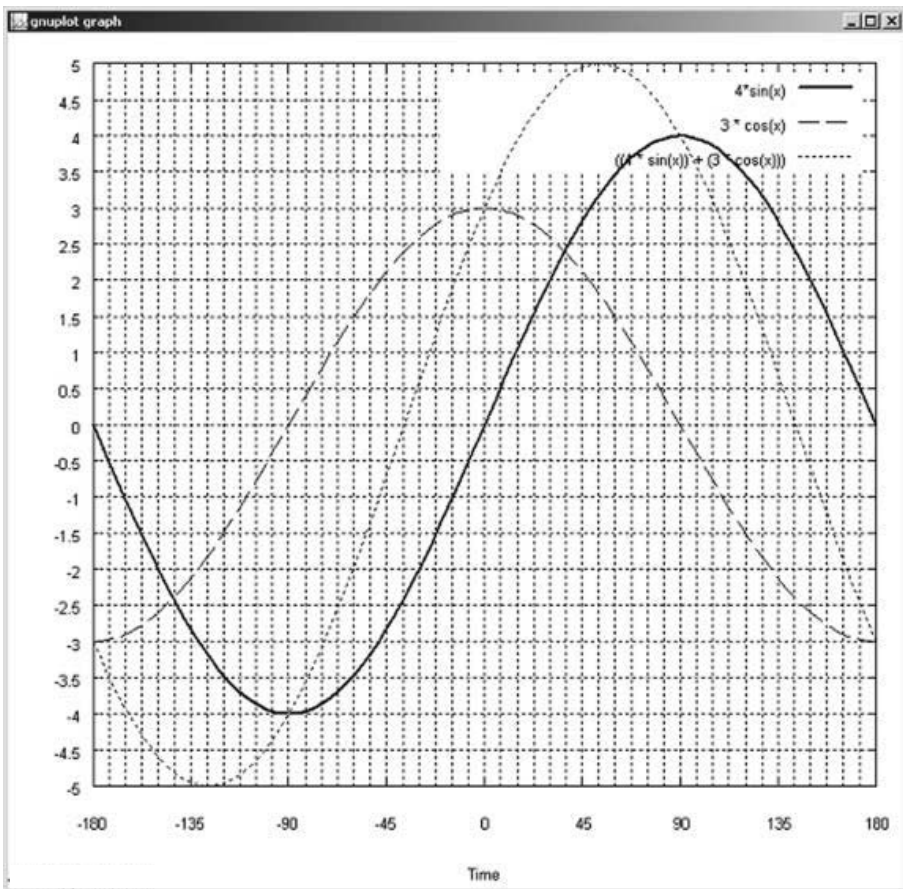


Figure 1 — This screen capture shows the *Gnuplot* graph from a file that plots a cosine with an amplitude of 3 (dashed line), a sine with an amplitude of 4 (solid line) and the sum of those waveforms (dotted line).

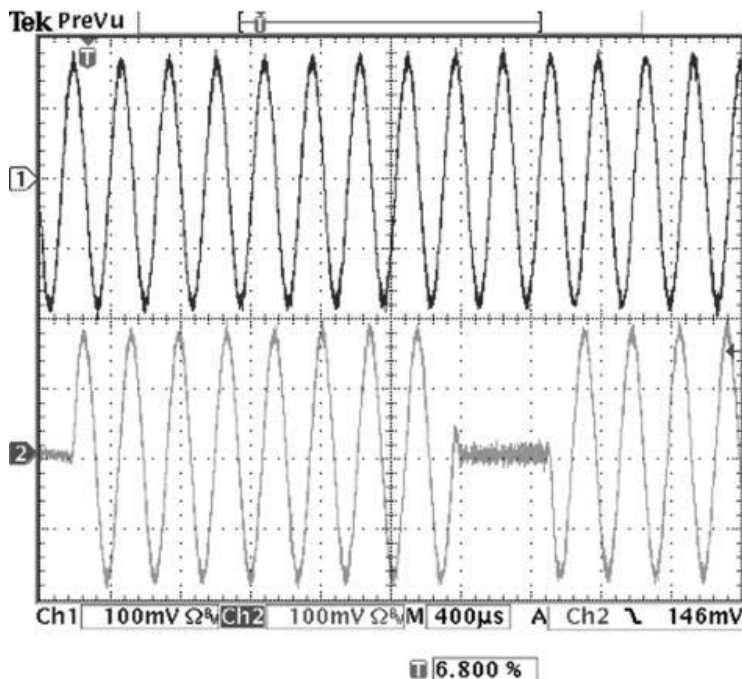


Figure 2 — This oscilloscope display shows a cosine waveform at trace 1 and a phase shift keyed waveform at trace 2. Notice that trace 2 is delayed 90° from the cosine reference at first, and then the phase shifts part way through the sweep, so that the trace is now shifted 90° ahead of the cosine reference signal.

you through the command history. This is very useful as you edit your batch file and rerun it to see the results.

You set the appearance of the plot with the set commands. The last command beginning on line 15 of `iq.plt` tells `Gnuplot` what to plot in the graph window. Notice in our example that there are “\” characters at the end of lines 15, 16, and 17. These allow you to split a single command across multiple physical lines (another Unix/Linux concept). The second thing to notice is that each waveform equation is separated from the next by a comma. If you leave out the comma, you will get an unhelpful error message. You can see this if you take out the comma on line 17 of `iq.plt`. The error says “line 18: undefined variable: x” even though the error is really on line 17. You just have to struggle through trying to find what the problem is. This is a “normal” programming problem where the error is on line 17, but the software doesn’t see the problem until the next line. You may encounter similar issues when we start writing programs in C.

There are some aspects of plots that must be set in `wgnuplot.ini`. Each computer and operating system has a different “terminal.” The lines that you use for plotting in Windows are set up with the variables “Line1” through “Line15.” The first 3 numbers set the color of the line (R, G, and B). The fourth number sets the line density for solid lines and the fifth sets the type. The types are 0 — solid, 1 — dash, 2 — dot, 3 — dashdot and 4 — dashdotdot.

`Gnuplot` has a reasonable set of help pages, especially when you consider that the folks who write the software do it for free. If you have good programming experience, the commands are pretty easy to figure out. There are a very large number of features for 2D and 3D plotting, as well as both polar and rectangular presentations.

Experiments with I and Q

We can generate I and Q signals with the PC sound card by creating WAV files and playing them. Again, all of the files are on the ARRL Web site under `QEX`. Our experiment for this issue will be to create a Binary Phase Shift Keyed waveform. We will define a Zero to be a $+45^\circ$ angle with respect to the cosine and One to be a -135° angle with respect to the cosine. The amplitude of the waveform during each bit will be 1. The file `iq_wave.c` creates a C program that will generate and play a demonstration of I-Q modulation. The left channel produces the reference cosine, and the right channel produces our modulated signal. You can see the two waveforms in both the oscilloscope plots of Figures 2 and 3, and the Sound Editor screen shot of Figure 4. Notice that the screen shot shows the individual samples. The PC sound card

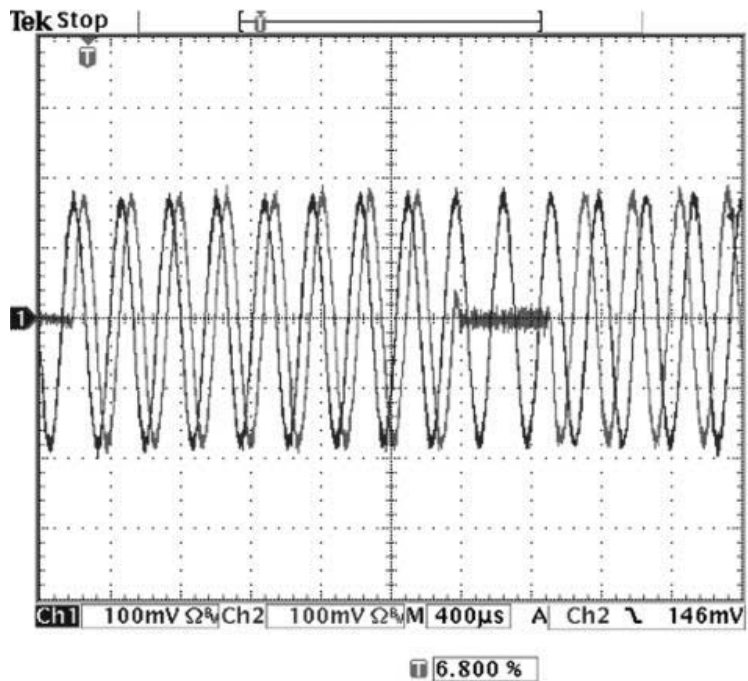


Figure 3 — This oscilloscope display makes it easier to see the phase shift that occurs in trace 2 as compared to the reference cosine waveform.

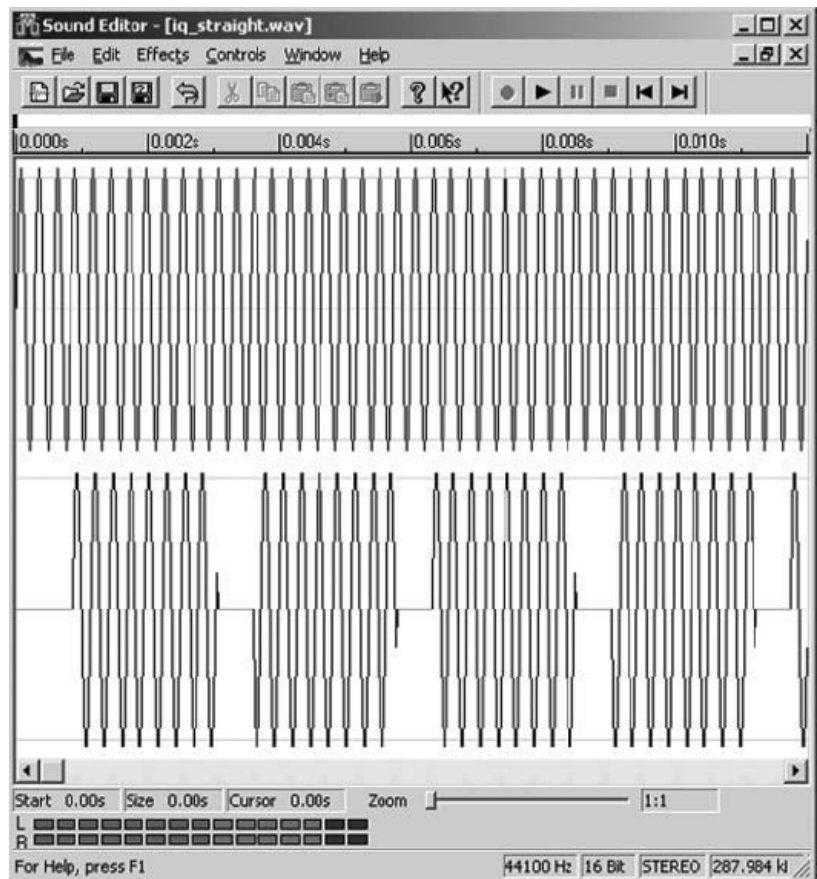
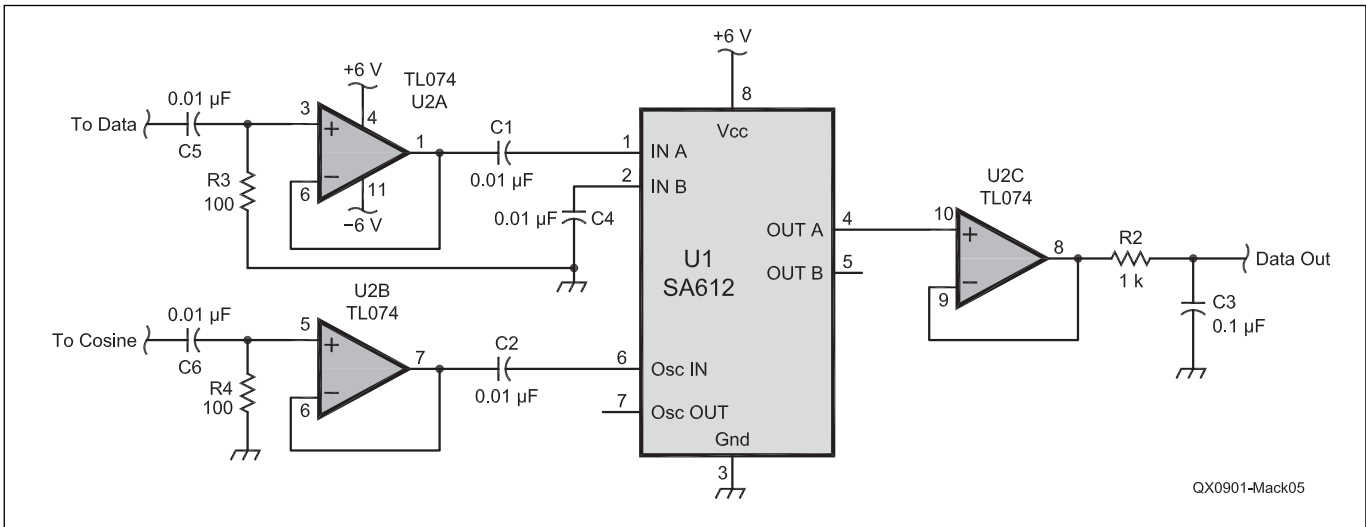


Figure 4 — This screen capture from the Roxio Wave Editor display shows a cosine reference signal at the top and a phase shift keyed signal at the bottom.



QX0901-Mack05

Figure 5 — This schematic diagram shows a simple demodulator that will recover the I signal from a modulated waveform. In the next installment of SDR: Simplified, we will use this circuit to analyze some signals.

We Design And Manufacture To Meet Your Requirements
*Prototype or Production Quantities

800-522-2253

This Number May Not Save Your Life...

But it could make it a lot easier!
Especially when it comes to ordering non-standard connectors.

RF/MICROWAVE CONNECTORS, CABLES AND ASSEMBLIES

- Specials our specialty. Virtually any SMA, N, TNC, HN, LC, RP, BNC, SMB, or SMC delivered in 2-4 weeks.
- Cross reference library to all major manufacturers.
- Experts in supplying "hard to get" RF connectors.
- Our adapters can satisfy virtually any combination of requirements between series.
- Extensive inventory of passive RF/Microwave components including attenuators, terminations and dividers.
- No minimum order.



NEMAL ELECTRONICS INTERNATIONAL, INC.
12240 N.E. 14TH AVENUE
NORTH MIAMI, FL 33161
TEL: 305-899-0900 • FAX: 305-895-8178
E-MAIL: INFO@NEMAL.COM
BRASIL: (011) 5535-2368

URL: WWW.NEMAL.COM

filters the samples and smoothes the samples into sinusoids.

The C program is rather simple. It uses data arrays of interleaved left and right samples that I write to the output file in sequence. The logic is much simpler, since the program is just a sequence of writes. I used the values in an Excel spreadsheet to calculate the samples for the cosine, the sine and the one and zero data values. If you don't have Excel, you can see the equations I used under each heading in the PDF file. The C program can be set up for either 48 kHz sampling to get an exact 8 kHz carrier, or you can use 44.1 kHz, to create a CD-compatible WAV file. The Excel spreadsheet computes the sample values of $((\cos(\text{angle}) + \sin(\text{angle})) / 1.414)$ for a one. The sample values for a zero are $((-\cos(\text{angle}) - \sin(\text{angle})) / 1.414)$. Each of these values is rounded to the nearest integer value. The range of values is restricted to -32767 and $+32767$ to maintain symmetry around zero.

Don't be surprised if your waveforms don't match up. My Dell computer running Windows 2000 allowed Musicmatch Jukebox and Roxio Wave Editor to play the 48 kHz file. My HP computer running Windows XP Professional would only play the 44.1 kHz file using Windows Media Player. Another difference between computers was that the Dell played the signals with exact phase and the HP played the signals with a 180° phase shift. The differences can be attributed to driver differences and hardware differences.

We can build simple hardware that will use the reference cosine to convert the modulated BPSK signal back to the original binary signal. This hardware is your laboratory assignment until the next column. The schematic of Figure 5 shows a simple demodulator that just recovers the I signal. We don't have enough channels in the PC sound card to generate both the I and Q reference. With BPSK, we really only need one clock that is synchronized to the data, and our reference cosine provides that sync.

In the next issue, I will explain the Nyquist criteria and begin our work with the Blackfin part.

Notes

¹Gerald Youngblood, AC5OG (now K5SDR), "A Software Defined Radio for the Masses, Parts 1 - 4," QEX, Jul/Aug 2002, Sep/Oct 2002, Nov/Dec 2002, Mar/Apr 2003.

²The software files associated with this column are available for download from the ARRL QEX Web site. Go to www.arrl.org/qexfiles and look for the file **1x09_SDR_Simplified.zip**.

³Mark Wilson, K1RO, Ed, *The ARRL Handbook*, 2009 Edition, ARRL, 2008 ISBN: 0-87259-139-5; ARRL Publication Order No. 1395, \$44.95. ARRL publications are available from your local ARRL dealer, or from the ARRL Bookstore. Telephone toll-free in the US 888-277-5289, or call 860-594-0355, fax 860-594-0303; www.arrl.org/shop; pub-sales@arrl.org.



Letters to the Editor

VHF Frequency Multiplication Using the SA602 IC (Jul/Aug 2008)

Dear John and QEX Editor,

In the article "VHF Frequency Multiplication Using the SA602 IC," there are a few misunderstandings. Briefly, in my opinion:

1) This kind of multiplier must function in linear mode to produce the second harmonic effectively.

2) The SA602 is a low-level device, its RF input is linear only up to -30 dBm input and limits hard at -20 dBm. Therefore, its output here is a square wave that doesn't contain even harmonics. Also, its core is meant to be a switching mixer, so the oscillator input is out of linear mode, too.

3) AN1983 does not mention any gain figures. It states only that the second harmonic is 10 to 15 dB higher than the fundamental, in output.

The circuit should be tested with much smaller signals and attenuation between stages to keep the device in linear mode in both inputs. Lower frequencies and an oscilloscope will reveal the signal forms, needed for linear multiplication. After all, AN1983 is not so bad.

— Kindly, (Mr) E-P Mänd, Finland. (Member of ARRL and SRAL, Technical class from 1970; BsC); e-p.mand@pp.inet.fi.

Dear Mr. Mänd,

Thank you for your interest in my article and for the questions that you raise. (For those readers not familiar with all of the literature that concerns the NE/SA602, Application Note 198, published in 1987, states that the 1 dB compression point, which defines the upper limit of the effective mixer dynamic range, is about -25 dBm.) If I understand your letter correctly, you are concerned that the amplitude of the signal fed to the mixer is such that the mixer output waveform is a square wave, which contains no even harmonic energy, preventing the circuit from operating as a frequency doubler.

This concern is valid, but does the mixer run completely out of linearity for input signals larger than -25 dBm? In order to answer this question, I went back to the lab to measure the overtone oscillator/mixer circuit formed by U1, L1, R1, Y1, and C1–C5 only, in both the time and frequency domains.

The first test was to view the output waveforms at pins 4 and 5 of U1 with a Tektronix 2246A 100 MHz oscilloscope. The periodic

Table 1

	36.425 MHz	72.85 MHz
Osc. Output (U1 pin 7)	-1.7 dBm	-15.8 dBm
Mixer Output (U1 pin 4)	-4.0 dBm	-4.3 dBm
Mixer Output (U1 pin 5)	-5.7 dBm	-4.3 dBm

waveforms were definitely not square waves (more generally, the waveforms were not half-wave symmetric — mathematically required if they contain no even harmonic energy). Next, I used an HP4195A Network/Spectrum Analyzer to view the frequency spectrum of the oscillator (U1 pin 7) and mixer output (U1 pins 4 and 5) at the fundamental (36.425 MHz) and second harmonic (72.85 MHz).

An advantage I had gained since my original work was due to an HP41800A Active Probe I had just obtained. The HP41800A probe has a bandwidth of 5 Hz to 500 MHz, with an equivalent input resistance of 100 k Ω in parallel with 3 pF. This essentially eliminates the loading effect of the spectrum analyzer when making measurements. Table 1 gives the results I obtained from the spectrum analyzer.

As the table shows, the oscillator output power of the second harmonic is about 14 dB below the fundamental, while at the output of the mixer the second harmonic is only about 3 dB below the fundamental — equivalent to a conversion loss of about 3 dB. The presence of such a large second harmonic indicates that the mixer still maintains enough linearity to perform frequency conversion sufficient for my design, albeit at a 3 dB conversion loss.

A second test that I ran on this circuit was to attenuate the oscillator signal prior to feeding it to the mixer, as you suggested. With C1 and C2 removed (equivalent to infinite attenuation) I measured -2.5 dBm at 72.85 MHz at pin 4 and pin 5, while with C1 and C2 in place (equivalent to zero attenuation) I measured -4.3 dBm at 72.85 MHz as shown in Table 1. Resistor values of 4 k Ω , 2 k Ω and 1 k Ω placed in series with C1 resulted in power levels in between the values for infinite attenuation (-2.5 dBm) and no attenuation (-4.3 dBm). This seems to be about a zero sum game. Any gain in conversion efficiency because of lower signal levels seems to be offset by the concomitant reduction in the amplitude of the input signal itself, resulting in approximately the same output power level.

— 73, John E. Post, KA5GSQ, 5635 Four O'Clock Ln, Prescott, AZ 86305; john.post@erau.edu

Receiver Performance Measurement and Front End Selectivity (Sep/Oct 2008)

Dear Larry,

I was very interested in Henry Rech's article on Receiver Performance Measurement and Front End Selectivity in the Sep/Oct issue of QEX, especially as Henry quotes some of my work. Some of his references took me back, too — I worked briefly with John Dingley and Roger Winn at Racal, for Sosin at Marconi and for a subcontractor to Redifon where Ron Barrs was Chief Engineer! It should be remembered that much of the work published in the 1970s was the result of the fashion in the late '60s and early '70s to use broadband circuitry to minimize tuning time in service, and production and test costs in manufacture. The resultant downturn in performance was an unwanted and unexpected side effect. Examples of this appeared in the marine field, where receivers meeting the mandatory Type Approval tests in the lab proved useless on board ship.

Pat Hawker, G3VA, in his Technical Topics column in the RSGB *RadCom*, advocated the advantages of front end selectivity over a good many years, and I cannot disagree. One point that Henry does not mention is reciprocal mixing: in its way, this is more insidious than intermodulation, since reducing signal levels reduces reciprocal mixing dB for dB, rather than for n dB, as in the case of intermodulation. Improved front end selectivity helps with reciprocal mixing as well.

The noise testing methods using a notch have been described in *Marconi Instrumentation* magazine back in the early 1960s: one occasionally sees the *MI* test equipments at flea markets. The method was also described in the same magazine in the 1970s as applied to transmitter testing. The FT-102 used in my measurements does indeed have a relatively narrow front end. It is used only to establish the noise floor, however, with the actual signal measurements being carried out with a spectrum analyzer. The noise floor can be varied with a step attenuator to check the "dB for dB," indicating that intermodulation is not

Table 2

Number of signals at various noise levels in 2002 and in 2007 using a dipole at 7 MHz


Time (UTC)	Number of signals Jan 2002			Number of signals Oct 2007		
	-10 to -20 dBm	-20 to -30 dBm	-30 to -40 dBm	-10 to -20 dBm	-20 to -30 dBm	-30 to -40 dBm
00-01						
01-02						
02-03	1	12	12	2	3	6
03-04				2	1	8
04-05						
05-06					1	2
06-07		1	4		3	2
07-08				1	1	3
08-09						
09-10						2
10-11						
11-12						
12-13						
13-14						
14-15		1	1			2
15-16			2			2
16-17	1	3	18		1	9
17-18	5	5	20		5	9
18-19	2	8	23		5	10
19-20	1	4	18			8
20-21	2	6	27		3	13
21-22		6	25			13
22-23	1	3	23		3	11
23-24	2	5	7			

Table 3

Noise floor and signal levels measured during a 20-hour period in 2007

Time (UTC)	Number of signals Noise floor (dBm)	-10 to	-20 to	-30 to
		-20 dBm	-30 dBm	-40 dBm
0215	-96	2	3	4
0230	-100		3	6
0300	-99	1	2	8
0315	-98	2	1	6
0505	-102		1	2
0530	-102		1	2
0610	-99		3	2
0640	-103		2	2
0715	-102	1	1	2
0730	-100		1	3
0945	-100			2
1440	-101			2
1530	-95			2
1620	-99		1	8
1640	-100		1	9
1700	-96		5	7
1730	-95		3	9
1800	-95		5	10
1920	-95			8
1935	-102			5
2015	-102		3	11
2045	-95		1	13
2130	-100			13
2200	-98		3	9
2215	-97		2	11



from **MILLIWATTS to KILOWATTS**SM
More Watts per Dollar



Taylor TUBES

Quality Transmitting & Audio Tubes




- COMMUNICATIONS
- BROADCAST
- INDUSTRY
- AMATEUR

Immediate Shipment from Stock

3CPX800A7	3CX15000A7	4CX5000A	813
3CPX5000A7	3CX20000A7	4CX7500A	833A
3CW20000A7	4CX250B	4CX10000A	833C
3CX100A5	4CX250BC	4CX10000D	845
3CX400A7	4CX250BT	4CX15000A	866-SS
3CX400U7	4CX250FG	4X150A	872A-SS
3CX800A7	4CX250R	YC-130	5867A
3CX1200A7	4CX350A	YU-106	5868
3CX1200D7	4CX350F	YU-108	6146B
3CX1200Z7	4CX400A	YU-148	7092
3CX1500A7	4CX800A	YU-157	3-500Z6
3CX2500A3	4CX1000A	572B	4-400A
3CX2500F3	4CX1500A	807	M328/TH328
3CX3000A7	4CX1500B	810	M338/TH338
3CX6000A7	4CX3000A	811A	M347/TH347
3CX10000A7	4CX3500A	812A	M382

- TOO MANY TO LIST ALL -






ORDERS ONLY:
800-RF-PARTS • 800-737-2787
Se Habla Español • We Export

TECH HELP / ORDER / INFO: 760-744-0700
FAX: 760-744-1943 or 888-744-1943

An Address to Remember:
www.rfparts.com

E-mail:
rfp@rfparts.com



RF PARTS COMPANY

affecting matters. The measured noise levels are consistent with those expected in a quiet rural location from on a dipole in accordance with Recommendation ITU-R P.372-8 "Radio noise."

The measurements in my original *QEX* article were made at what was about the peak of the sunspot cycle, and the question remained as to how different the results are at the bottom of the cycle. That may be found in my March/April 2008 *NCJ* article. Since there is no copyright problem between *NCJ* and *QEX*, those tables are shown here as Tables 2 and 3.

The measurements still suggest that about 100 dB of dynamic range is all that is required for most amateurs, but the major point is where that 100 dB begins. The use of an antenna attenuator with as much as 40 dB of available attenuation seems justified. Phase noise is a more subtle problem, in that multiple low level signals add in ways that does not happen with intermodulation. A good front end preselector helps in many ways, as the designers of such classic receivers as the HRO, AR88, SX28 and SuperPro apparently appreciated.

— 73, Peter Chadwick G3RZP, Senior Radio Systems Consultant, Medical Products Group, Zarlink Semiconductor, Cheney manor, Swindon SN2 2QW, United Kingdom; peter.chadwick@Zarlink.Com

Dear Larry,

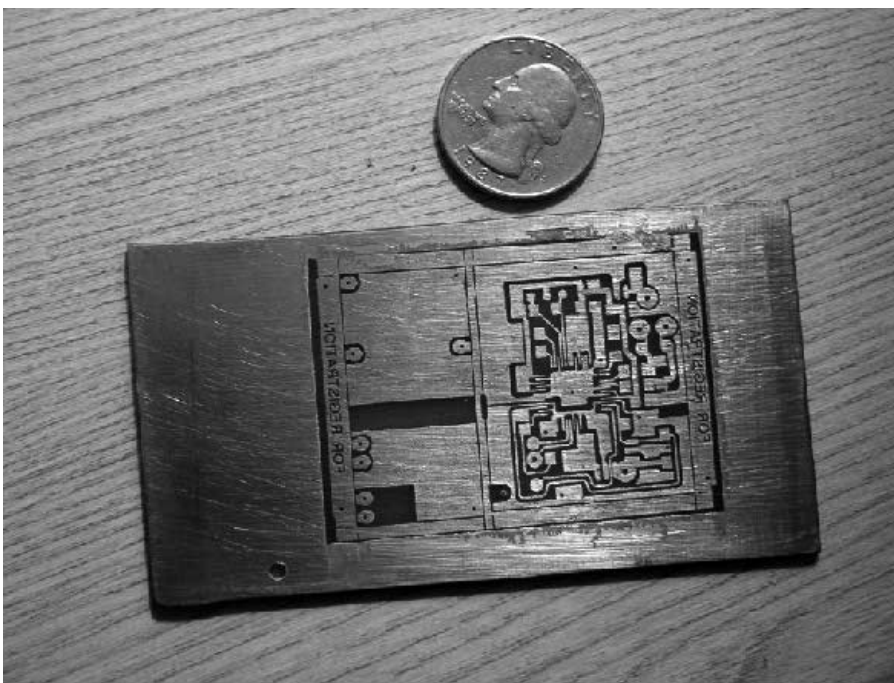
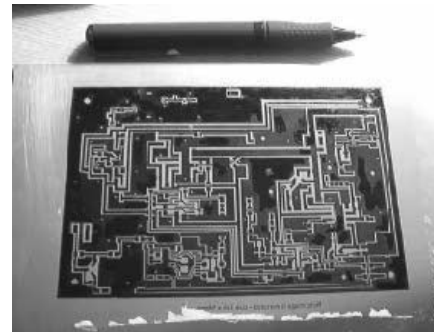
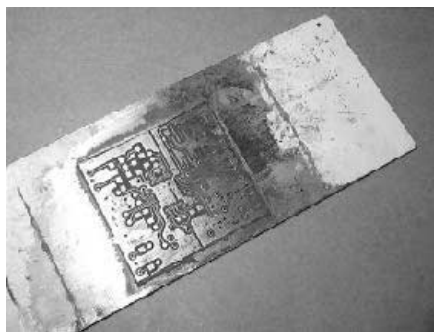
I read Peter Chadwick's letter to you and was fascinated to find that he had an involvement with some of the references cited in my article. This was a time when receiver design was in a state of rapid development.

Peter noted that I omitted a mention of reciprocal mixing. His point is valid.

Receiver overall performance is largely dependent on front end linearity, first oscillator phase noise behavior, front end selectivity, roofing filter bandwidth and inherent sensitivity. All of these also affect the receiver dynamic sensitivity (that is, how a receiver noise floor varies as the signal environment in which it is embedded changes) in particular. I believe the notion of "dynamic sensitivity" has to be looked at in more detail.

It would seem to me that the conventional battery of tests that are used do not adequately address the comparative performance of receivers. My article focuses on IMD performance and front end selectivity and how the Noise Power Ratio Figure of Merit (NPRFOM) might be a way out of this.

Given that the IMD characteristic of a receiver may not be only third order, as discussed in my article, point measurements may not describe the complex IMD behavior of a particular receiver, and hence receiver comparisons based on such measurements may not be valid. For instance,



two receivers may have the same calculated IP3 but may vary in actual IMD performance. This is another point I could have emphasized in my article.

I would argue that the NPRFOM test fits the bill as a general figure of merit test very well and is a means by which the overall performance of a receiver can be characterized, taking account of all the determinants of receiver performance in one test.

— 73, Henry Rech, 55 King St, Dandenong, Victoria, Australia, 3175; hjrech@optusnet.com.au

Press-n-Peel Circuit Boards (Sep/Oct 2008)

Dear Larry:

If only WA9PYH's article on Press-n-Peel had appeared last year, before I embarked on building a G3XJP reference-design STAR (software transmitter and receiver), I would have saved time and effort. His notes

are invaluable for any builder that home-brews circuit boards. There are some points I'd like to add to Jim's excellent article, however.

Two of the many boards for my STAR project housed surface-mount ICs with leads measuring 0.27-mm on 0.5-mm pitches. Once I perfected my technique through trial and error, I was able to readily make fine-line double-sided boards to accommodate tiny DDS and CODEC chips.

I found that 2-oz. Copper fiberglass FR4 material, obtained at low cost on eBay, was the best substrate. I etched my boards with a mixture of ferric chloride and hydrochloric acid. I used Chip Quik flux to ease attachment with an ordinary soldering iron.

Rather than using Press-n-Peel, which is somewhat expensive, I used ordinary glossy photo paper intended for inkjet printers. I bought 10-mil heavyweight paper called Special Moments, made by

Greenbrier International, Inc. It was available at my local Dollar Tree store, priced at eight sheets for a dollar.

Although some people have warned that running this glossy stock through a laser printer can ruin the printer's fuser, I have never experienced that problem, not even after making dozens of prints. To be on the safe side, however, it might be worthwhile purchasing a surplus printer, as Jim did for his projects. My printer is a Hewlett-Packard Laserjet 2300.

I print my layouts on the Special Moments paper, and then transfer them to the polished and cleaned copper, using an iron, as Jim explained. The clothes iron is dedicated to this purpose, as the process leaves a brown stain on the iron that is almost impossible to remove. (Ask me why I gave my wife a gift of a brand new iron!) The clothes iron deposits the plastic-based laser toner onto the copper boards in the same manner as Press-n-Peel. The deposited image is a great resist.

Depending on the size of the board and the thickness of the copper, and how much heat and pressure is applied, there can be places on the board where the laser toner resist doesn't adhere. These areas show up clearly when you peel off the paper, but they can be touched up manually with a Sharpie pen prior to etching. These pens are now available with ultra-fine points. I use a broad-point black Sharpie to touch-up large areas on the image, and a fine-point black Sharpie pen for the tiniest traces.

I found I could also partially peel off the Special Moments paper after heating, and if I observed any traces that didn't transfer, I could fold the paper back down, and hit the board with more heat. Partially peeling off the paper preserves the registration of the original artwork, as there is a portion of unpeeled paper that still adheres to the underlying copper.

Lastly, I always scratch my call sign and date onto my boards, prior to etching. It's nice to have your call sign etched forever on homebrew circuit boards.

I've attached a few photographs of some of my boards.

I hope these hints will help others to make fine-line boards. It's now easier than ever to homebrew advanced radio projects on your kitchen table!

— 73, Alex Mendelsohn, AI2Q, 164 Sea Road, Kennebunk, ME 04043; ai2q@arrl.net

Optimum Lossy Broadband Matching Networks for Resonant Antennas (Sep/Oct 2008)

Hi Larry,

When I received my copy of the Sept/Oct issue of QEX in the mail, I did a quick read of the article; it came out very well. Thanks for all your efforts. I detected a few minor errors that I did not pick up before.

On page 35, Figure 11, y-axis: The top number should be 120 instead of 3.

On page 36, in the second paragraph, line 11: Figure 12D should say Figure 12C.

On pages 36-40, Figures 12, 16, 17 and 18: The y-axis of each graph is dual-use and is intended to show SWR values from 1.0 to 3.0 and loss values from 0 to 2.0 with a label of "Loss (dB)." This can be accomplished by moving the "SWR" label upward to make some space for the loss label.

Thanks again. I enjoyed working on this project with you.

— 73, Frank, AI1H, 41 Glenwood Rd, Andover, MA 01810; ai1h@comcast.net

Hi Frank,

Thanks for pointing out those errors and incomplete labels on some of the graphs with your article. I also enjoyed working with you on this article, and look forward to doing it again soon.

— 73, Larry Wolfgang, WR1B, QEX Editor; lwolfgang@arrl.org

Broadband Impedance Matching (Nov/Dec 2008)

Dear Larry,

The article "Broadband Impedance Matching" in the Nov/Dec 2008 issue of QEX contains an error. In Figure 17, page 29, the source impedance (R_S) should be 50Ω , not 750Ω . The graphs of Figure 18 are based on $R_S = 50$, as is the "With Inverter" graph of Figure 16. Sorry I didn't catch this when I reviewed the final layout PDF file.

— Sincerely, Frederick B. Huber, 9422 Deer Ridge Dr, Cedar Rapids, IA 52411; fhubler@msn.com

Hi Frederick,

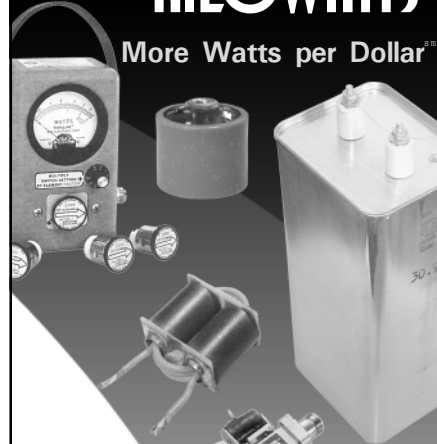
Thank you for pointing out the mistake that we made when drawing Figure 17. We sincerely apologize to our readers for that error.

— 73, Larry, WR1B; lwolfgang@arrl.org

QEX

From
MILLIWATTS
to **KILOWATTS**SM

More Watts per DollarSM



- **Wattmeters**
- **Transformers**
- **TMOS & GASFETS**
- **RF Power Transistors**
- **Doorknob Capacitors**
- **Electrolytic Capacitors**
- **Variable Capacitors**
- **RF Power Modules**
- **Tubes & Sockets**
- **HV Rectifiers**



ORDERS ONLY:

800-RF-PARTS • 800-737-2787

Se Habla Español • We Export

TECH HELP / ORDER / INFO: 760-744-0700

FAX: 760-744-1943 or 888-744-1943



An Address to Remember:
www.rfparts.com

E-mail:
rfp@rfparts.com



RF PARTSSM
COMPANY

Upcoming Conferences

Southwest Ohio Digital and Technical Symposium

January 10, 2009
Middletown, OH

You are invited to attend the 23rd Annual Southwest Ohio Digital and Technical Symposium, to be held on Saturday, January 10, 2009, from 8:30 AM to approximately 4:30 PM. The location is Thesken Hall, Miami University, Middletown Campus, Middletown, Ohio. Details of the program and activities are on the web at www.swohdigi.org. A number of very interesting presentations will be part of this conference.

This is an ARRL sanctioned conference, and we are pleased to have Great Lakes Division Director, Jim Weaver, K8JE, host an ARRL forum.

Larry Phipps, N8LP, will explain how his LP-PAN panadapter works. This exciting product enhances your operating ability by allowing you to visually observe activity

across a large segment of the band. More information on this product and other of Larry's products may be found at www.telepostinc.com/n8lp.html.

Tony Gargas, KB8WOW, has developed a text messaging gateway that allows you to send text messages to cell phones or e-mail addresses from your amateur station. This has potential uses in an Emcomm situation, and will hopefully spark others to develop new Emcomm applications.

Do you remember the popular column in *Popular Electronics* from the 1950s and 60s about the adventures of two young ham friends named Carl and Jerry? The author of those columns was John Frye, W9EGV (SK). John lived in Ft. Wayne, IN. Jeff Dunteman, K7JPD, has received permission to republish all of the Carl & Jerry columns and the entire collection is now available in five volumes. Jeff will do a remote presentation on his experiences in this project.

In today's age of computers, we continue to see applications for their use in Amateur

Radio. Bill Erwin, N9CX, will give us a practical presentation on how to use micro controllers and microcomputer chips in the shack. Bill's presentation will explain how he designed and built a digital based controller to do AZ/EL (azimuth/elevation) rotator control with a couple of old U-100 TV rotators. This same principal will work with other rotators, such as the AR-22. More importantly, it is a practical demonstration of how you can get started in designing your own control application.

AMSAT will be represented by Gerd Schrick, WB8IFM, and Steve Coy, K8UD, with an update on what is new and what is planned for space.

There will be an optional catered lunch, with an expected cost of \$8, and a "feed the kitty" can for morning coffee and snacks. There are numerous fast food and other types of restaurants within a mile of Thesken Hall, if you wish to go off site.

For further information please contact Jay Slough, K4ZLE; k4zle@embarrmail.com.

Larry Wolfgang, WR1B

QEX Editor; qex@arrl.org

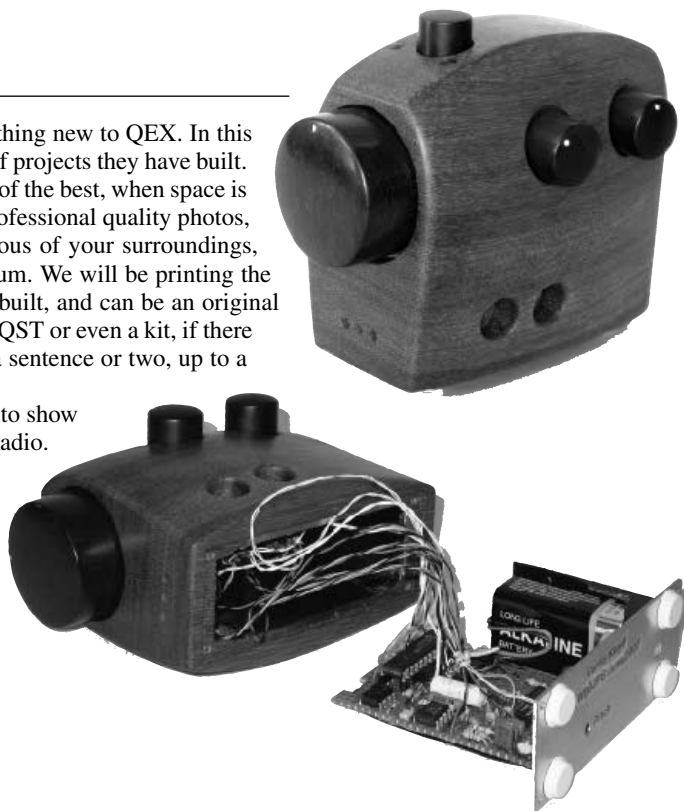
Reader's Page

At the suggestion of Gary Johnson, WB9JPS, we are trying something new to QEX. In this column we are offering our readers an opportunity to publish photos of projects they have built. Send in your photo ideas, with a short caption, and we will pick some of the best, when space is available. As I wrote in *Empirical Outlook*, you don't have to send professional quality photos, but they should be sharply focused and carefully lighted. Be conscious of your surroundings, and try to keep background clutter and other distractions to a minimum. We will be printing the photos in black and white. Photos should show something you have built, and can be an original project design or your interpretation of something presented in QEX, QST or even a kit, if there is something interesting or unique about your construction. Include a sentence or two, up to a short paragraph to describe your project. Show us what you've got!

To start things off, here are some photos that Gary, WB9JPS, sent to show off some of his woodworking projects that cross over into Amateur Radio.



Morse keys are an old favorite of radio craftsmen. This one is made from a block of cocobolo and features custom-made hardware, silver contacts, and sealed ball bearings. The knob is carved asymmetrically to fit the owner's hand.



This unusual keyer enclosure is made of purpleheart with ebony knobs, and fits in the palm of your hand. It's based on a Curtis keyer chip, and runs on a 9 V battery. The keyer circuit includes a sidetone oscillator for practice, with volume, weight, and speed adjustment knobs, along with a button for the message memory.

2008 QEX Index

Feature Articles

- A 2256 MHz PLL Local Oscillator (Kocsis): Jan/Feb, p 16
- A Great Teacher: The Crystal Set (Anderson): Sep/Oct, p 10
- A Low-Cost, Flexible USB Interface (Baier): Jan/Feb, p 11
- A Modern Discrete-Method for Signal Analysis and Design (Sabin): Nov/Dec, p 36
- A Software Controlled Radio Preselector (de Fortuny and de Onate): May/Jun, p 11
- A Squelch Amplifier (Laughlin): Jan/Feb, p 32
- An Advanced Direct-Digital VFO (Hagerty): May/Jun, p 19
- An All-Digital SSB Exciter for HF (Ahlstrom): May/Jun, p 3
- Broadband Impedance Matching (Hubler): Nov/Dec, p 23
- Building Electrodes (sidebar to Using Morse Code for Computer and Ham Station Control) (Connell): Nov/Dec, p 10
- Buying or Building Your Own NUE-PSK (sidebar to NUE-PSK Digital Modem): Mar/Apr, p 7
- Carbon Composition, Carbon Film and Metal Oxide Film Resistors (Smith): Mar/Apr, p 46
- Computing the R and N Register Values for a 10 MHz Reference And 2256 MHz Output (sidebar to A 2256 MHz PLL Local Oscillator) (Kocsis): Jan/Feb, p 22
- D-STAR Uncovered (Loveall): Nov/Dec, p 50
- Dual Output Power Supply (DeHoney and Murphy): Nov/Dec, p 30
- From Spark Generators to Modern VHF/UHF/SHF Voltage Controlled Oscillators (Rohde): Jul/Aug, p 42
- Fully Automated DDS Sweep Generator Measurement System (Green): Nov/Dec, p 13
- Ground System Configurations for Phased Vertical Arrays (Christman): Jul/Aug, p 13
- Linux Under Windows? (Kluck): May/Jun, p 25
- More Octave For Transmission Lines (Wright): Jan/Feb, p 26
- NUE-PSK Digital Modem (Cram and Heron): Mar/Apr, p 3
- Observations on Ferrite Rod Antennas (Smith): Jul/Aug, p 22

- Offset Matching Of Yagi-Uda Beams (Zimmerman): Nov/Dec, p 39
- Optimum Lossy Broadband Matching Networks or Resonant Antennas (Witt): Sep/Oct, p 31
- Oscillator Noise Evaluation with a Crystal Notch Filter (Hayward): Jul/Aug, p 6
- Parallel or Series Resistance? (Sidebar Carbon Composition, Carbon Film and Metal Oxide Film Resistors) (Smith): Mar/Apr, p 54
- Press-n-Peel Circuit Boards (Kocsis): Sep/Oct, p 22
- Receiver Performance Measurement and Front End Selectivity (Rech): Sep/Oct, p 26
- Setup and Using EasyPLL (sidebar to A 2256 MHz PLL Local Oscillator) (Kocsis): Jan/Feb, p 24
- SID: Study Cycle 24, Don't Just Use It (Spencer): Sep/Oct, p 3
- Some Thoughts on Crystal Parameter Measurement (Koehler): Jul/Aug, p 36
- The Mystery of the Q-section... Revealed by a Science Teacher (Raffaele): Nov/Dec, p 33
- The Rechargeable Battery "Cycler" (Zauhar): Sep/Oct, p 15
- The Star-10 Transceiver (Dretea): Part 2: Mar/Apr, p 15; Part 3: May/Jun, p 33
- The Z100 CW Tuning Aid (Smith): Jan/Feb, p 3
- Using Morse Code for Computer and Ham Station Control (Connell): Nov/Dec, p 3
- Using Udpcast to IP Multicast Data over Amateur Packet Radio Newtorks (Wiedemeier): Nov/Dec, p 43
- VHF Frequency Multiplication Using the SA602 IC (Post): Jul/Aug, p 3
- Why Should I Care About My CW Frequency? (sidebar to The Z100 CW Tuning Aid) (Smith): Jan/Feb, p 7

About the Cover (Wolfgang)

- A Software Controlled Radio Preselector: May/Jun, p 1
- NUE-PSK Digital Modem: Mar/Apr, p 1
- "Simple" Crystal Set (Anderson): Sep/Oct, p 1
- The Z100 CW Tuning Aid (Smith): Jan/Feb, p 1
- Using Morse Code for Computer and Ham Station Control (Connell): Nov/Dec, p 1

- VHF Frequency Multiplication Using the SA602 IC: Jul/Aug, p 1

Antenna Options (Cebik)

- Beam Matching: Mar/Apr, p 58
- Horizontally Polarized Omni-Directional Antennas: Some Larger Choices: Jan/Feb, p 40
- In Memoriam — L.B. Cebik, W4RNL (Wolfgang): Jul/Aug, p 50
- One Wavelength Loops: Jul/Aug, p 51
- Reflections on Reflectors: May/Jun, p 50

Circulation Statement Nov/Dec, p 56

Empirical Outlook (Wolfgang)

- 27th ARRL/TAPR Digital Communications Conference: Nov/Dec, p 2
- Ah, Spring!: May/Jun, p 2
- L.B. Cebik, W4RNL, Silent Key; Paul Rinaldo, W4RI, reminiscing: Jul/Aug, p 2
- Miscellaneous; Share Your Work: Sep/Oct, p 2
- Out and About: Jan/Feb, p 2
- Writing for QEX: Mar/Apr, p 2

Index of Advertisers:

- Jan/Feb, p 1; Mar/Apr, p 1; May/Jun, p 1; Jul/Aug, p 1; Sep/Oct, p 1; Nov/Dec, p 1

Letters to the Editor

- A New Subscriber (Niles): Mar/Apr, p 63
- A Direct-Reading Reflection Coefficient and Power Meter (Nov/Dec 2007) (Gaze): Jan/Feb, p 45
- A High-Efficiency Filament Regulator For Power Tubes (Nov/Dec 2006) (von Valtier): Jul/Aug, p 57
- A Large Aperture, Resonant, Regenerative Frame Antenna (LARRFA) (Jan/Feb 2007) (Young): Mar/Apr, p 64
- A Low-Cost Atomic Frequency Standard (Nov/Dec 2007) (Goedecke, Haselwood and McCulla): Jan/Feb, p 48
- A Low-Cost, Flexible USB Interface (Jan/Feb 2008) (Baier): May/Jun, p 58
- A Software Controlled Radio Preselector (May/Jun 2008) (Wolfgang): Jul/Aug, p 57
- A Squelch Amplifier (Jan/Feb 2008) (Laughlin and Lund): May/Jun, p 58

Antenna Options (Jul/Aug 2007) (Riley and Cebik): May/Jun, p 58
 Carbon Composition, Carbon Film and Metal Oxide Film Resistors (Mar/Apr 2008) (Czuhajewski): May/Jun, p 58
 Empirical Outlook (Mar/Apr 2008) (Nichols): May/Jun, p 58
 Empirical Outlook (Nov/Dec 2007) (Premena): Mar/Apr, p 63
 May/June Issue of *QEX* (McCulla): Sep/Oct, p 41
 Signal Resilience to Ionospheric Distortion of HF Digital Chat Modes (Nov/Dec 2007) (Greenman): May/Jun, p 59
 Some Thoughts on Crystal Parameter Measurement (Jul/Aug 2008) (Bloom and Koehler): Sep/Oct, p 41
 The Direct-Reading Reflection Coefficient and Power Meter (Nov/Dec 2007) (Gaze): May/Jun, p 58
 The Star-10 Transceiver (Nov/Dec 2007) (Drentea, Kunde, Wolfgang and Zavrel Jr): Jan/Feb, p 45
 Transmission Line Paradigm (Jul/Aug 2007) (Thompson): Mar/Apr, p 64

In the Next Issue of QEX

Jan/Feb, p 48
 Mar/Apr, p 61
 May/Jun, p 32
 Jul/Aug, p 61
 Sep/Oct, p 43
 Nov/Dec, p 56

Out of the Box (Mack)

Atmel Microcontroller Design Tools: May/Jun, p 57
 CADSTAR Express Version 10.0 Available; New L Band FETs; New RF Power Detector IC: Sep/Oct, p 44
 New Sources for UHF and Microwave Semiconductors: May/Jun, p 57
 Unusual Local Sources for Parts: May/Jun, p 57

Tech Notes

Feeding the Thing (sidebar to Tech Notes: The Goofy-Foot Yagi) (Nichols): Jul/Aug, p 48
 The Goofy-Foot Yagi (Nichols): Jul/Aug, p 47

Upcoming Conferences

12th Annual Southeastern VHF Society Conference: Jan/Feb, p 48
 Mar/Apr, p 62
 2008 AMSAT North America Space Symposium: Sep/Oct, p 43
 2008 Eastern VHF/UHF Conference: Mar/Apr, p 62
 42nd Annual Central States VHF Society Conference: Jan/Feb, p 48
 Mar/Apr, p 62
 May/Jun, p 63

ARRL/TAPR Digital Communications Conference (2008): Jul/Aug, p 61
 Sep/Oct, p 43
 Microwave Update 2008: Mar/Apr, p 62
 May/Jun, p 63
 Jul/Aug, p 61
 Sep/Oct, p 43

In the Next Issue of QEX

Tom Allread, VA7TA, continues the description of his NimbleSig III dual output DDS RF generator. In Part 2, Tom describes the software design, computer interfacing, MPU programming and initial testing procedure aspects of this project.

NimbleSig needs to be connected to a computer for programming, testing and calibration. Tom describes a simple USB to 3.3V UART adapter for this connection. He leads us through the program flow chart and describes the process of programming the RF generator. He then takes us through the initial testing for the project and describes the procedure for calibrating the NimbleSig generator.

Down East Microwave Inc.

We are your #1 source for 50MHz to 10GHz components, kits and assemblies for all your amateur radio and Satellite projects.

Transverters & Down Converters, Linear power amplifiers, Low Noise preamps, coaxial components, hybrid power modules, relays, GaAsFET, PHEMT's, & FET's, MMIC's, mixers, chip components, and other hard to find items for small signal and low noise applications.

We can interface our transverters with most radios.

Please call, write or see our web site
www.downeastmicrowave.com
 for our Catalog, detailed Product descriptions and interfacing details.

Down East Microwave Inc.
 19519 78th Terrace
 Live Oak, FL 32060 USA
 Tel. (386) 364-5529

10111 Jorie Blvd. #332
 Oak Brook, IL 60523
 1-800-985-8463
www.atomictime.com

ATOMIC TIME



14" LaCrosse Black Wall
WT-3143A \$21.45
 This wall clock is great for an office, school, or home. It has a professional look, along with professional reliability. Features easy time zone buttons, just set the zone and go! Runs on 1 AA battery and has a safe plastic lens.



Digital Chronograph Watch
ADWA101 \$49.95
 Our feature packed Chrono-Alarm watch is now available for under \$50! It has date and time alarms, stopwatch backlight, UTC time, and much more!



LaCrosse Digital Alarm
WS-8248U-A \$49.95
 This deluxe wall-clock features 4" tall easy to read digits. It also shows temperature, humidity, moon phase, month, day, and date. Also included is a remote thermometer for reading the outside temperature on the main unit. approx. 12" x 12" x 1.5"



LaCrosse WT-3143A - \$21.45



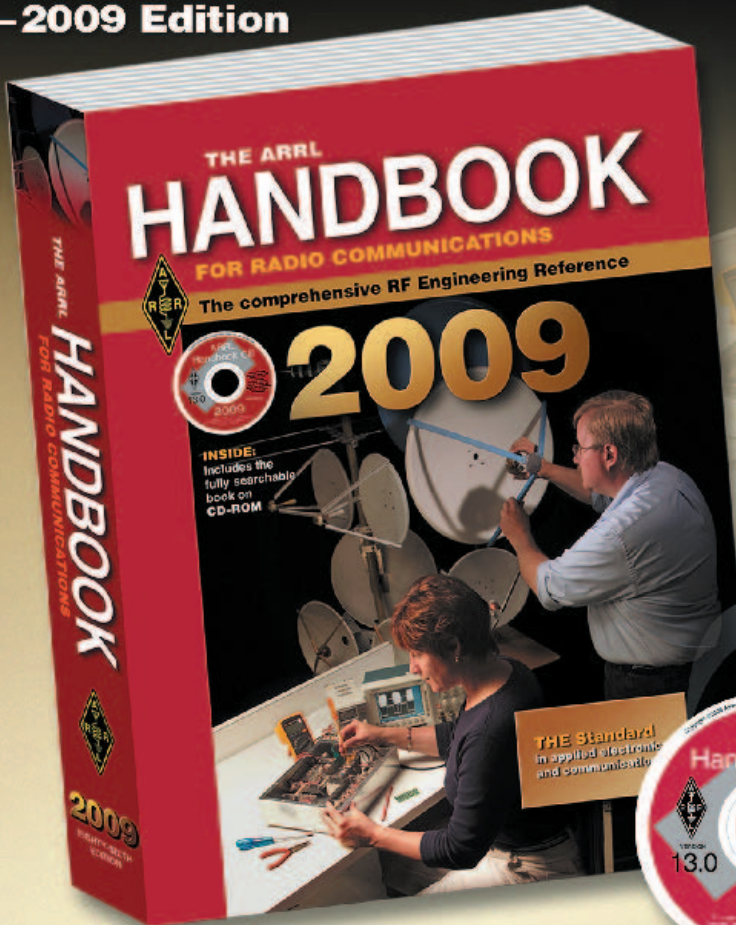
LaCrosse WT-5720U Clock \$24.95
 This digital projection clock is great for travel and fits in a small space. Shows 12 or 24 hour time, time zone, and alarm time. Size 5.25" x 1.25" x 4"

1-800-985-8463
www.atomictime.com
 Quantity discounts available!

Tell time by the U.S. Atomic Clock - The official U.S. time that governs ship movements, radio stations, space flights, and warplanes. With small radio receivers hidden inside our timepieces, they automatically synchronize to the U.S. Atomic Clock (which measures each second of time as 9,192,631,770 vibrations of a cesium 133 atom in a vacuum) and give time which is accurate to one second every million years. Our timepieces even account automatically for daylight saving time, leap years, and leap seconds. \$7.95 Shipping & Handling via UPS. (Rush available at additional cost) Call M-F 9-5 CST for our free catalog.

NEW!

The ARRL Handbook —2009 Edition



Must-Have

For the radio amateur...
 For the technician and engineer...
 For the newcomer...

This 86th Edition stays ahead of the pack—taking its place as the most comprehensive source of applied electronics and communications know-how. Featuring the most current material on the state-of-the-art, topics include:

Principles of electronics—including basic theory, components, analog and digital circuit construction.

Radio communication fundamentals and design—including modes and systems, filters, EMI, digital signal processing and software radio design, and RF power amplifiers.

Real-world applications and operating—including practical projects, station setup, antennas, transmission lines, and methods for testing and troubleshooting.

References—filled with hundreds of detailed tables, illustrations and photos. You will turn to **The Handbook** again and again!

CD-ROM Included! The CD-ROM at the back of the book includes the fully searchable text and illustrations in the printed book, as well as companion software, PC board templates and other support files.

ARRL *The national association for*
AMATEUR RADIO
 225 Main Street, Newington, CT 06111-1494 USA
 SHOP DIRECT or call for a dealer near you.
 ONLINE WWW.ARRL.ORG/SHOP
 ORDER TOLL-FREE 888/277-5289 (US)

Brand-new material:

- Updated **amateur satellite** content, including details for today's fleet of operational satellites.
 - Updated versions of **accessory software** on the CD-ROM.
 - **New Projects:**
 - **RockMite QRP CW transceiver.** Now expanded to cover 80, 40, 30 or 20 meters.
 - **Audio Interface** for Field Day or Contesting. Audio and mic connections for two operators sharing a radio.
 - **Remote Power Controller.** Turn high current devices off and on.
 - **Audible Antenna Bridge.** Tune for the lowest SWR by ear.
- ...and MORE!

**Order Today www.arrl.org/shop
 or Call Toll-Free 1-888-277-5289 (US)**

2009 ARRL Handbook Hardcover. Includes book and CD-ROM.
 ARRL Order No. 0292 **\$59.95***

2009 ARRL Handbook Softcover. Includes book and CD-ROM.
 ARRL Order No. 0261 **\$44.95***

*Shipping and Handling charges apply. Sales Tax is required for orders shipped to CA, CT, VA, and Canada. Prices and product availability are subject to change without notice.

KENWOOD

Listen to the Future



TM-G707A



TM-V7A



TM-D700A

With the supplied accessories the RC-D710 is a full upgrade to the TM-V71A. The TM-V71A will have full functionality of the TM-D710A by exchanging the TM-V71A panel with the RC-D710.

This is where it gets interesting!

PG-5J connection kit makes the RC-D710 a complete standalone APRS/TNC for your current radio. This option allows connectivity with previous and current Kenwood models* as an external modem.

*Compatible models include: TM-D710A / TM-V71A / TM-D700A / TM-G707A / TM-V7A / TM-733A / TM-255A / TM-455A
SmartBeaconing™ from HamHUD Nichetronix

KENWOOD U.S.A. CORPORATION

Communications Sector Headquarters

3975 Johns Creek Court, Suite 300, Suwanee, GA 30024-1298

Customer Support/Distribution

P.O. Box 22745, 2201 East Dominguez St., Long Beach, CA 90801-5745

Customer Support: (310) 639-4200 Fax: (310) 537-8235



www.kenwoodusa.com
ADS#42908



JQA-1205
ISO9001 Registered
Kenwood Corporation
ISO9001 certification